ISRU-BASED ROBOTIC CONSTRUCTION TECHNOLOGIES FOR LUNAR AND MARTIAN INFRASTRUCTURES

NIAC Phase II Final Report

Behrokh Khoshnevis, Anders Carlson, Madhu Thangavelu

University of Southern California

CHAPTER 1

INTRODUCTION

Economically viable and reliable building systems and tool sets are being sought, examined and tested for extraterrestrial infrastructure buildup. This project utilizes a unique architecture weaving the robotic building construction technology with designs for assisting rapid buildup of initial operational capability Lunar and Martian bases. The project intends to develop and test methodologies to construct certain crucial infrastructure elements in order to evaluate the merits, limitations and feasibility of adapting and using such technologies for extraterrestrial application. High priority infrastructure elements suggested by our NASA advisors to be considered include landing pads and aprons, roads, blast walls and shade walls, thermal and micrometeorite protection shields and dust-free platforms utilizing the well-known in-situ resource utilization (ISRU) strategy. Current extraterrestrial settlement buildup philosophy holds that in order to minimize the materials needed to be flown in, at great transportation costs, strategies that maximize the use of locally available resources must be adopted. Tools and heavy equipment flown as cargo from Earth are proposed to build required infrastructure to support future missions and settlements on the Moon and Mars.

Several unique systems including the Lunar Electric Rover, the unpressurized Chariot rover, the versatile light-weight crane and Tri-Athlete cargo transporter as well as the habitat module mockups and a new generation of spacesuits are undergoing coordinated tests at NASA's D-RATS. This project intends to draw up a detailed synergetic plan to utilize these maturing systems coupled with modern robotic fabrication technologies based primarily on 3D Printing, tailored for swift and reliable Lunar and Martian infrastructure development. This project also intends to increase astronaut safety, improve buildup performance, ameliorate dust interference and concerns, and reduce time-to-commission, all in an economic manner.

The goal stated in our Phase I proposal was a high fidelity demonstration at D-RATS to be conducted at the conclusion of the Phase II study. In the course of the Phase I study, however, it became clear that such demonstration was neither possible (due to the maximum Phase II budget limitation and the cost of NASA assets and related overhead expenses to support such demonstrations), nor necessary (due to NASA's low TRL expectation of Phase II results). These important facts were revealed to us only after interacting with the NIAC administrators and meetings with potential future partners at JPL and KSC. Accordingly, it was decided by the team that in order to make best use of resources we should investigate novel directions in the adaptation of our fabrication technologies by using in-house laboratories and to produce truly useful technologies and data, and then proceed with high fidelity demonstration at a later opportunity when sufficient resources become available. Furthermore, we have recognized that in addition to our building scale 3D printing technology called Contour Crafting, variations of some of our other fabrication technologies under development are suitable for construction of infrastructure elements such as regolith based ceramic tiles and hence we have decided to include some related preliminary research in this Phase II proposal. The Phase II project title and overview reflect these changes in direction but the ultimate goal remains the same: A high fidelity to-scale demonstration to construct the above mentioned infrastructure elements, all meant for repeated and frequent use during build-up operations and for routine service afterward.

In the course of our Phase I and Phase II studies and through the informative NIAC conferences, we have made highly synergetic alliances with esteemed groups of NASA researchers and KSC and MSFC. The KSC colleagues are specialized in planetary materials and materials processing. In the course of the Phase II study we have continued to benefit from the advice and direction of the KSC team in our highly relevant experiments. MSFC has prior experience in using USC's flagship fabrication technology, Contour Crafting. Our partner at MSFC have focused on radiation shielding analysis of our proposed structures.

A robotic construction system can also provide tremendous benefits for human habitation on Earth. Construction is the last frontier of human endeavor to be automated. The recently published "Roadmap for US Robotics" has identified several key areas and related enabling technologies for co-robotics which will result in US economic expansion. Robotic construction falls into two categories of manufacturing and professional services identified in that Roadmap. The economics of the proposed approach will enable the construction of durable, low-cost housing in the US and worldwide, and can enable much faster disaster recovery. Replacing human workers with robots on construction sites will reduce the injuries and fatalities of construction, which has long been recognized as the most hazardous occupation. Some of the specific proposed research modules will also have broad impacts. For example, construction using sand and without the use of water would be extremely useful for dry climates, and the work on radiation shielding may lead to terrestrial benefits such as improved and more economical shielding at nuclear power plants and nuclear waste storage sites. Student involvement will develop uniquely experienced future US construction robotic engineers and researchers.

We intend to continue to publicly disseminate our related research results through presentations and publications in conferences and journals in the fields of aerospace, fabrication, civil engineering, construction and architecture.

PROGRESS SUMMARY

Our activities have advanced on many fronts. We have successfully engaged in team building efforts, we have conducted extensive literature review in related domains and engaged in architectural conceptual design of planetary outpost elements, we have performed materials and process studies, built experimental machines and conducted numerous laboratory experiments, conducted structural design and analysis studies, jointly taught a new Moon Studio architecture course, created several high fidelity visuals, made presentations at several conferences, published several research articles on various aspects of our project in engineering and architectural proceedings and journals, and participated in several interviews for related articles and television programs that appeared in acclaimed international media. The following sections present some of these activities in more detail.

Team Building:

Shortly after the start of the project our team visited the D-RATS site where we made numerous useful contacts with NASA researchers and administrators who were working at D-RATS or visiting the site. At the fruitful NIAC meeting in November 2011 we initiated contact with the KSC team (thanks to the NIAC Program Director who wisely arranged for our poster presentations to be adjacent to one another). Since then we have had numerous interactions with the KSC team and this April we had an extensive

meeting with five researchers from KSC who visited USC and our laboratories. Our group has been exploring other synergetic partnerships as well. Notably, we had a meeting with the JPL ATHLETE group with whom we have had several useful meetings and exchanges. The PI also visited MSFC to meet with the group specialized in radiation shielding. The result of these interactions is the synergetic partnerships from which our NIAC project benefits. We have also engaged two engineering graduate students (one being under scholarship support and working as a 50% RA solely on the NIAC project), two graduate architecture students who concentrated on visualization projects, and one undergraduate astronautics student (also under scholarship support).

Conceptual Infrastructure Designs:

We first concentrated on the landing pad and road requirements and will be concentrating on blast walls and hangars for the remaining part of the project. Lunar vacuum and low gravity will make it very difficult to contain or curtail high energy debris that results from direct lander exhaust plume impingement on the exposed, free and loose surface regolith. The extreme natural environment of the Moon coupled with the reference Altair-class (45-50MT) lunar lander touchdown profile will create a very challenging dust and debris environment for safe sortie operations. Ground effects will be far more severe than experienced during Apollo missions (Mason 1970). Review of recent literature clearly points to the need to provide stabilized surfaces for landing heavy payloads (Lumpkin 2007, Metzger 2008, Khoshnevis 2012, Sengupta 2012).

Site Selection: Site selection for lunar lander sortie operations is of the utmost importance. A strategic location will provide several advantages. They include:

- Safety - Good approach and lift-off trajectories (and abort), and maximum windows of opportunity for routine operations, avoiding overflights above sensitive locations, landmark identification and pilot landing target visibility (Eppler1992, Kerrigan 2012)
- Least fuel expenditure (depending on landing site altitude)
- Terrain character – plains vs. highlands, bedrock vs. loose regolith
- Steady surface/terrain temperature

Lander Terminal Phase Effects: The reference RL-10B main engine cluster core exhaust of the lander, during the terminal descent and touchdown phase of operations, upon low velocity translation toward and hovering maneuver over the touchdown area, just before main engine cut-off and setting down, will exert around 50MT reaction loads over a very small footprint of approximately 10 m^2. This force will be compounded by the intense heat and pressure of the exhaust, even if only for a small period of time. The rapid transient temperatures and pressures, further aggravated by low lunar surface ambient (depending on site), will cause severe stresses on the landing pad materials and need to be carefully studied and taken into account for safe and reliable design over the commissioned life cycle (assumed to be 100 landings over a 10 year timeframe).

Landing Pad Options Under Study: One way to accommodate this extreme transient temperature and dynamic pressure pattern is to reinforce the core of the landing pad with appropriate materials and design features to mitigate the exhaust effects. The CC technology and other augmenting methods that we have newly explored may offer a way to create and inlay refractory tiles in such a manner as to be able to dissipate the heat and energy of the lander engines effectively.

Several other options for landing pads exist including locating and appropriately preparing (tooling and shaping) naturally occurring expanses of bedrock before applying CC technology, and we are studying these alternatives.

The landing pad apron has much less stringent requirements than the landing pad center segment and as such sulfur concrete may be a reasonably good candidate for its construction. We are considering several different methods or a combination of these methods for road construction. These include construction by sulfur concrete, by extruded molten regolith, by melting regolith in place without extrusion, and by using strong ceramic tiles made of sintered regolith and possibly grouted by sulfur concrete or molten silica.

Our concept designs of landing pad, apron, blast walls, and road and hangar robotic construction scenarios are depicted in visualization shown in Figures 1, 2 and 3.

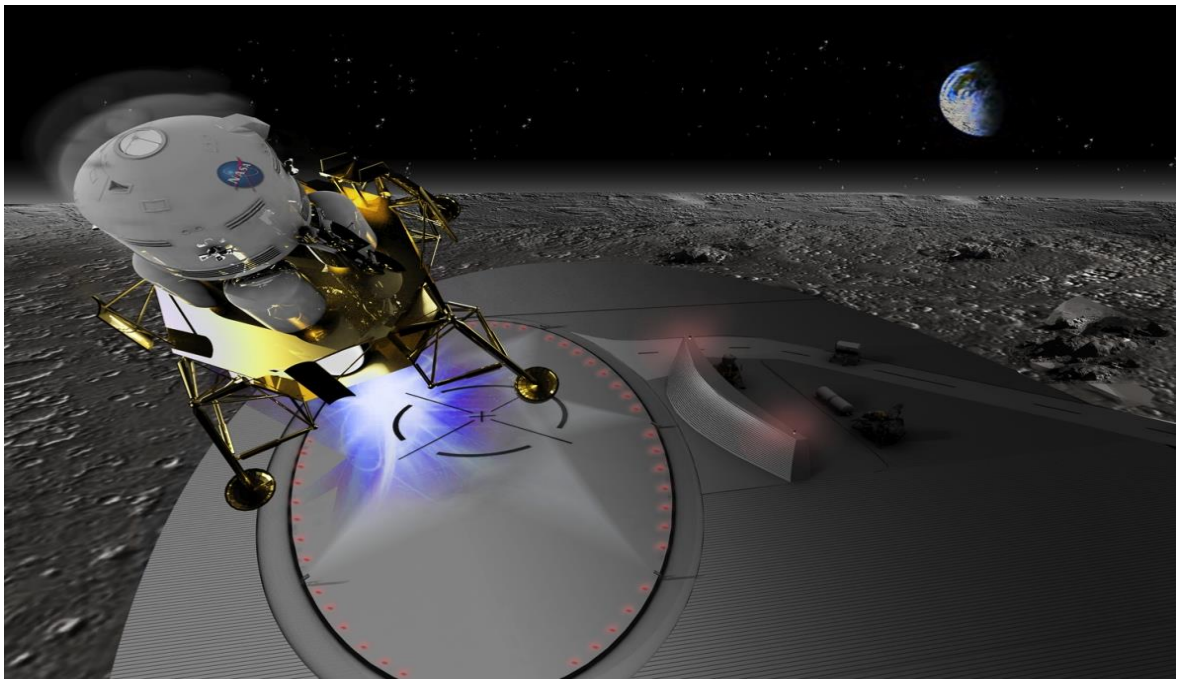

Figure 1. A lander is shown coming in to land on a lunar landing pad. The landing pad has been designed as an ellipse with its length in line with the direction of landing and takeoff with a central landing area lit up by lights, surrounded by a broader dust-free apron. A blast wall is also visible, protecting the entire settlement and items of equipment stored behind it.

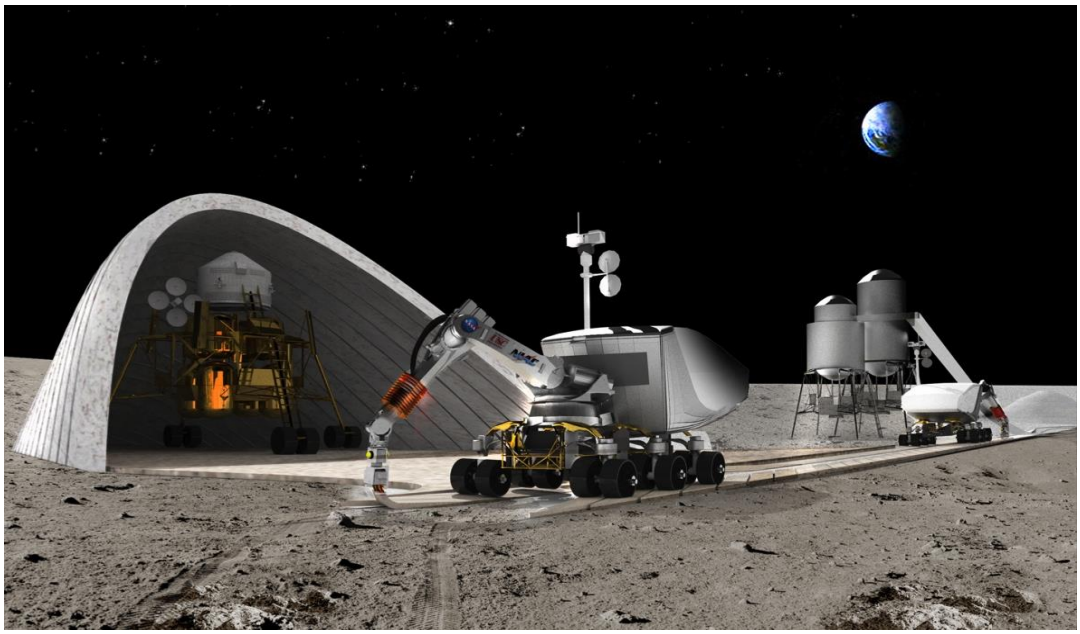

Figure 2. A Contour Crafting robot is shown here printing a road in front of a parabolic hangar structure housing a lunar lander. In the background can be seen a plant intended for processing regolith that will be used in the construction process.

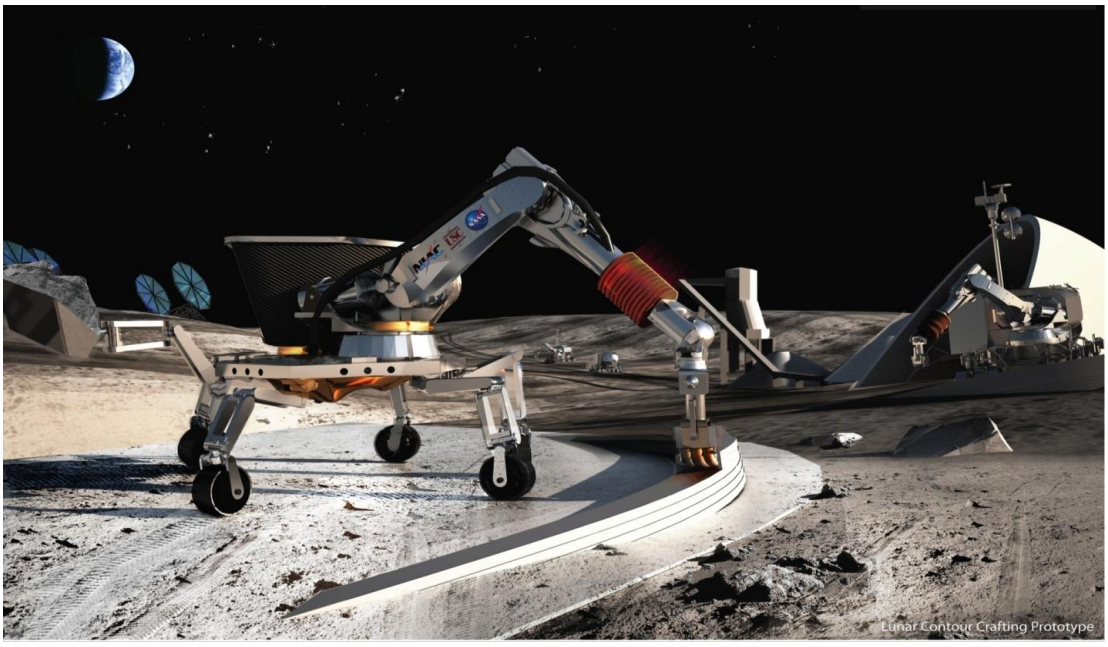

Figure 3. A Contour Crafting robot, housed on an 'ATHLETE' rover, is shown here printing a parabolic vault structure out of processed regolith. The structure is intended to house a lunar lander or other equipment, and is unpressurized. The parabolic form has been adopted, because it is structurally efficient and lends itself to the Contour Crafting mode of construction. In the background can be seen an array of solar panels intended to supply power to the robot.

Construction Materials and Fabrication Technologies:

In the course of our current project we have considered a variety of practical construction material for different planetary structural applications. Having become aware of the diversity of structural performance requirements and suitability of alternative fabrication processes, we have also investigated a number of other novel digital fabrication alternatives, all conceived in-house, in addition to Contour Crafting (our mega-scale 3D printing technology), which was the sole technology of choice proposed in our NIAC Phase I proposal.

Water is present on Moon and Mars and other researchers have demonstrated the possibility of creating hydraulic (water based) concrete on these planets. Accordingly, our years of research on hydraulic concrete construction for terrestrial applications using Contour Crafting and the resulting technological solutions are applicable to extraterrestrial condition with relatively minor alterations beyond handling water in a high or low temperature near-vacuum environment. We have hence decided to focus our attention on other construction materials including sulfur based concrete, molten regolith concrete, and sintered regolith. We have performed some preliminary successful studies with sulfur based concrete by mixing and hot-extruding sulfur and JSC1-A regolith stimulant. We have also melted regolith stimulant by means of concentrated sunlight using a 70 cm diameter Fresnel lens. The silica component in the regolith melts at about 1100 C and acts as the cement in binding other regolith constituents (primarily metal oxides) that serve as concrete aggregates. We then tested the compressive and tensile strengths of the resulting solid. To improve tensile strength we have performed a number of experiments, the most successful of which was mixing regolith with 5% metal powder (we used bronze powder which was readily available to us due to our ongoing research on 3D printing of metallic parts) and melting the mix. Finally, using our small sintering furnaces we have examined the sintering process of regolith.

PLAN SUMMARY

Our planetary infrastructure construction strategy is based on robotic system deployment, digital fabrication using 3D Printing, and ISRU for feedstock. As with all space missions, cost of transport of equipment to site is the dominant part of extraterrestrial technology deployment and operations. Current values are around $10,000 /kg to low Earth orbit, $100,000 for lunar orbit and another order of magnitude for landing payloads on Mars. These are exorbitant transportation costs, and once again, robotic construction technology-derived solutions offer great promise. A lunar setup based on existing CC machine components, for example, could weigh as low as 500 kg on the launch pad[1], depending on the choice of robotic rover system on which the CC module will be installed. We expect such a CC system to be compactly packed into a payload volume of 5 m x 2 m x 2 m and could be adapted as auxiliary payload on a variety of launchers. We also expect the cost of transportation to drop significantly as private launchers like SpaceX Falcon 9 become serviceable for lunar and Mars missions.

An extraterrestrial robotic construction system offers tremendous advantages over crew doing complex building tasks manually. First of all, it eliminates the risk associated with EVA. By relegating crew to supervisory tasks and anomaly resolution alone, robotic fabricators allow the builder to hold to schedule

[1] Our largest CC machine which has a fabrication envelope of 5 m x 7 m x 2.2 m weighs 250 kg

with minimal slippage. The ability of such systems to work continuously allows for rapid infrastructure buildup.

Our current estimate suggests that a 500 kg robotic fabricator setup, once deployed on the lunar terrain, could fully make use of one lunar day (14 Earth days), to prepare and build a 30 m diameter, stabilized landing pad for an Altair-class lander in sortie operations. This pad could be surrounded by a 70 m band of stabilized regolith for dust suppression during lander operations. Robotic fabricator performance is enhanced when multiple copies of a structure need to be commissioned. When coupled with ISRU materials and technologies like real time tele-robotics or co-robotics, such fabricators offer a versatile building system which over a period of time could construct numerous structures and vast settlements. At the end of our Phase II effort we will have identified alternative digital fabrication technology development and demonstration architectures that may be tailored to NASA needs and applications.

Phase II has so far allowed us to build test samples of the materials we will be depositing using robotic construction methods. We have performed several mechanical property tests on the materials and have managed to better assess the viability of materials to build initial infrastructure on the Moon or Mars. This will allow us to determine if any of the desired infrastructure components can be fabricated without further processing of ISRU materials to enhance the tensile capacity of our unreinforced regolith concretes. Working closely with NASA KSC's experts in Granular Mechanics and Regolith Operations Laboratory as well as their Electrostatics and Surface Physics Laboratory we will look at techniques to make reinforce regolith concrete with either a matrix of ISRU metal melted into the regolith mix to form a tensile matrix or discreet elements formed with robotic construction techniques and assembled into the concrete similar to our reinforced concrete here on earth.

During the extension period of Phase II we will continue our fabrication studies and will create much larger scale sulfur concrete structures. The end result of our Phase II structural behavior and performance studies of robotic construction will be a figure of merit analysis that will help determine timelines for future missions to the Moon or Mars to create scientific bases or settlements. Our analytical studies and physical tests of samples will raise the knowledge of major infrastructure components for the Moon or Mars to TRL-3.

WHAT IS ANTICIPATED AFTER PHASE II

Fortunately, we have received words that NASA and the Army Corps of Engineers are planning to fund the Phase III of our project to further development of our promising technologies and the structures they can produce. As an initial next step beyond Phase II, samples of infrastructure elements subject to lunar and Martian environmental loadings would be made using robotic construction technology (TRL-4). This will help validate FEA simulations and the feedback may influence refinements to the infrastructure designs. After that, samples of infrastructure elements would be made with robotic construction methods in an environment similar to the Moon or Mars and subject to Lunar and Martian environmental loadings (TRL-5). This will also help validate FEA simulations and the feedback may influence refinements to the infrastructure designs. Further maturity of the robotic construction technology and structures it can make would lead to full scale prototypes of infrastructure components built in vacuum or Martian-like

atmosphere and be subjected to thermal and blast loading (TRL-6). This test performance will be used to demonstrate agreement with FEA simulation predictions.

In addition to research that will advance the maturity of this architecture, we anticipate other divisions of NASA to be interested in expanding the robotic construction methods to build other types of ISRU based components beyond basic infrastructure. Robotic construction technologies could build tools, other robots, scientific equipment and many other objects that can be formed from excavated and processed extraterrestrial materials. We also anticipate major contributions by robotics researchers at NASA divisions to integrate our proven fabrication technologies with space-worthy advanced class of NASA robotics hardware and intelligent software. Once such integration materializes exciting demonstrations at sites such as D-RATS can be performed and following successful demonstration and refinement the ultimate dream of actual Lunar and Martian settlement construction will be materialized.

Automated building technologies will revolutionize the way structures are built on Earth, in dense urban environments, in difficult-to-build and difficult-to-service sites, or in remote and hostile regions of the globe. The technologies under development by our group have the potential to simplify construction logistics, reduce the need for hard physical labor by assigning humans to a strictly supervisory role, eliminate issues relating to human safety, and produce intricate and aesthetically refined designs and structures at significantly reduced construction cost. Space architecture in general and Lunar and Martian structures in particular will also provide a rich new aesthetic vocabulary for architects to employ in the design and creation of buildings that employ high technology and building information modeling that is vital for optimizing use of materials and energy that is critical to building economics.

We have established the Contour Crafting Corporation in order to advance terrestrial as well as some extraterrestrial applications of our NIAC-supported technologies using private as well as public funds. We anticipate this NIAC initiated endeavor to ultimately lead to revolutionizing construction on our planet and significantly impacting the quality of life for billions of people and improving the state of the earth environment, in addition to making breakthrough contributions to development of technologies that make creation of human settlements on other planets a possibility.

WORK PLAN

The chart in Figure 9 demonstrates the research thrusts, responsible teams, major research activities, minor and major milestones, and project timeline that we predicted for NIAC Phase II.

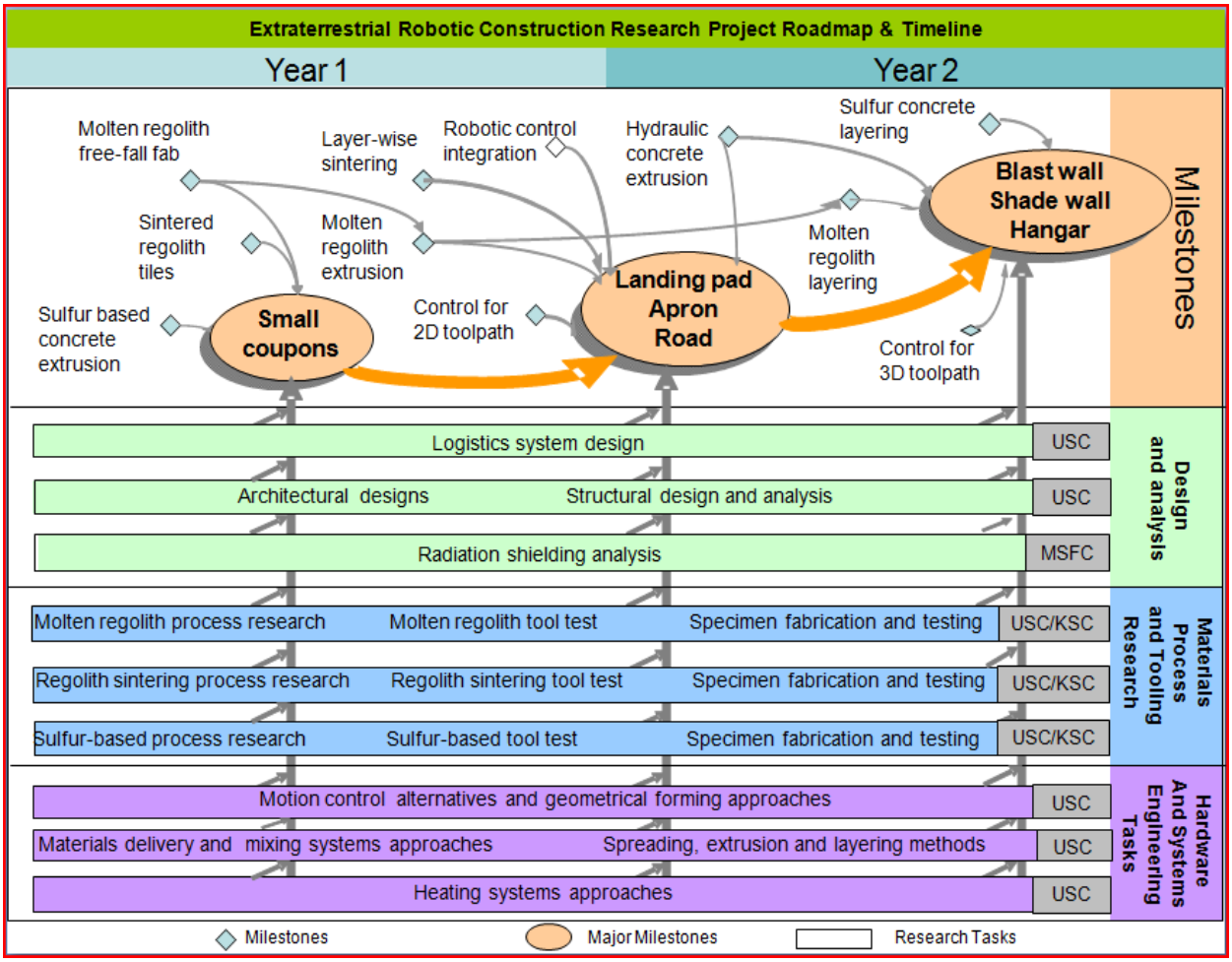

Figure 4. Chart showing project roadmap, timeline and activity breakdown

We have attempted and carried out most of what we planned. Following are some deviations from the plan:

- We discontinued to pursue fabrication with molten regolith, primarily due to the requirement of high power heating systems and the potential danger of accidental severe burns or even explosions of molten materials.
- We have not yet constructed large structures with sulfur concrete because of the difficulties that we encountered in extruding large volumes of sulfur concrete. This problem has now been resolved and integration of our new nozzle system with the large industrial robot is now advancing.
- Fabrication and testing of ceramic tile varieties for suitability for landing pad and roads has not been completed although we have nearly perfected the fabrication method.

- Structural design and analysis has advanced to a reasonable extent but still certain activities are still ongoing and should complete by the end of the extension period.
- Details of energy requirement analysis is yet to be performed.

CHAPTER 2

Construction of Structures with Sulfur Concrete

1. Introduction

1.1 Robotics Approach

Contour crafting can quickly build structures such as houses out of hydraulic (water-based) concrete using an extrusion based fabrication system that implements a gantry robot structure such as the one shown in Figure 1.

Figure 1: Gantry robot structure for contour crafting

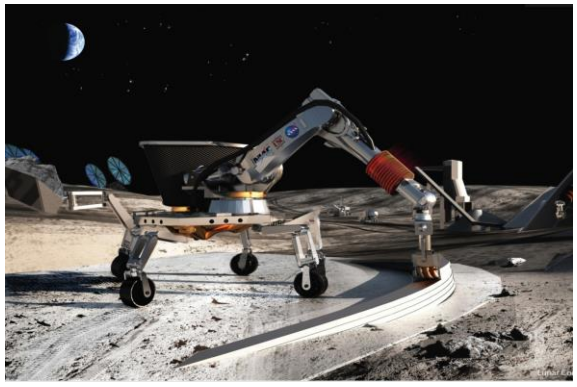

Figure 2: 6-axis robot used for contour crafting

The gantry structures is less attractive for planetary construction because of the large size of the gantry which makes fitting in cargo area of launch systems problematic, and implementation problems due to the requirement of autonomous assembly of the gantry upon deployment. Furthermore, the gantry structure cannot build anything larger than its footprint. Accordingly, a mobile robotic system such as the one shown in Figure 2 is proposed which will be a) more compact when its elements are retracted hence making it more suitable for launching, b) will be possible to deploy much easier after being landed, and c) can build structures with practically unlimited size.

1.2 Sulfur Concrete

Sulfur concrete is a composite construction material composed of sulfur as the binding agent and aggregate (coarse aggregates such as gravel rocks and stones and fine aggregates such as sand and ash). Compared to regular Portland cement, sulfur concrete has the following advantages:

(a) Excellent resistance to acid and salt environment (Figure 3 compares regular and sulfur concretes when exposed to acid)
(b) Superior water (and most likely air) tightness
(c) 100% recyclability
(d) High solidification speed (Figure 4) [3]

Figure 3: Resistance to acid environment

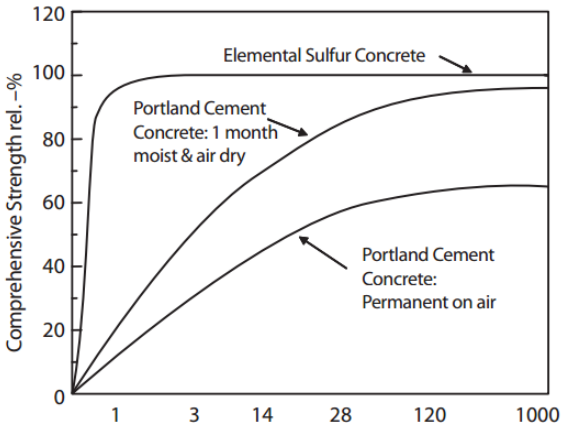

Figure 4: Solidification speed of sulfur and Portland cement

Besides the advantages enumerated above, the rich-in-sulfur mines, especially on Mars, encourages the use of sulfur concrete for extraterrestrial settlement infrastructure construction. King [4] points out that sulfur enriched environment of Mars may have resulted in an Fe–(Ni–)S core and illustrates the sulfur concentration in the upper few decimeters of Martian surface in Figure 5.

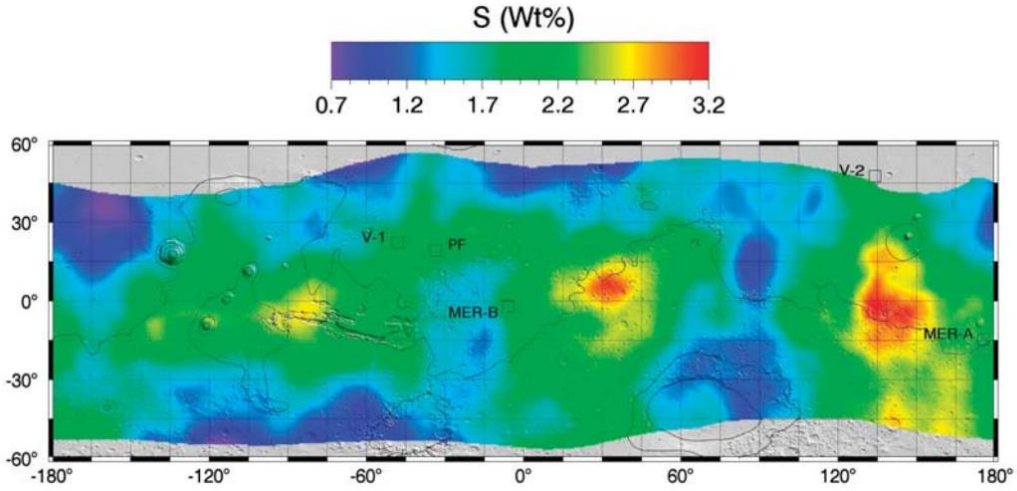

Figure 5. Sulfur concentration on Mars

2. Sulfur cement extruder design

Prior to this project the proven extrusion process for Contour Crafting was designed only for processing several specific Portland cement based concrete types. The system included heavy mixers, massive concrete pumps, and air compressor. To apply Contour Crafting in the environment of Mars and the Moon and using sulfur concrete, an entirely different extruder is necessary considering the large temperature variation, vacuum, low gravity, dust effects and the

necessity for durability. Since construction materials provided by ISRU may be different for different terrains, a new extrusion concept must be developed for sulfur concrete with different types of constituents, viscosity and plasticity [1, 2].

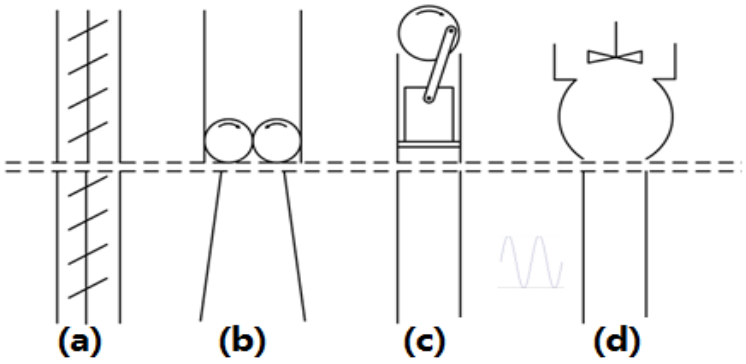

Figure 6: Design of extrusion system

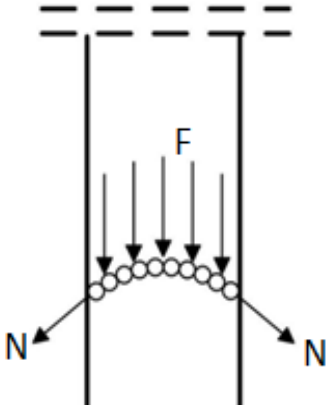

Figure 7: Illustration of bridging effect

The extrusion nozzle is composed of two sub-stages: a compression stage and a forming stage. Some options for granular material compression are shown above the dotted line in Figure 6. Compression was used to deliver the mixture of sulfur and regolith into the heated nozzle, where it was melted and extruded. The figure shows four kinds of compression methods, from left to right: the auger rotation method, the double-roller method (developed by our team), the plunger method, and the preheated paste stirring/pressing method. In the auger method, single or double augers rotate to move the mixture. In the double-roller method, the knurled surface of the rollers captures and presses down the powder particles. In the plunger method, a piston connected to a crank periodically pushes against the mixture. In the preheated method, the blades rotate in a heated hopper and provide pressure to push the molten mixture into the nozzle.

2.1 Double roller Extruder

Method (b) in Figure 6 shows the concept which has been developed by our team, for which the CAD model is shown in Figure 8. First, the mixture of aggregates and sulfur was placed in the chamber. Second, the knurled rollers rotate while pressing together to drive the mixture into the nozzle. Vibration was added by a separate motor with an off-center load to prevent the bridging effect (Figure 7).

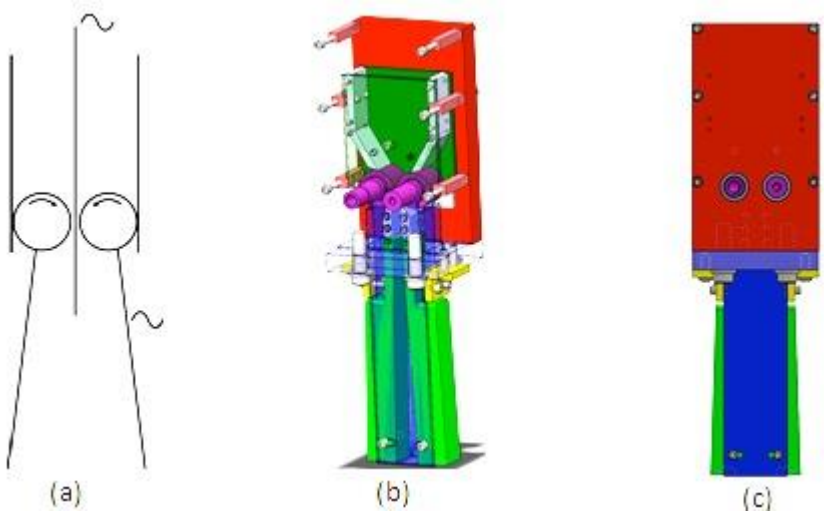

(a) The extrusion mechanism illustration (b) (c) Perspectives of extrusion system

Figure 8. Extrusion system of double-roller design.

As seen in Figure 9, the extruding system was fixed to a frame with a turntable. The nozzle was heated to roughly 130 ºC (the melting point of sulfur) and the mixture was extruded in the form of a viscous paste.

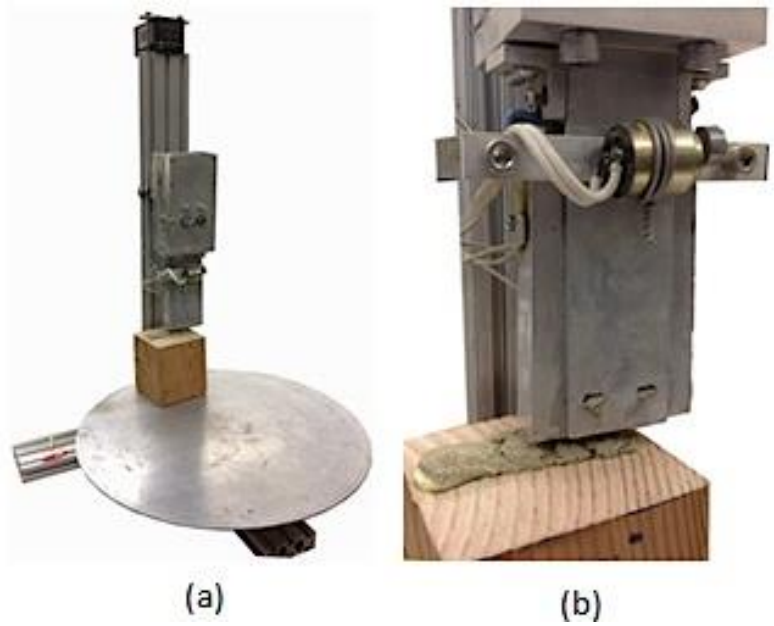

(a) Extrusion system (b) Extrusion process

Figure 9: Experimental setup of two-roller extrusion system

In this part of the research, we investigated the interaction of several variables in controlling the strength of the resulting parts. More experiments in this area are warranted to find the combination of parameters that uses the least sulfur while producing the greatest strength.

2.2 Mini-size auger extruder

In the mini-size auger extrusion system (Figure 10), the mixture was pushed downward to the nozzle by a rotating auger while it was heated by electrical heating elements. At the bottom of the nozzle, the nozzle head controls the flow of the paste and creates regular surfaces and edges. To increase the inter-layer binding strength, a contour profile (Figure 11) was machined at the nozzle outlet to create interlocking features.

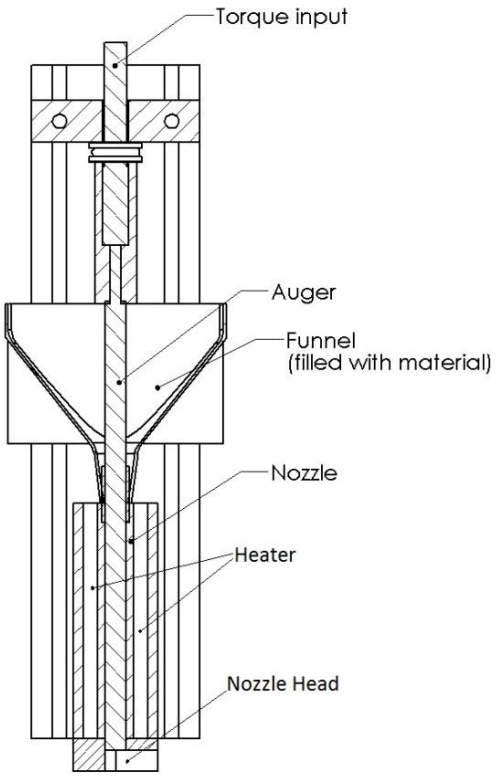

Figure 10: Diagram of Extrusion System

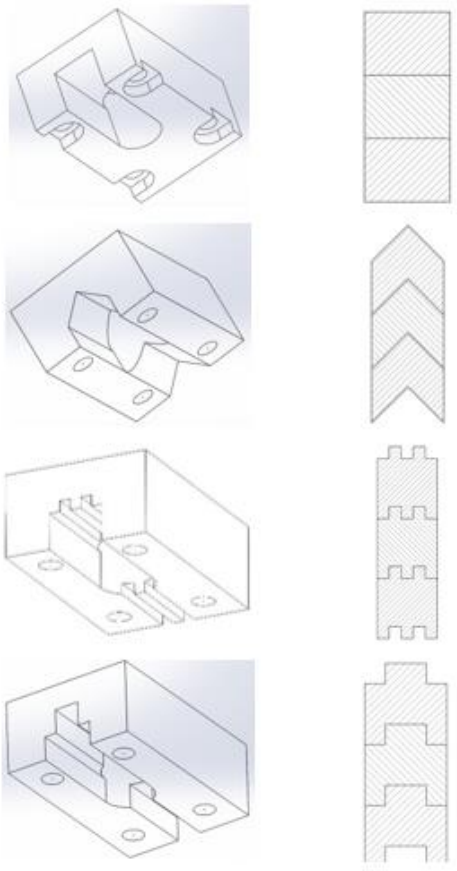

Figure 11: Diagram of nozzle head and layer binding

Extrusion of granular abrasive material is never straightforward. Lacking water which serves as lubricant to ease the concrete flow, the extrusion of the highly viscous and abrasive sulfur and regolith mix is undoubtedly challenging. To study the problem we have created a crude experimental device shown in the lower section of Figure 12 under our Phase I project. In this device a gear motor turns an auger that forces the dry mixture of sand and sulfur out of a vibrating hopper and into a hot barrel and nozzle. The auger was also equipped with a vibrator

to prevent possible clogging. As the mixture is pushed inside the hot barrel of the extrusion nozzle, the sulfur portion heats up in the upper portion of the barrel and melts in the lower portion. The extrusion process may take place without clogging only for a few seconds until the "bridging" phenomenon causes a few particles of sand to create an arch against the flow direction and the two arch bases push against the inner walls of the barrel causing complete clogging. Under such a circumstance vibration could overcome the static friction and clear the clogging problem. Vibration may be applied to the barrel or to the auger. Vibrating the barrel could be problematic as the barrel is solidly attached to the rest of the structure for stability. Barrel vibration may also eventually damage the heater filament that heats the barrel to melt the sulfur; therefore, it is best to vibrate the auger. Furthermore, it is best to minimize the vibration period only to occasions of clogging because too much vibration causes segregation of sulfur powder and aggregate particles in the upper portion of the extrusion barrel.

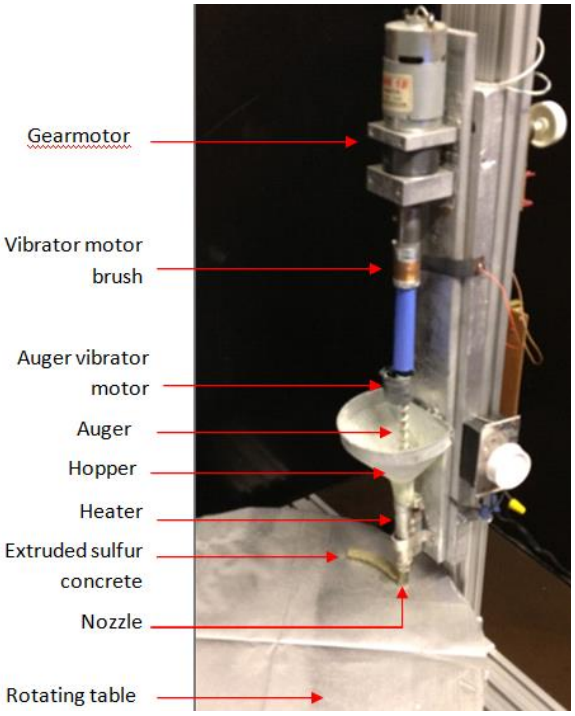

Figure 12: Experimental machine for extrusion testing of sulfur concrete

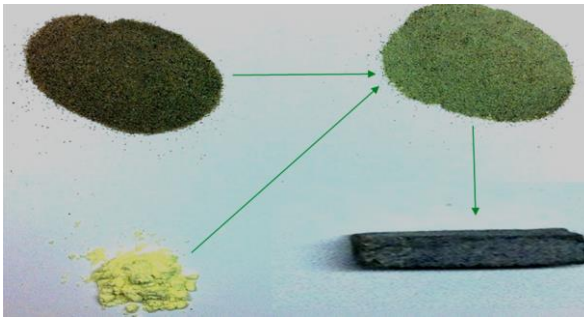

Figure 13: Sulfur, sand, sulfur/sand mix yielding sulfur concrete

We have devised a hard-wired controller that activates auger vibrator only at clogging times. This was done by sensing the gear motor current which increases as beginning of clogging increases the motor load. The more serious the clogging the higher the motor current becomes. A circuit activates the auger vibrator with a vigor that is proportional to the gear motor current. At normal gear motor load levels the vibration motor remains inactive.

In NIAC Phase II, a new mini-size auger with piezo vibrators was developed to investigate the possible difficulties in extruding sulfur concrete. As it is shown in Figure 14, well-mixed dry sulfur and Martian regolith simulant in the funnel were pushed downward through a nozzle by a rotating auger while sulfur was melted by electric heaters. When mixture arrives at the end of the nozzle the nozzle head controls the flow direction of sulfur cement and builds smooth surfaces

and edges. To increase the inter-layer bonding strength, an interlocking profile is also added to the nozzle outlet to create additional protuberant structure to interlock successive layers.

In this experiment, the rotation friction changes frequently and is not predictable due to the bridging effect which is caused by coarse aggregate in cement. To automatically counteract the bridging effect during the extruding process, a vertical vibration piezo transducer is added to the auger and a horizontal vibration piezo is added to the end of the extruder in Figure 14. These two piezo actuators partially alleviate the friction problem during extrusion process.

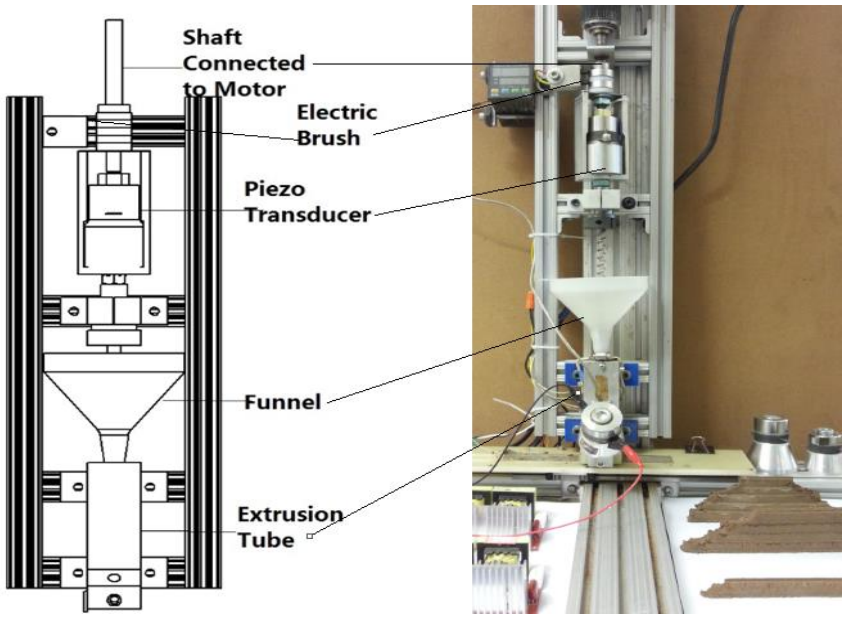

Figure 14: Schematic of Mini-size auger extruder

However, the surface quality of extruded parts during this process was not always acceptable, as some parts were smooth while others had many cracks. Considering this phenomenon, several factors such as heat transfer, hardness of the nozzle's inner wall (which impacts friction with abrasive particles) and shape of the channel of nozzle head were analyzed. After cutting and polishing some failed samples (Figure 15) it was revealed that the color of the material in the core of the layer is significantly different from the color of the peripheral regions, which indicates that the mixture was not completely melted in the nozzle during the extrusion process. To improve the heating efficiency a comparison experiment was carried out with pre-heating method. Well mixed sulfur and Martian regolith simulant were sealed and pre-heated in a water bath at 98 C for half an hour which dramatically improved the melting efficiency in the extrusion process (Figure 16). In comparison to the heating process from room temperature to melting temperature of sulfur at 115 C, pre-heating method further reduces the extrusion friction and improves the final surface of extruded Martian sulfur concrete.

Figure 15: Extruded sample with crack on surface

Figure 16: Extruded sample with smooth surface

Although the surface quality of the extruded layer has been optimized, the rotation torque has been excessive. Also, when the auger was taken out from the nozzle after approximately 50 hours of work, the auger blade was almost totally worn out, especially in the case of working with low temperature mixture on the upper part of nozzle. Note that while the original auger blade had width of 3mm, the worn-out blade width is only 0.3mm, as shown in Figure 17. Hard aggregate in regolith simulant is the primary cause of abrasion. Almost half of the content of the regolith simulants used is silicon dioxide whose hardness is between 4500~9500 MPa.

Figure 17: Auger worn-out during experiment

2.3 A vibration valve extruder

Our lab has previously developed a vibration valve extrusion method for hydraulic concrete. As shown in Figure18, the concrete is pushed by a plunger through a pipe with the valve. The idea behind the vibration valve is that the friction with the material can be changed by using a "friction element," as shown in Figure 18. The abrasive particles of the concrete would be stopped by the friction when they come through the blades of the friction elements. The friction is neutralized when vibration is applied to the friction element, letting the abrasive particles flow

away. The concrete flow rate is controlled by changing the vibration frequency and intensity of the friction element.

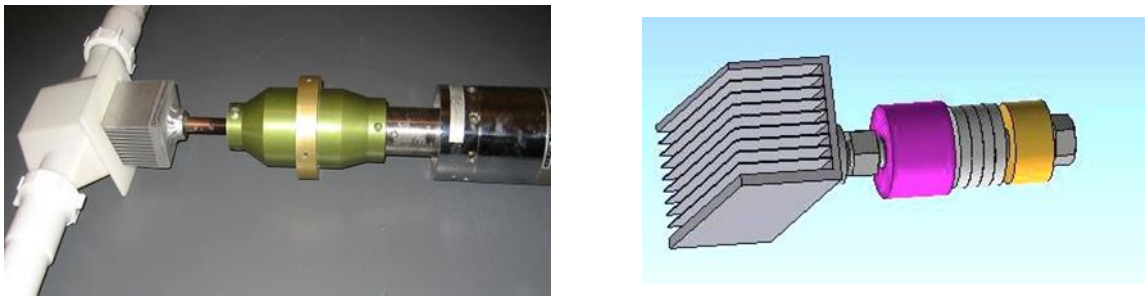

Figure 18: Application of vibration valve extruder on hydraulic concrete

For sulfur concrete, a variation on this process must be developed. As shown in Figure 19, the new vibration valve extruder includes a mixing system, extruding system, forming system, and curing system. Unlike hydraulic concrete, sulfur concrete must be kept near the melting temperature of sulfur throughout the process. First, the mixture of sulfur and aggregate is poured into the mixing tank, and heated with a flexible heater until melted. The friction element is connected to a vibration motor, which has eccentric wheels on both sides. When the vibrator is turned on, the abrasive particles which are stuck between the blades are broken away and pushed downwards into the forming chamber. The accumulator in the forming system is made of high-temperature silicone rubber that releases pressure in order to avoid a blockage in the forming chamber. The reducer is designed to exert pressure on the sulfur concrete to remove porosity.

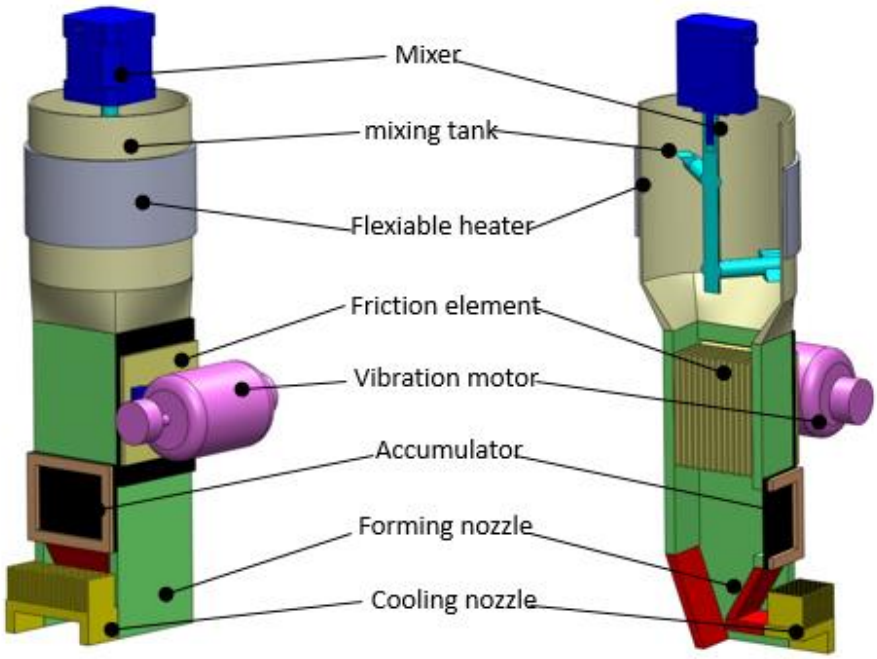

Figure 19: Principle of vibration valve extruder

2.4 A novel extruder

To ensure durability, stability and reliability of sulfur concrete extruder, a new universal concrete extruder was invented by the PI. As shown in Figure 20, the new extruder is built up by multiple propelling blades, forming system and curing system. Different from the previous auger extruder, the double-propellers at the end of the nozzle provides the main extruding force, while the multiple blades at the upper stages push cement downward against the resistance of extrusion tube. In addition, the mixture is completely melted before entering the nozzle and as such its friction with the walls of the nozzle is far less than the mixture at the room temperature or even pre-heated mixture. Besides these two alterations, an aluminum extender end which also acts as heat sink is added to the outlet of the nozzle to accelerate cooling. Fuzzy logic control is employed to control the DC motor that rotates the propellers. This control system is proven to be more consistent and accurate.

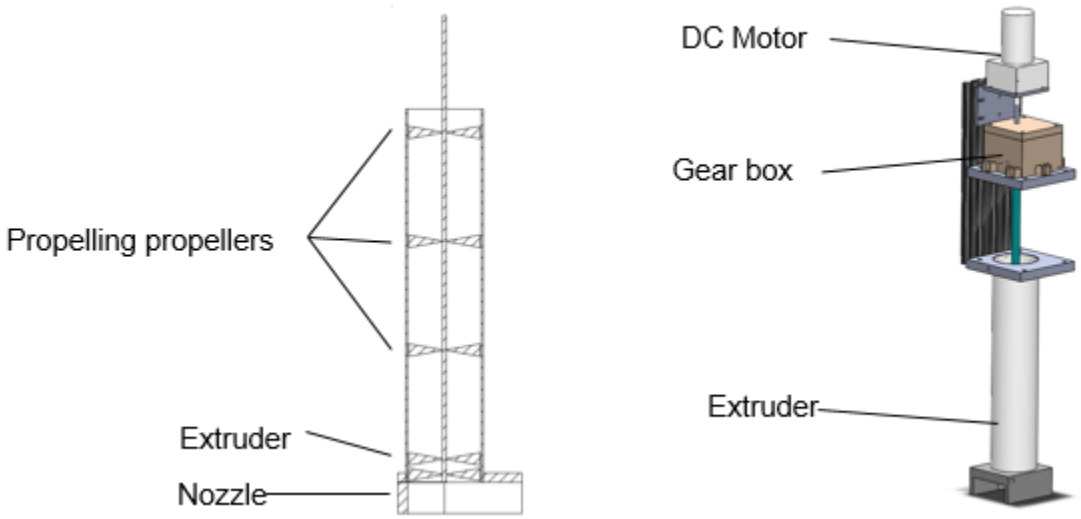

Figure 20: Schematic of multiple propellers extruder

To test the properties of the sulfur concrete extrusion process, a simple linear motion platform was developed prior to using the 6-axis robot. As shown in Figure 21, the linear motion platform contains a linear rail system, a belt drive system and control unit. Figure 22 is a three layers extrusion sample made by this platform.

Figure 21: Linear test bench

Figure 22: Three layers extrusion sample

2.5 Improving the new extrusion system

Several extrusion experiments have been carried out with the multiple propellers extruder and the influences of temperature, sulfur proportion, extrusion speed and linear speed in different stages are investigated for each experiment. However, the volume of extrusion tube limits the maximum length of extrusion. To study the extrusion in a continuous process, an improved extruder with a reservoir and feeding system has been developed. (Figure 23)

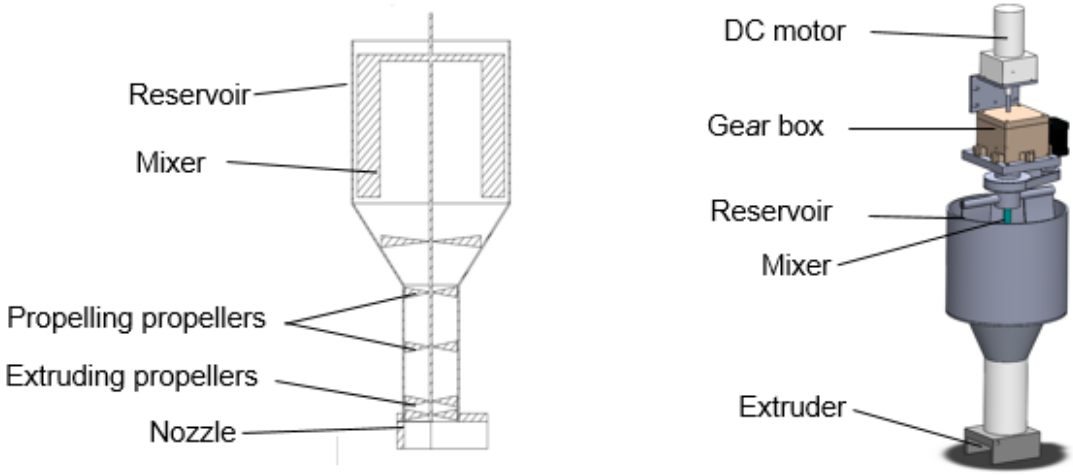

Figure 23: Improved multi propellers extruder

Figure 24 shows the new extrusion system concept where raw aggregate and dry sulfur are transported into a hopper installed on top of the nozzle. The hopper heats and mixes it at 150 C. When the sulfur concrete mixture in the reservoir is depleted the robot can move the extrusion system along with its reservoir under the hopper to the refill station.

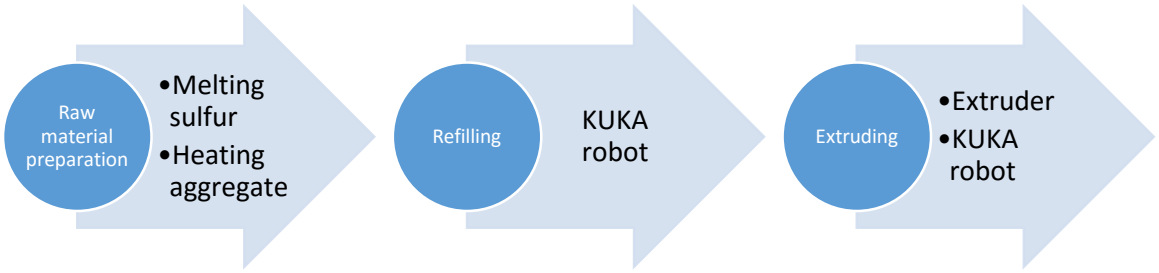

Figure 24: The construction process

3. Research on sulfur concrete

3.1 Sulfur concrete

Sulfur concrete is a composite construction material composed of elemental sulfur and aggregates, such as sand and crushed rocks. Compared to regular Portland cement which reaches the maximum strength only after 28 days of curing, sulfur cement reaches its final strength within several hours. The humidity and temperature of the external environment do not influence the strengthening process at all. The compressive strength of final sulfur concrete product reaches up to 50MPa which is comparable with high strength concrete. Its excellent resistance to acid and salt environments as well as its superior water tightness makes sulfur concrete an ideal construction material for marine construction [3] and a wide range of other applications.

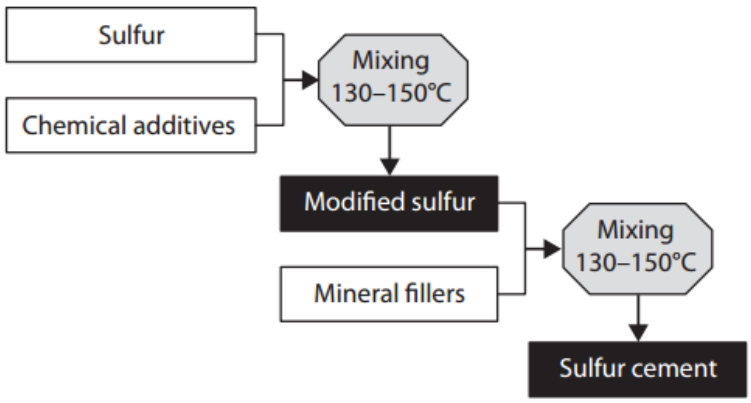

Figure 25: Sulfur cement production process

However, due to the variations of elemental sulfur crystal, sulfur cement displays great expansion and shrinkage rate in thermal cycles. According to the report, the daily temperature differences on Mars and moon are about 100C and 300C, respectively. Therefore, it is essential to modify the property of elemental sulfur to overcome expansion/retraction issue. Nimer [5] tried to add chemical additives, such as dicyclopentadiene, styrene or acrylic acid, to elemental sulfur to plasticize sulfur in its polymeric form. As shown in Figure 25, sulfur and chemical additives are melted and mixed at the temperature range from130C~150C for more than 3 hours.

Then, modified sulfur is mixed with mineral fillers at the same temperature until the sulfur is completely plasticized [3]. The availability of comparable additives on Moon and/or Mars should be studies to evaluate the possibility of making such modifications to sulfur.

In the sulfur extrusion process, the viscosity and surface tension of mixture are considered as two main factors. Blight [6] approves that elemental sulfur and DCPD react in an exothermic reaction, which would increase the temperature of reaction and make the sulfur tremendously viscous. Allan and Neogi [7] also carried out research on the impacts of heating time and DCPD proportion on viscosity and surface tension of modified sulfur. Both viscosity and surface tension of sulfur with 5 wt% DCP gradually increase with time, while these parameters in sulfur with 20 wt% DCP increase to 2~3 times more after 3 hours heating.

So far, research is concentrated on the extrusion process. Further effort will be dedicated to improve the strength, durability and stability of modified sulfur cement using in-situ materials.

3.2 Research on simulant regolith extrusion process

Martian regolith simulant JSC-Mar1A (aggregate of Martian sulfur cement) and Lunar regolith simulant JSC-1A (aggregate of Lunar sulfur cement) made by Orbital Technology Corporation are chosen in this extrusion experiment. (Table 1) The purity of sulfur powder used in this experiment is higher than 99.0%.

Table 1: Major Element Composition of JSC-Mar1A and JSC-1A

Major Element Composition	Martian regolith simulant JSC-Mar1A	Lunar regolith simulant JSC-1A
Silicon Dioxide (SiO_2)	34.5-44	46.67
Titanium Dioxide (TiO_2)	3-4	1.71
Aluminum Oxide (Al_2O_3)	18.5-23.5	15.79
Ferric Oxide (Fe_2O_3)	9-12	12.5
Iron Oxide (FeO)	2.5-3.5	8.17
Magnesium Oxide (MgO)	2.5-3.5	9.39
Calcium Oxide (CaO)	5-6	9.90
Sodium Oxide (Na_2O)	2-2.5	2.83
Potassium Oxide (K_2O)	0.5-0.6	0.78
Manganese Oxide (MnO)	0.2-0.3	0.19
Diphosphorus Pentoxide (P_2O_5)	0.7-0.9	0.71

Sulfur and regolith may be premixed prior to being poured into the extrusion machine. However, movement and vibration can displace the fine sulfur powder particles, making the mixture less homogeneous. We have therefore devised a method to assure mix consistency. First, sulfur and regolith were thoroughly mixed, and then heated to the melting point of sulfur. The mixture was then cooled down to form a solid lump, which was crushed into fine chunks so each chunk retained the correct proportion of sulfur to regolith. This method creates sulfur-coated regolith particles that are very stable and resist settling back into their components.

Regolith simulants and sulfur were mixed together uniformly, and the mixture was extruded with the parameters shown in Table 2.

Table 2 Materials and Processing Parameters

	Sulfur Concentration (wt%)	Processing Temperature (^{o}C)	Auger Rotation Speed (RPM)	Raw Material Density (g/cm^3)	Sulfur Concrete Density (g/cm^3)
Martian Regolith Simulant (JSC Mars-1A)	40	150	120	1.05	1.86
Lunar Regolith Simulant (JSC-1A)	35	135	60	1.84	2.26

Lunar concrete was heated at 135 ^{o}C, and the auger rotation speed was set to 60 rpm. Martian concrete was heated at 150 ^{o}C, and the auger rotation speed was set to 120 rpm. The relatively slow auger speed for lunar regolith is due to the high friction of the simulant, and its lower extrusion temperature is due to its increased time in contact with heating elements. The temperature for Martian regolith, in contrast, is higher because the material moves faster through the barrel.

Upon extrusion the nozzle is moved linearly at a constant speed to produce straight extrudates as shown in figures 26 through 29.

For both materials, the auger experiences a changing frictional force, as noted earlier. Lunar concrete has a significantly higher friction than Martian concrete, leading to generally better quality for Martian samples.

Smoothly extruded layers with smooth surfaces and sharp edges were obtained with Martian sulfur concrete (Figure 26). A rougher layer was obtained for lunar sulfur concrete (Figure 27) due to intermittent nozzle flow caused by the high friction. Short walls with multiple layers were built with both materials (Figure 28 and Figure 29). They are fairly strong, difficult to break or separate layers by hand.

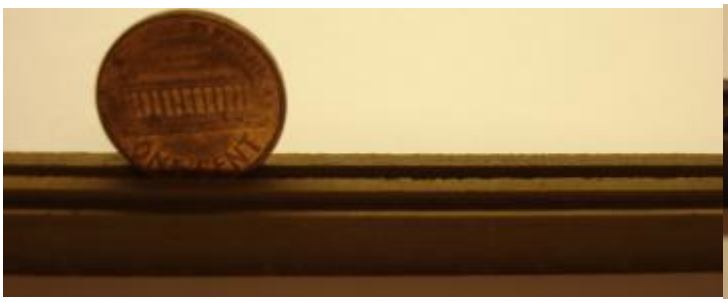

Figure 26: Single layer of Martian sulfur concrete

Figure 27: Single layer of lunar sulfur concrete

Figure 28: Multiple layers wall of Martian sulfur concrete

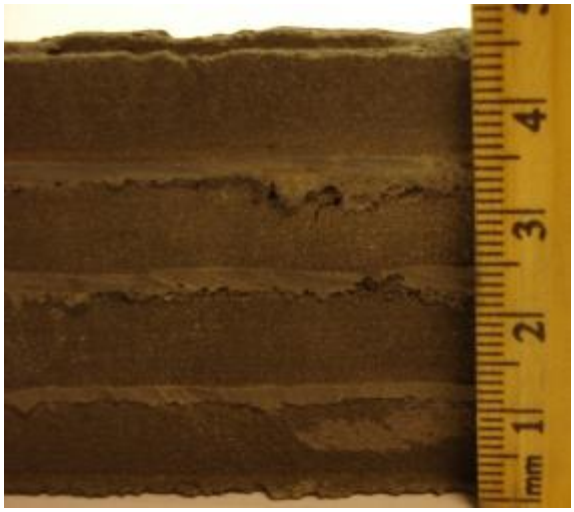

Figure 29: Multiple layers wall of lunar sulfur concrete

Due to the interactions among the auger surfaces, abrasive particles, and nozzle wall, the auger experiences a changing friction. For the Martian simulant JSC-Mars1A, the powder is loosely bonded together (Figure 30), and can be pulverized into fine grains by finger pressure. In the case of the lunar simulant JSC-1A (Figure 31), the particles are hard and abrasive. This makes JSC-1A have poor friction characteristics, for it flows into the gap between the auger blade and the nozzle wall, slowing the rotation of the auger. If the lunar regolith could be ground into a flour-like powder, the extrusion process might be smoother.

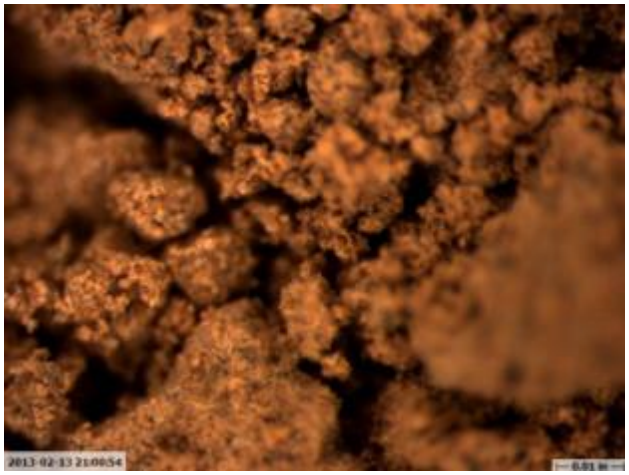

Figure 30: Crushed JSC Mars-1A simulant (×92)

Figure 31: Sifted JSC-1A Lunar regolith stimulant (×92)

The compression effect during extrusion is obvious in the case of JSC-Mars1A. The density of JSC-Mars1A is 1.05g/cm^3 alone versus 1.86g/cm^3 for the extruded part, whereas for JSC-1A these values are 1.84g/cm^3 and 2.26g/cm^3, respectively. For a solid mixture without any compression, the mixed density can be given as follows:

The calculated densities are 1.30g/cm^3 for the Martian mixture and 1.89g/cm^3 for the lunar mixture. The measured densities for the extruded parts are 1.86g/cm^3 and 2.26g/cm^3. The compression ratios are therefore 1.42 and 1.19 for Martian concrete and lunar concrete, respectively.

The surface smoothness of Martian sulfur concrete is better than that of lunar sulfur concrete due to the better wettability of sulfur to JSC-Mars1A. The flour-like Martian simulant holds sulfur tightly, and the melted paste does not flow freely as it does in the case of lunar concrete.

The material feeding rate must be proportional to the extrusion rate, for if the feeding rate is higher than the extrusion rate, the nozzle will overflow; if the feeding rate is lower than the extrusion rate, the product will be discontinuous. The ideal system would incorporate feedback to properly match these two speeds.

As an initial forming experiment, parts were extruded with Martian regolith because of its superior plasticity. A 3D model of an incomplete circular wall was built in SolidWorks (Figure 32). Next, based on the dimensions of the nozzle head, the model was divided into layers with a thickness of 3/8 inch and converted into tool paths, as shown in Figure 33. Finally, using pre-heating and anti-bridging vibration, an incomplete circular wall (shown in Figure 34) was built by the CC machine. Subsequently, a Martian regolith dome was constructed, as shown in Figure 35.

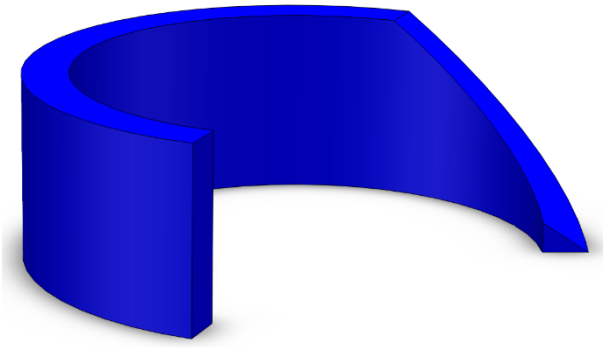

Figure 32: 3D model of incomplete circle wall

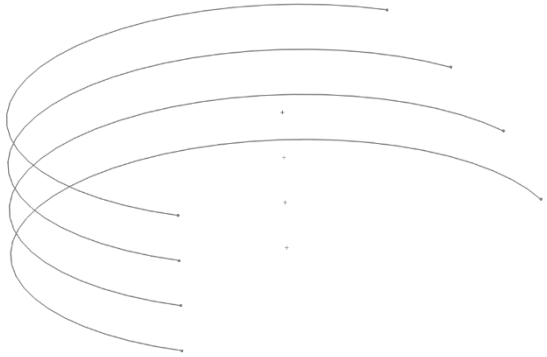

Figure 33: Tool path

Figure 34: Incomplete circle wall

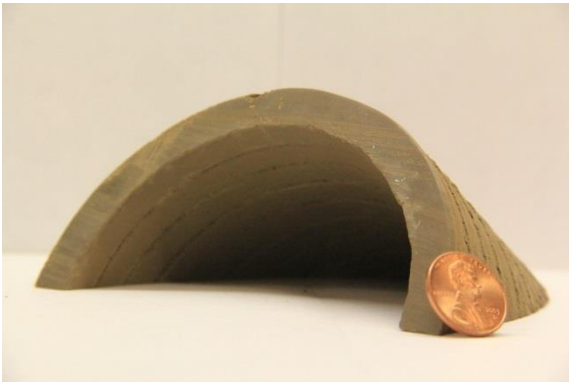

Figure 35: Martian regolith dome

3.3 Research on sulfur concrete extrusion process

The performance of the extrusion process varies considerably with different proportions of sulfur. When sulfur level is high, the sulfur cement has low viscosity, which makes it easy to extrude, however, low viscosity also causes the problem of high slump and leakage. On the other hand, low proportion sulfur cement lowers the slump, but low viscosity mixture is hard to extrude as it always sticks to extrusion barrel and propellers.

To explore the significant factors that may influence the extrusion process a 2k factorial experiment is designed based on temperature at different stages, proportion of sulfur and extrusion/moving speed as shown in Table 3.

Table 3: A 2k factorial design on extruding process

Factors	Level -	Level +
A. Sulfur Proportion	30 wt%	35 wt%
B. Sulfur Concrete Temperature	140 C	150 C
C. Extruder Temperature	150 C	160 C
D. Extrusion Rate	3 kg/min	5 kg/min

This experiment shows that the extruder temperature and extrusion rate have little effect on the extrusion process, but only if the sulfur concrete does not stick to inner wall of the barrel and flows to the working zone of next propellers smoothly by the force of gravity.

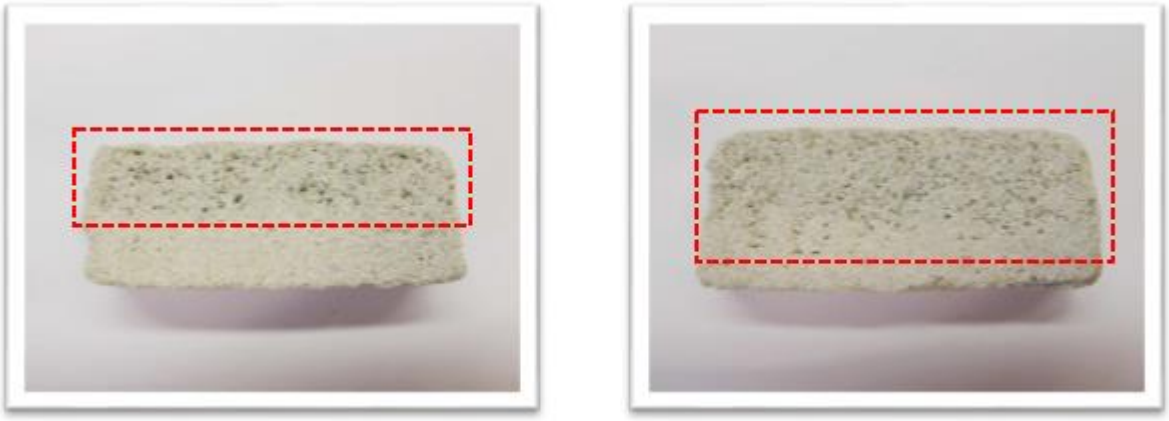

(a) Sample built in 140C *(b) Sample built in 150C*

Figure 36: Extrusion process with different sulfur cement temperature

In the experiment, it is obvious that the mixture at 150C has less viscosity and better flow rate. Some extrusion cross-sections are observed under optical microscope, as shown in Figures 36 and 37. The porous structure is more equally distributed in the sample built at 150 C; while most of porous structure is in the upper part of the extrusion sample built at 140 C. It is deduced that sulfur in mixture at 150C had a longer time for curing process and sank into the lower region by

gravity. The uneven sulfur content between upper and lower parts may considerably reduce the strength of multi-layer structures.

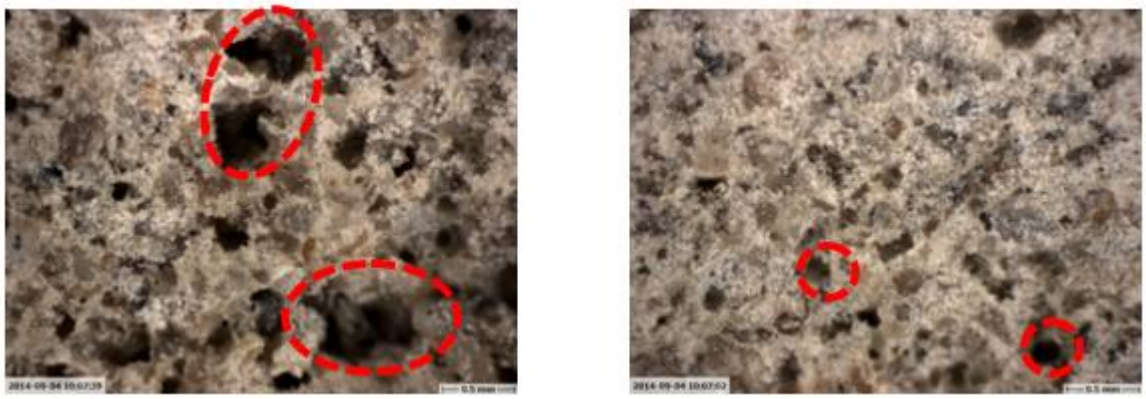

(a) Sample built in 140C *(b) Sample built in 150C*

Figure 37: Extrusion process with different sulfur cement temperature

Sulfur plays the role of binder in solidified sulfur cement and lubricant during the extrusion process. By increasing sulfur proportion, the sulfur cement viscosity decreases considerably hence liquidity increases. Compared to 30 wt% sulfur concrete samples, the 35 wt% sulfur concrete is saturated with sulfur and porosity level is not so significant. However, the plasticity of 35 wt% sulfur cement in the molten state is less than that of 30 wt% sulfur concrete as it may be concluded from the rounded shape at both edges and top surface of the sample on the right in Figure 38. This necessitates adding side trowels behind the nozzle to keep the extruded surface smooth.

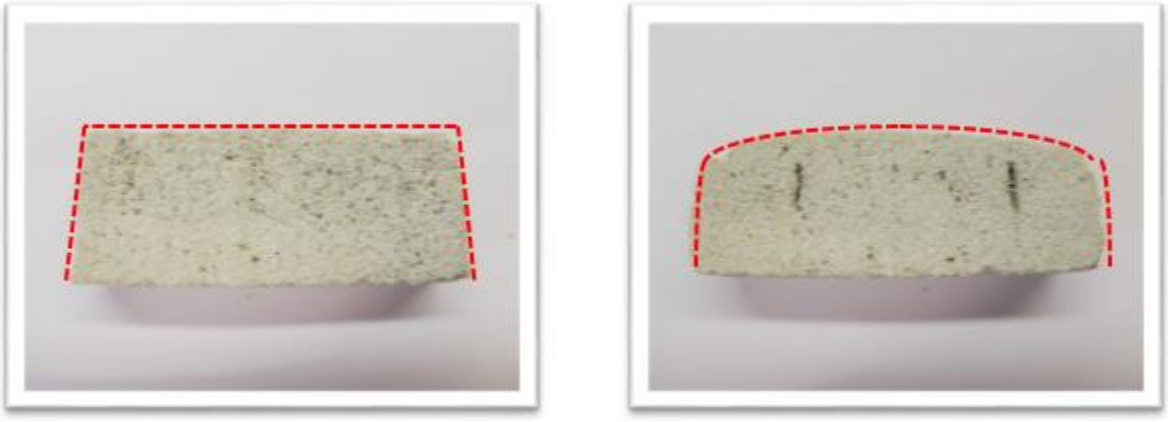

(a) Sample with 30wt% sulfur *(b) Sample with 35wt% sulfur*

Figure 38: Extrusion process with different mixture temperature

From Figure 39 it is clear that the microscopic characteristics of two samples are different. The sizes of microscopic holes in the two samples differ greatly. The porosity directly impacts the strength of the structures made with these materials. By choosing the appropriate weight ratio for sulfur in the mixture the porosity can be decreased.

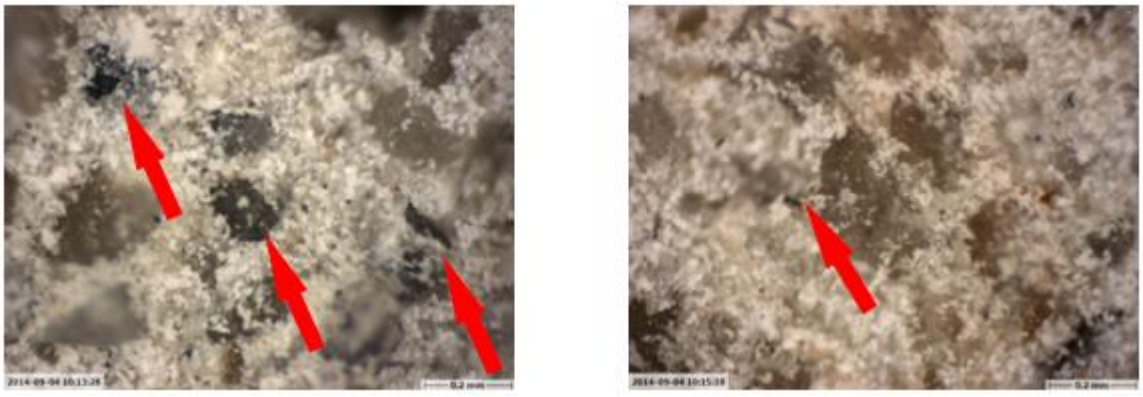

(a) Sample with 30wt% sulfur *(b) Sample with 35wt% sulfur*

Figure 39: Extrusion process with different mixture temperature

4. Construction with KUKA 6-axis robot

4.1 Operation of KUKA 6-axis robot

For the construction of full-scale structures a 6-DOF industrial robot is being used in the Contour Crafting Laboratory. The KUKA robot consists of six rotational actuators which provide six degrees of freedom within the robot's workspace. As explained earlier, one of the most important advantages of using such robot over a gantry robot is that for any type of structure the gantry has to be designed in such a way that the structure falls within the gantry's workspace, that is, the gantry always has to be larger than the structure; but a joint robot like the KUKA robot used in this experiment can be mounted on top of a rover to eliminate the size restriction.

Figure 40: KR150 KUKA robot

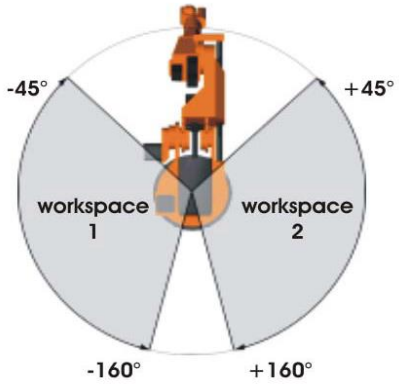

Figure 41: Working zone

Figure 40 shows the KUKA robot and Figure 41 shows the axis-specific workspace for the actuator A1. The rotational range of each actuator (A1 to A6) is limited which in turn limits the total workspace of KUKA robot. Each layer in the construction must then be carefully arranged so that it falls within KUKA's workspace. The robot can handle up to maximum force of 1.5 KN exerted to its TCP (Tool Center Point).

Table 4: KUKA KR150L ROBOT

Voltage	480V	
Capacity	150KG	
Repeatability	±0.12mm	
Horizontal Reach	2410mm	
Vertical Reach	2700mm	
Axis	Robot Motion Range	Robot Motion Speed
1-Axis	±185°	110 °/s
2-Axis	+93 to -40	110 °/s
3-Axis	+155° - 119°	110 °/s
4-Axis	±350°	170 °/s
5-Axis	±125°	170 °/s
6-Axis	±350°	238 °/s

4.2 Construction of multi-layers walls and half-domes

For construction of vertical walls linear motion is generated by the robot. The speed of the linear motion is adjusted so that it is synchronized with the feeding rate that the reservoir can provide. When the robot shifts to subsequent layer, the moving direction of end nozzle has to be reversed, which is executed by using the KUKA's ending flange rotational degree of freedom. Figure 42 shows the KUKA's TCP path for vertical wall and dome constructions.

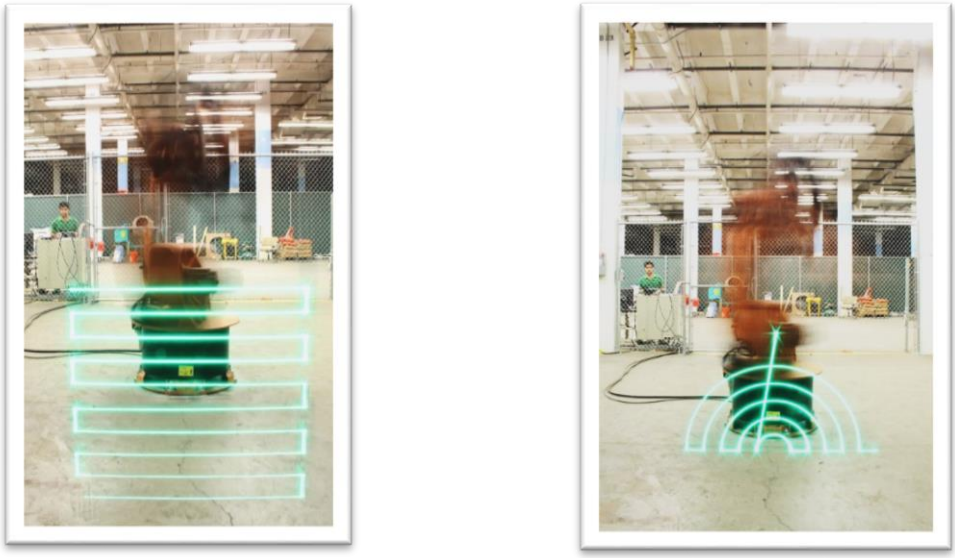

Figure 42: Tool path of straight wall and half dome taken with long exposure camera

Building 3D dome structures requires following more complicated pathways. The starting layer position in the global coordinate system is selected in such a way that the whole dome structure falls completely within KUKA's workspace. Different shapes and geometries can be selected for the dome-like structures. One of the candidates for the 3D dome structure is depicted in Figure 43. For this structure, inclined layers are built consecutively such that each layer has a slight angle with respect to the horizontal floor. This angle has to be small enough so that the support for each layer is assured by the previous layers.

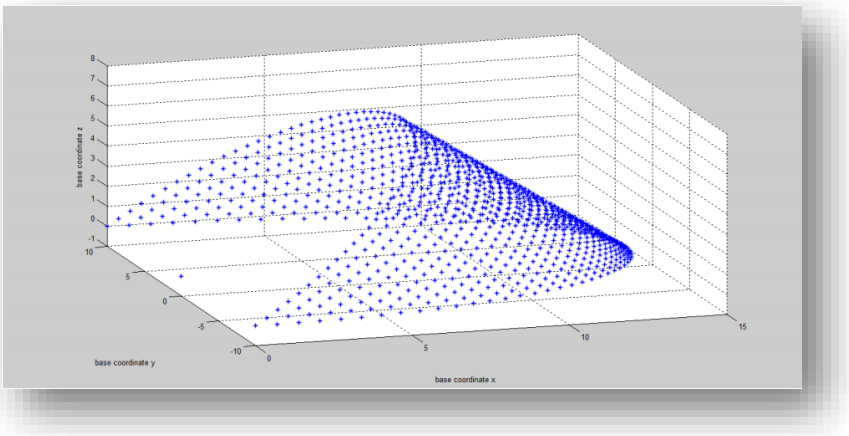

Figure 43: Tool path coordinates for dome-like structure

Other patterns to achieve dome-like structures are also being considered. For instance patterns which inherit geometric advantages of domes and cones can be used to build optimum structures by horizontal, rather than inclined, layering method. We plan to investigate relevant merits of

different geometric structures in order to determine the optimum shape such that each layer has sufficient support and the whole structure shows robust stability and strength.

Theoretical Analysis of Deformation

Molten sulfur concrete is similar to fresh hydraulic concrete and can be approximately analyzed using Bingham model.[4] In this model, molten sulfur concrete that shear stress is less than yield stress are able to stand without flowing under its own mass. The one dimensional law of Bingham model is:

$$\tau = \mu_p \dot{\gamma} + \tau_0 \qquad (1)$$

where τ Yield stress

μ Plastic viscosity

$\dot{\gamma}$ Shear stress

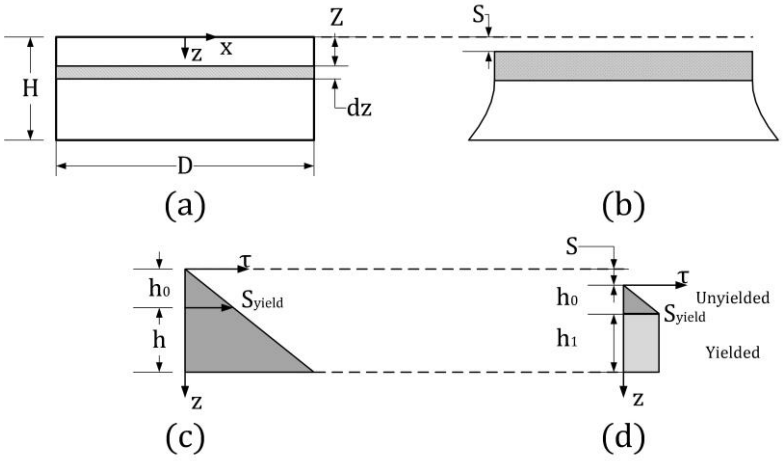

(a) Initial shape (b) Final shape (c) Initial stress distribution (d) Final stress distribution

Figure 10: Deformation of slump process

The molten sulfur concrete can keep the shape without flowing and support the material above until the shear stress is larger than the yield stress. To study the deformation of extrusion, a two-dimension model is built.[5] Figure 10(a) shows the cross section shape of extrusion. At the height of z, the pressure p(z) can be calculated as,

$$p(z) = \frac{F}{S} = \frac{\rho g z D}{D} = \rho g z \qquad (2)$$

Where H Extrusion height

z Axial position

ρ Material density

g	Gravity
D	Width of extrusion

Assume the maximum shear stress at the position of z is half of the pressure. Then, the maximum shear stress τ(z) can be calculated as,

$$\tau(z) = \frac{1}{2}\rho g z \qquad (3)$$

The shear stress distribution of extrusion before deformation can be illustrate as Figure 10(c). The material on top of the boundary z_0 where the shear stress value is less than the yield value keeps the same shape and remains as a rigid body. While, the material below this point yields as shown in Figure 10(b). And, Figure 10(d) shows the shear stress distribution after the slumping process is complete.[6]

Since the top material remains undeformed in the slumping process, only the material underneath is discussed in the following. In the slump process, the material under the boundary flows until the shear stress reduce to the yield value.

Assumption:

1) The material above the boundary keeps the same shape and remains as a rigid body.
2) The boundary of yield and un-yield keeps a flat surface and sink down as the material underneath flows.
3) The yield material flow outward horizontally along the x axis.
4) The volume of the yield material stay unchanged.

After the deformation, the initial height of unyeild material h_0 remains the same, but the initial height of yield material decrease to the final height h_1. This change is illustrated in Figure 10(d). [7]

The final height of yield material h_1 can be calculated by intergrading dz_1 as

$$h_1 = \int_{h_0}^{H} dz_1 \qquad (4)$$

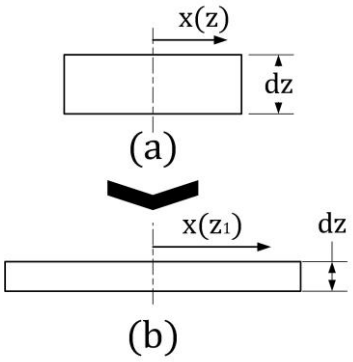

(a) An element before deformation (b) The element after deformation

Figure 11: Deformation process of an element

Since the volume of the yield material stay unchanged, the later thinness of dz_1 can be calculated as,

$$dz_1 = \frac{x(z)}{x(z_1)}dz \qquad (5)$$

When the slump is completed, the shear stress value of yield material become identical S_{yield}.[8] Since the weight of material above the x(z) remains the same, the relationship of original element thickness x(z) and the deformed element thickness x(z1) can be calculated as,

$$\tau(z)x(z) = \tau(yield)x(z_1) \qquad (6)$$

Substitute equation 5 and equation 6 into equation 4:

$$h_1 = \int_{h_0}^{H} \frac{S_{\text{yield}}}{\tau(z)}dz \qquad (7)$$

Then, substitute equation 3 into equation 7:

$$h_1 = 2\int_{h_0}^{H} \frac{S_{\text{yield}}}{\rho g z}dz \qquad (8)$$

Last, calculate this integration and get:

$$h_1 = \frac{2}{\rho g} ln\left(\frac{H}{h_0}\right) \qquad (9)$$

The slump value can be calculated by:

$$S = H - h_0 - h_1 = \text{H} - \frac{2}{\rho g}\left[S_{\text{yield}} + ln\left(\frac{H}{h_0}\right)\right] \qquad (10)$$

Finite Element Analysis

A finite element analysis for the deformation behavior of sulfur concrete immediately after extrusion was conducted by using the finite element code. The details of analysis are given below.

a) Description of constitutive model and selection of material parameters

Mohr Coulomb Plasticity model, provided within the material library of ABAQUS, was selected for the description of the rheological behavior of uncured sulfur concrete right after extrusion. According to Mohr-Coulomb model, failure in the element begins when the shear

stress in a material reaches a threshold that depends linearly on the normal stress in the same plane. By plotting Mohr's circle for states of stress at failure in the plane of the maximum and minimum principal stresses, the failure line is defined as the best straight line that touches these Mohr's circles as shown in Figure 12 [9].

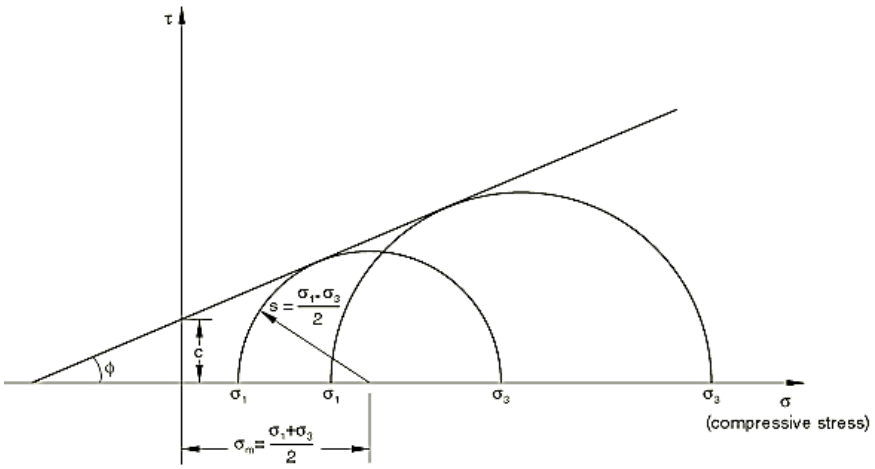

Figure 12: Mohr-Coulomb failure model [9]

According to figure 12, the Mohr-Coulomb model is defined by [9]

$$\tau = c - \sigma \tan \phi \qquad (11)$$

Where σ would have a positive sign in tension and a negative sign in compression. In Equation (11) ϕ is the friction angle and c is the cohesion of the material. With some manipulation in Equation (1), the Mohr-Coulomb model can be written as

$$s + \sigma_m \sin \phi - c \cos \phi = 0 \qquad (12)$$

This model can also be written in the general form as:

$$F = R_{mc} q - p \tan \phi - c = 0 \qquad (13)$$

Where

$$R_{mc}(\Theta, \phi) = \frac{1}{\sqrt{3} \cos \phi} \sin\left(\Theta + \frac{\pi}{3}\right) + \frac{1}{3} \cos\left(\Theta + \frac{\pi}{3}\right) \tan \phi \qquad (14)$$

The essential components of the Mohr-Coulomb model are described below:

- Friction angle: In Equation (11-14), ϕ is the friction angle which is the slope of the Mohr-Coulomb yield surface in the $p\_R_{mc}q$ stress plane (see Figure 13), which is commonly referred to as the friction angle of the material and can depend on temperature and predefined field variables.

- Dilation angle measured in the $p\_R_{mc}q$ plane at high confining pressure and can depend on temperature and predefined field variables.
- Cohesion: In Equation (11-14) c is the cohesion of the material.

The geometry of the yield surface in the deviatoric plane is controlled by the friction angle ϕ as shown in Figure 13. The range for friction angle variation is from $0 \leq \phi < 90$. In the case of $\phi = 0$, the Mohr-Coulomb model reduces to the pressure-independent Tresca model with a perfectly hexagonal deviatoric section. In the case of $\phi = 90$ the Mohr-Coulomb model reduces to the "tension cut-off" Rankine model with a triangular deviatoric section and $R_{mc} = \infty$ [9].

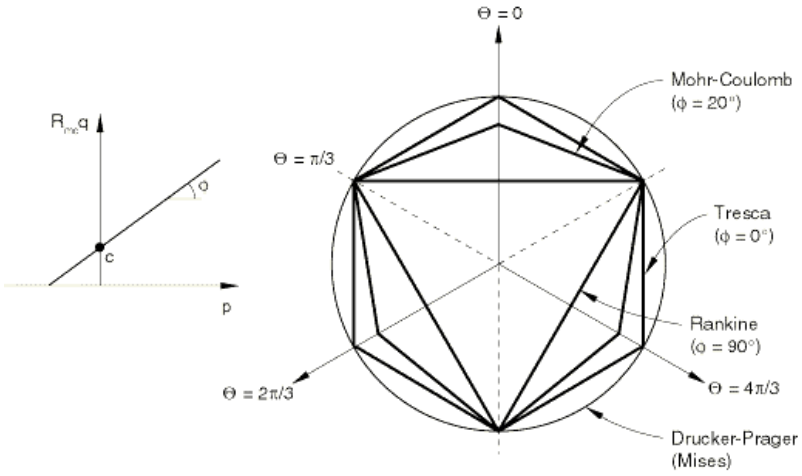

Figure 13: Mohr-Coulomb yield surface in meridional and deviatoric planes [9]

b) Geometry and boundary conditions

The geometry of the specimen is shown in Figure 14. Only one half of the specimen could also be modeled for the analysis to get the results since the deformation analysis of the concrete has axisymmetric nature. The specimen was meshed using four-node axisymmetric elements. The surface beneath the specimen was modeled as a rigid body with friction interaction with the model.

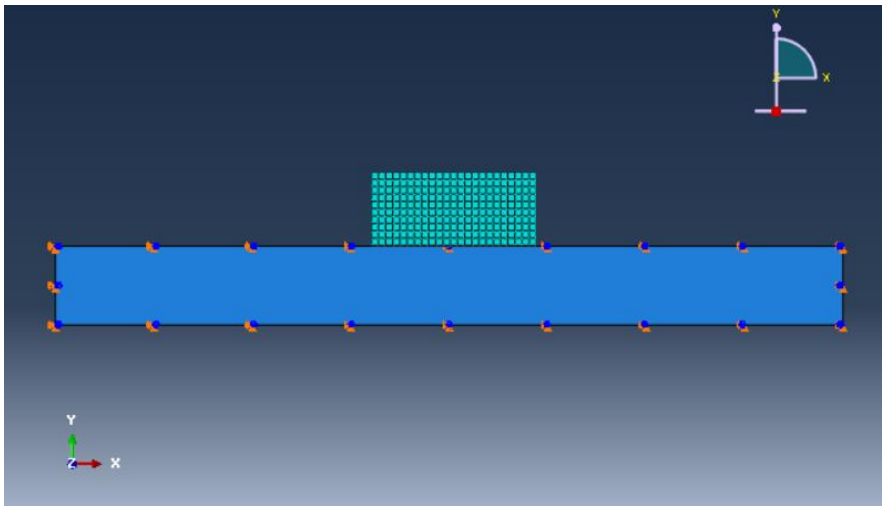

Figure 14: The geometry of the specimen and the initial mesh used to implement the finite element analysis.

c) Numerical results and a comparison with the experimental data

The relative geometrical deformation from the FEA model was obtained and compared to the experimental results (Figure 15, 16). By changing the viscosity in each experiment and using an iterative recursive curve fitting method, we are able to obtain an FEA model for uncured sulfur concrete which can predict the deformation of the extruded mixture as a function of viscosity.

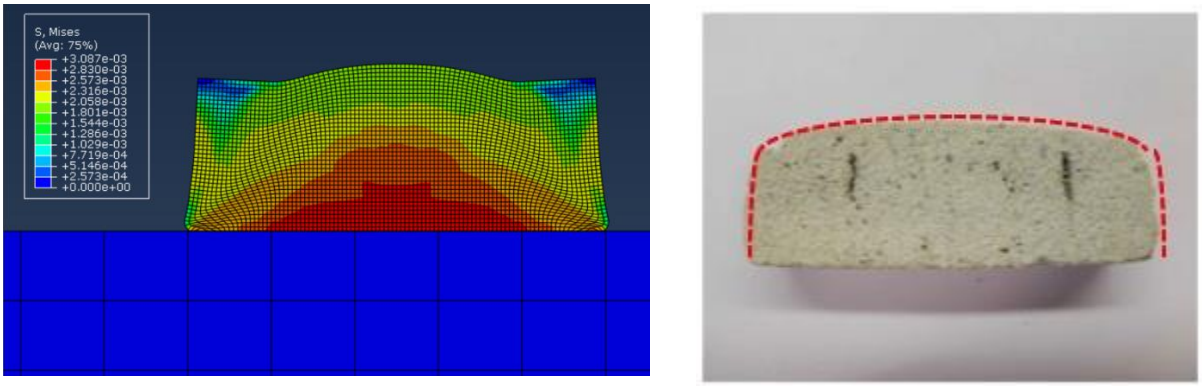

Figure 15: The Mohr-Coulomb based FEA model and the extruded sample 35%wt

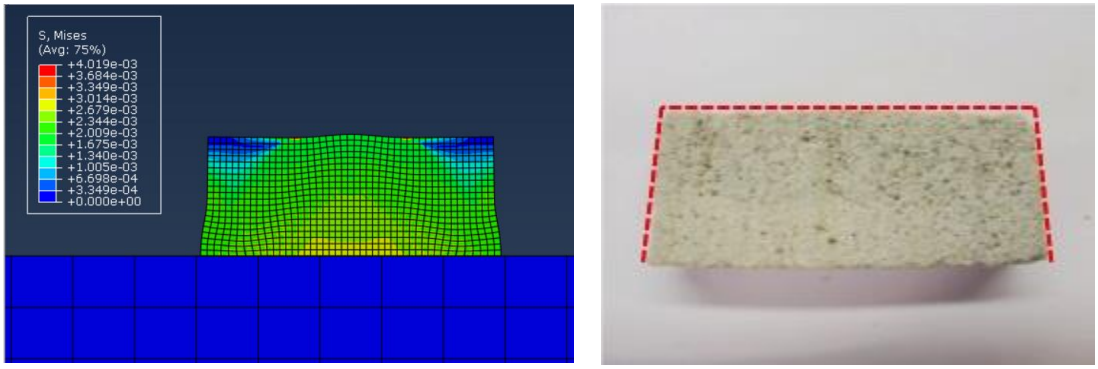

Figure 16: The Mohr-Coulomb based FEA model and the extruded sample 30%wt

Figures 15 and 16 show the FEA models versus the experimental samples. The essential parameters in the Mohr-Coulomb model is different for the two samples with different sulfur contents. The appropriate friction coefficients between the samples and the base were found by comparing the experimental results with the FEA results so that the friction coefficients were in the best agreement between the predicted and experimental deformation patterns.

6. Conclusion

Experimental samples of sulfur concrete were fabricated using a novel mixer/extrusion system. The mechanism was proven to be durable and stable after more than 500 hours of work. The extrusion experiment showed that the temperature of the mix and proportion of sulfur influenced the final shape of extrusion. Higher extrusion temperature made the samples less porous. Less sulfur in the mix improved the shape and surface of the extrudate but increased the porosity. Relative deformation of different samples with different proportions of ingredients were studied. The experimental results obtained were compared with those found from a FEA analysis. A model based on Mohr Coulomb Plasticity model was used for the FEA calculations. The simulations based on the FEA model closely predict the experimental results and hence show the potential applicability for improving the deformations of the sulfur concrete extrusion process.

Reference

[1] A.-M. O. Mohamed and M. El-Gamal, *Sulfur concrete for the construction industry: a sustainable development approach*. J. Ross Publishing, 2010.

[2] B. Khoshnevis, M. Bodiford, K. Burks, E. Ethridge, D. Tucker, W. Kim, H. Toutanji, and M. Fiske, "Lunar contour crafting—a novel technique for ISRU-based habitat development," *Autom. Constr.*, vol. 13(1), no. January, pp. 5–19, 2004.

[3] P. Bartos, *Fresh concrete: properties and tests*. Elsevier, 2013.

[4] W. R. Schowalter and G. Christensen, "Toward a rationalization of the slump test for fresh concrete: comparisons of calculations and experiments," *J. Rheol.*, vol. 42, no. 4, pp. 865–870, 1998.

[5] P. F. G. Banfill, "Rheology of fresh cement and concrete," *Rheol. Rev.*, vol. 2006, p. 61, 2006.

[6] G. Christensen, *Modelling the flow of fresh concrete: the slump test*. ProQuest, 1991.

[7] N. Roussel, "Three-dimensional numerical simulations of slump tests," *Ann. Trans. Nord. Rheol. Soc.*, vol. 12, pp. 55–62, 2004.

[8] N. Pashias, D. V Boger, J. Summers, and D. J. Glenister, "A fifty cent rheometer for yield stress measurement," *J. Rheol.*, vol. 40, no. 6, pp. 1179–1189, 1996.

[9] M.H Yu, "Generalized Plasticity", Springer Science & Business Media, May 20, 2006

[10] ABAQUS (2011) `ABAQUS 6.11 Analysis User's Manual'. Online Documentation: Dassault Systèmes.

[11] Menétrey, Ph., and K. J. Willam, "Triaxial Failure Criterion for Concrete and its Generalization," ACI Structural Journal, vol. 92, pp. 311–318, May/June 1995.

Supplementary references

Khoshnevis, B., Carlson, A., Leach, N., 2012, "Robotic Construction by Contour Crafting: The Case of Lunar Construction," International Journal of Architectural Computing, 10(3) pp. 423-438.

King, P. L., and McLennan, S. M., 2010, "Sulfur on Mars," Elements, 6(2) pp. 107-112.

Squyres, S. W., Arvidson, R. E., Bell, J. F.,3rd, 2004, "The Opportunity Rover's Athena Science Investigation at Meridiani Planum, Mars," Science (New York, N.Y.), 306(5702) pp. 1698-1703.

Blight, L., Currell, B.R., Nash, B.J., Scott, R.A.M., and Stillo, C. (1978) “Preparation and properties of modified sulfur systems,” In New Uses of Sulfur–II, Advances in Chemistry Series,No. 165, p.13-30.

Allan, G. G., and Neogi, A. N., 1970, "Copolymer Characterization by Surface Tension," Journal of Applied Polymer Science, 14(4) pp. 999-1005.

Khoshnevis, B. M. Thangavelu, X. Yuan and J. Zhang, “Advances in Contour Crafting Technology for Extraterrestrial Infrastructure Buildup”, American Institute of Aeronautics and Astronautics – Space Conference, San Diego, September 2013.

`

CHAPTER 3

Fabrication of Inter-locking Ceramic Tiles for Landing Pads and Roads and Fabrication of other Objects using Selective Separation Sintering (SSS)

Introduction

Selective separation sintering (SSS) is a novel powder based additive manufacturing method that can build parts of various scale out of metals, ceramics and composites. This can be done at relatively high speed and with minimal machine complexity. In the SSS process, a thin wall of high temperature separator powder material is deposited within the base material powder to form a barrier on the boundary of each layer. This barrier creates a separation between the part and surrounding material, which allows for the separation of the part from the surrounding powder after sintering is complete. Preliminary experiments with ceramic and metal base materials have demonstrated the feasibility of the approach. The method has also been used with JSC-1A lunar regolith simulant material and a potential in-situ separator powder to produce interlocking ceramic tiles. These tiles may be utilized for planetary construction of various structures including landing pads. We have also demonstrated the capability of the process in producing functional inter-locking metallic parts.

1. Planetary Construction

Planetary construction will provide the basic infrastructure for human outposts and will shield human beings from loose hazardous dust, cosmic radiation and micrometeorites, it is a prerequisite to extraterrestrial colonization. Various approaches have been proposed for planetary construction.

- Concrete construction proposed by T.D. Lin [1] - In this proposal, cement is obtained by high temperature processing of lunar rocks and water is formed by reaction of terrestrial hydrogen with lunar mineral ilmenite.
- Lava tubes reconstruction proposed by F. Horz [2] - Lava tubes formed by volcanic activities measure tens to hundreds of meters with some roofs expected to be thicker than 10 meters. These lava tubes might be reconstructed to serve as human habitats.
- Prefabrication shipped from the earth - Among the prefabrication shipped from the earth, there are concepts such as inflatable habitation which is readily available by inflation [3] and rigid structures which are used as mainframe for constructions [4].
- Construction by Contour Crafting using in-situ material proposed by the author [5,6] – Here a robot extrudes sulfur concrete to build planetary structures by a mixture of sulfur and sand, both extracted from locally, is extruded to build structures in a layerwise fashion.

The minimum guidelines of lunar construction include excavation, transportation, and construction [7]. Though these guidelines are set for lunar construction, the standards also apply to other planetary construction such as Martian construction. The aforementioned construction proposals have the merits of technological feasibility. The first three pose as costly approaches and require a great deal of human labor. Contour Crafting with sulfur concrete is feasible for habitat-like structures on Mars and in shady areas of the moon, but cannot be used for construction of structures such as landing pad which require high temperature resistance.

As the guidelines for planetary construction suggest, transportation counts as a significant factor and in-situ resource utilization (ISRU) is of high priority, which is especially true if the construction site is

`

farther away beyond the moon. The cost of shipping construction materials from earth to the moon, or to Mars will be too high to be economical.

2. Fabrication of smaller scale objects

There is a large set of objects such as tools, components of equipment and spare parts that would be needed for planetary exploration. Some of these may be needed rapidly on-demand. Shipping these objects from earth would be cost prohibitive as well, especially if an inventory of them is to be maintained on the Lunar or Martian outposts.

3. Operating Principle of SSS

SSS (Selective Separation Sintering), a 3D printing technology suitable for small and large scale fabrication, is proposed for planetary fabrication of functional objects such as metallic tools, and construction of structural elements such as interlocking tiles and bricks. In SSS, metals or ceramics may be used where high temperature and impact resistance are expected.

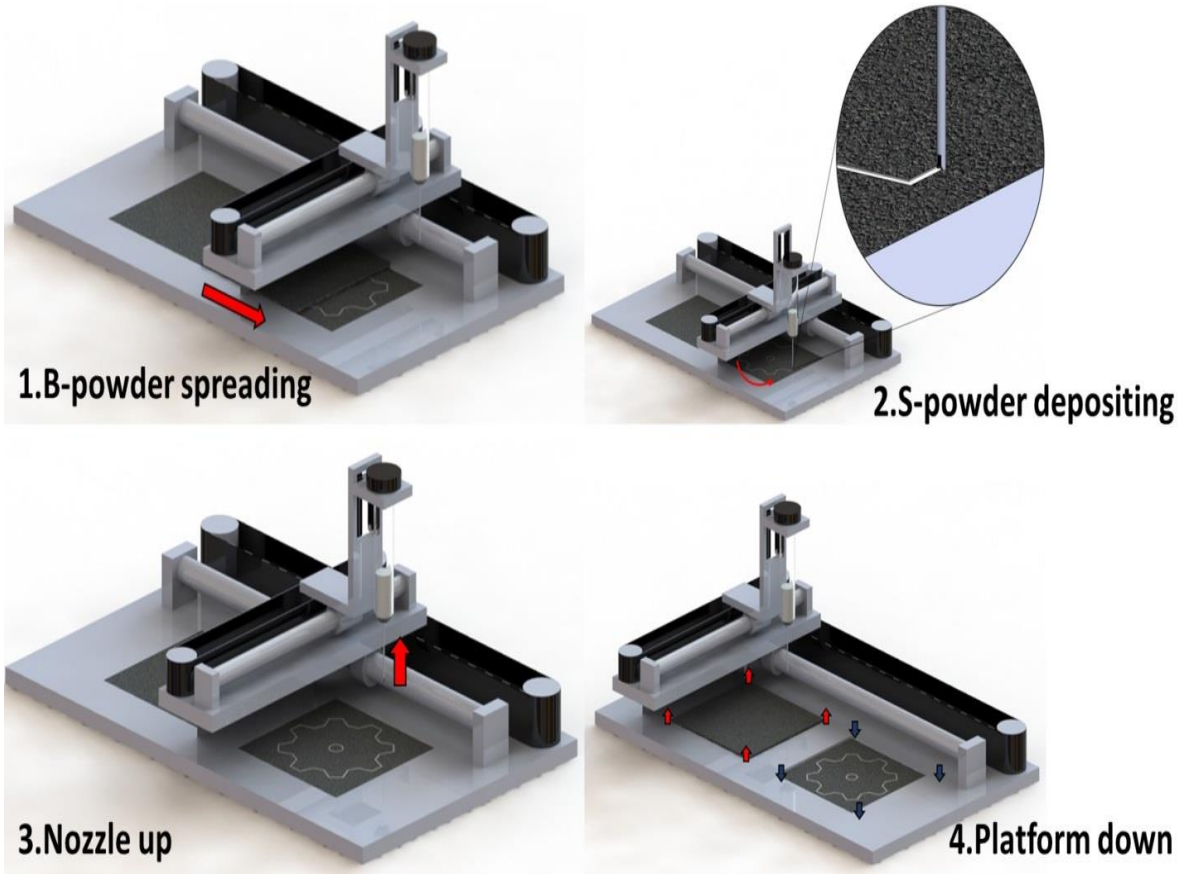

Figure 1 Printing process of SSS. 1. B-powder spread; 2. S-powder deposition; 3. Nozzle raised; 4. Part tank lowered, powder tank raised

`

In the SSS process two kinds of powders are used, the base powder (B-powder), which makes up the final part, and the separator powder (S-powder) which isolates the part from the surrounding B-powder region. The S-powder is selectively deposited into the B-powder layer, forming a barrier around the loose powder that eventually becomes the part. The printed green part is moved into a furnace for bulk sintering. After sintering, the S-powder remains unsintered and loose, making the part easily removable.

The SSS process can be described by the following steps as illustrated in Figure 1:

1. A thin layer of B-powder is spread over the part tank;
2. The S-powder deposition nozzle is lowered into the B-powder layer, selectively depositing the S-powder at the layer boundary;
3. The nozzle is raised to provide clearance for subsequent movement;
4. Raise up the B-powder storage tank and lower the platform for one layer thickness;
5. Steps 1-4 are repeated until all layers are completed;
6. The green part is moved to a sintering furnace.
7. The sintered part is removed from the furnace. The surrounding material is easily removed revealing the final part.

An animation of the SSS process is at:
https://www.dropbox.com/s/gxpo5by2g3f2kgs/SSS%20Animation.avi?dl=0

Successful separation of the part in SSS is dependent on the difference in sintering temperature between the S-powder and the B-powder. As illustrated in Figure 2, the green part in the furnace is heated up to a set sintering temperature. The actual sintering temperature (blue) is carefully chosen so that it is higher than the sintering temperature of the base material (green), but not high enough to sinter the S-powder (red line). As a result, the B-powder becomes well sintered, while the S-powder remains loose.

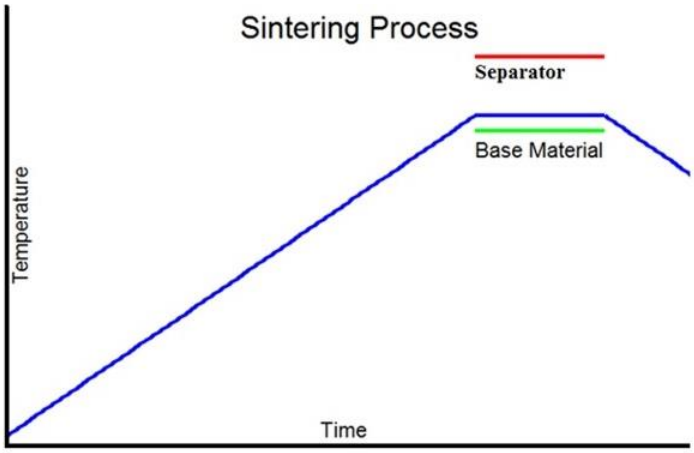

Figure 2 Sintering process for SSS. The blue line represents the heating ramp; the red line represents sintering temperature for the separator and the green line represents the sintering temperature for the base material.

An illustration is provided in Figure 3. The black spheres represent the B-powder and the white spheres represent the S-powder. Figure 3a illustrates the S-powder after deposition into the B-powder layer. In the course of sintering, the B-powder spheres only fuse with the neighboring B-powder spheres to form a solid piece while the S-powder regions are still loose. The part is then separated with ease by removing the loose S-powder.

`

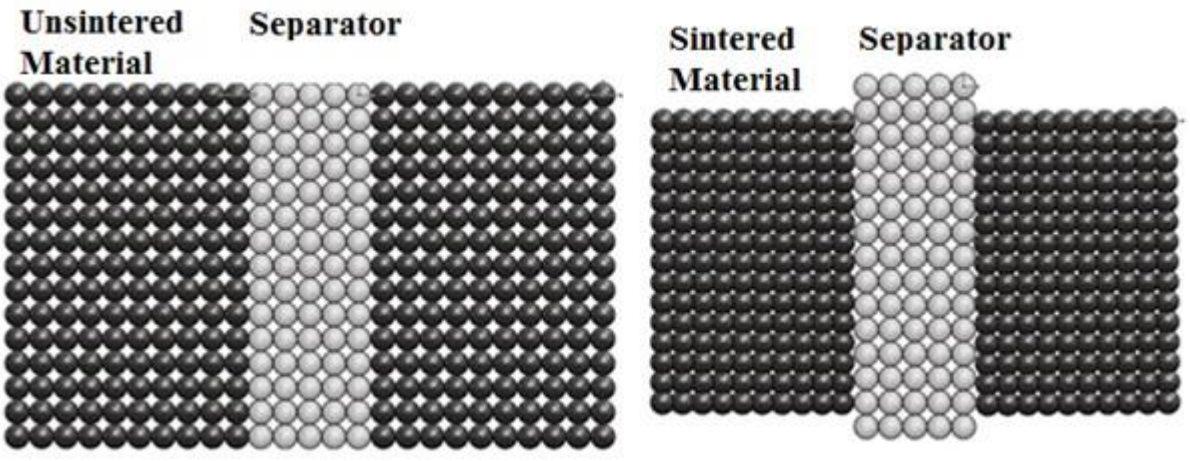

(a) (b)

Figure 3 Illustration for SSS principle (a) before sintering; (b) after sintering – B-material shrinks while S-material does not. (The black spheres represent the building material and the white spheres represent the separator)

A prototype SSS machine was built for experiments. The SSS machine consists of the B-powder spreading mechanism and the S-powder deposition mechanism. As illustrated in Figure 4, the B-powder spreading system includes two tanks that move up and down (z-direction) and a roller or blade for smoothly spreading thin powder layers. During B-powder spreading, the storage tank rises a set distance to provide a sufficient amount of powder. The part tank lowers exactly one layer thickness to receive the B-powder. The S-powder deposition system includes the motion actuators and a piezo vibrator. The motion actuators include an XY stage that moves the nozzle along the planned path, a Z stage that moves the nozzle up and down, and a rotation actuator that makes the nozzle opening opposite to the direction of movement. The rotation axis allows for the deposition nozzle to pave a path in the B-powder and deposit S-powder behind it as it moves through the layer.

The S-powder deposition is controlled together by movement of the nozzle as described above as well as the vibration of a piezoelectric disc. In a confined conduit, dry powders tend to form an arch or bridge that supports the weight of the powder above it. The existence of such an arch prevents the flow of powder under gravity as shown in Figure 5-b. In industry, the arching effect is generally considered undesirable for powder storage and transportation [9]. However, SSS takes advantage of this arching effect to serve as a “valve” for shutting off the flow of S-powder. The arch is stable under normal conditions, unless proper vibration is introduced. In SSS, vibration from the piezoelectric disc (Figure 5-a) is applied to the nozzle containing S-powder, effectively breaking the arch and allowing S-powder to flow through the nozzle freely as illustrated in Figure 5-c. Therefore, the movement of the nozzle must be coordinated with vibration to enable S-powder deposition.

`

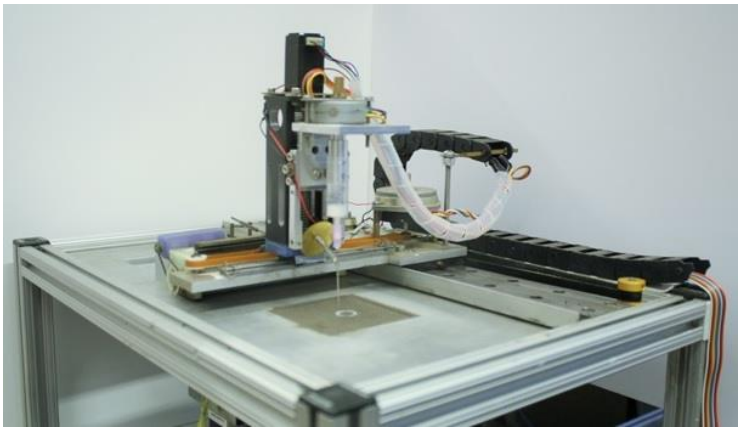

Figure 4 A Prototype SSS Machine

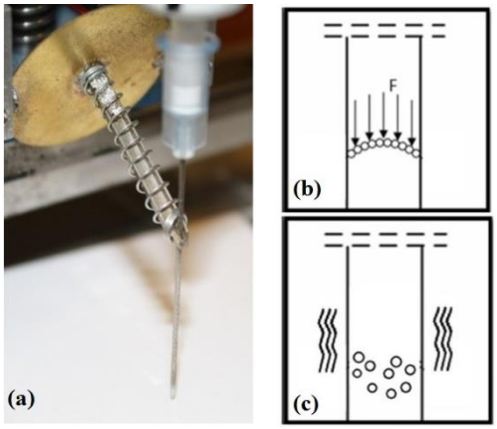

Figure 5 The dry powder delivery system (Left)The inhibitor deposition system (Right)Effect of vibration in breaking the powder bridge

4. In-Situ Resource Utilization by SSS

Construction materials by SSS will be obtained from in-situ resources. In SSS, the S-powder can be ceramics or metals of high sintering temperature. Major elements concentration for lunar regolith is shown in

Table 1[1]. Alumina and magnesia which have high sintering temperature all have high concentration with a weight ratio from 5% to 28% in the lunar regolith. Experiments show that alumina powder with d50 around 25um has a sintering temperature over 1500℃ without compaction and magnesia powder with d50 around 25 um has a sintering temperature over 1500℃. Research carried out for sintering of alumina and magnesia also demonstrated the necessity of using high pressure with much finer particles around 1 um[10,11] .

Table 1 Major Elements of Lunar Regolith

Element	*Major Elements, wt %* Mare Soil (10002)	Highland Soil (67700)	Basalt Rock (60335)	Anorthosite Rock (60015)	Glass (60095)
SiO_2	42.16	44.77	46.00	44.00	44.87
Al_2O_3	13.60	28.48	24.90	36.00	25.48
CaO	11.94	16.87	14.30	19.00	14.52
FeO	15.34	4.17	4.70	0.35	5.75
MgO	7.76	4.92	8.10	0.30	8.11
TiO_2	7.75	0.44	0.61	0.02	0.51
Cr_2O_3	0.30	0.00	0.13	0.01	0.14
MnO	0.20	0.06	0.07	0.01	0.07
Na_2O	0.47	0.52	0.57	0.04	0.28

`

On the moon, there is a sufficient supply of raw materials by excavation and extraction. Lunar regolith in the form of loose dust and raw materials such as metal can be extracted from lunar regolith. Experiments carried out in the lab use a lunar regolith simulant JSC-1A[1] which has similar physical and chemical properties. The melting temperature of JSC-1A is described as 1100℃[2] while experiments find sintering can be carried out from 1100℃ to 1150℃ by resistive heating in an ambient environment. Experiments carried out with Apollo 17 regolith sample showed microwave energy can be used to melt lunar regolith from 1200℃ to 1500℃ [12]. Therefore, large structure can be built by using lunar regolith as B-powder and alumina or magnesia as S-powder with microwave or radiation as the heat source. Metals, such as iron, aluminum have weight ratio from 4% to 14% depending on the minerals and can be extracted [13]. Steel is sintered at 1250℃ in the vacuum furnace [14] and aluminum is sintered at 650℃ [15] where alumina and magnesia can be used as the S-powder. Considering that there is perfect vacuum condition on the moon, large scale frames, bars and complex shapes can be fabricated by SSS technology.

A similar analysis can be carried out on Martian construction. Magnesia and alumina concentration by element weight in total accounts for more than 15% of Martian soil in Figure 6. More data are needed to find out if Martian soil can be used as construction material like that of lunar regolith. Commercial available Martian soil simulant JSC MARS-1A does not have a specified melting point or sintering temperature. While metals can still be extracted from the minerals and built into construction parts as needed.

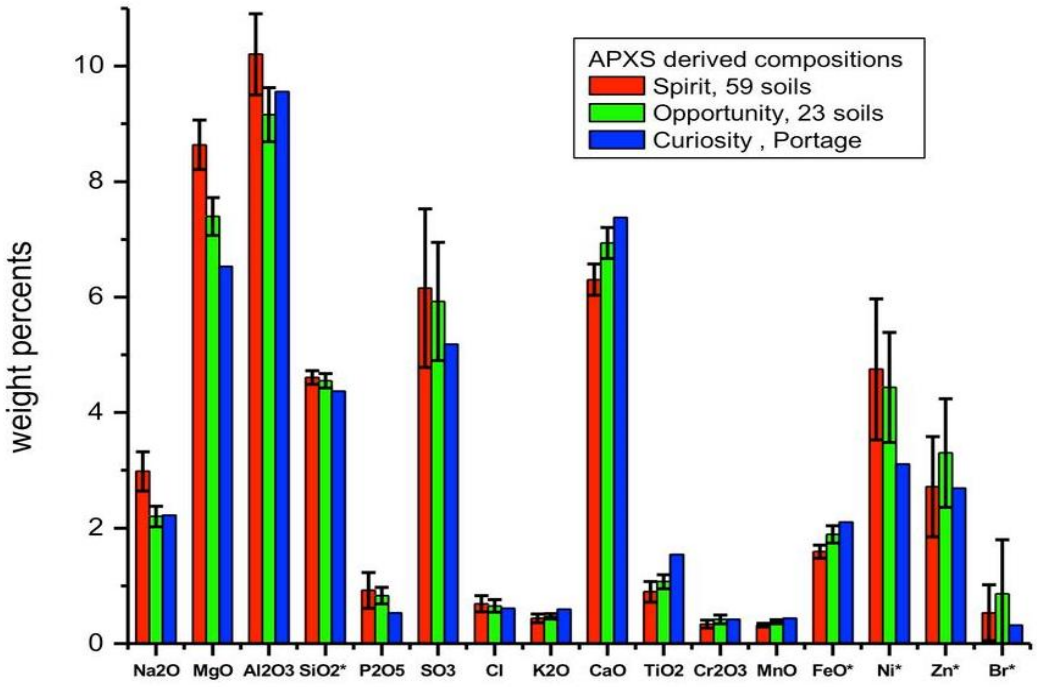

Figure 6 Elemental Composition of Typical Soils at Three Landing Regions on Mars (Image Credit: NASA/JPL-Caltech/University of Guelph)

[1] www.orbitec.com

[2] Data Safety Sheet from Orbitec.inc

`

5. Preliminary Results

In the experiments, lunar regolith simulant JSC-1A and bronze powder are tested as B-powder respectively. Alumina powder is used as S-powder for both B-powders. For JSC-1A, a layer thickness of 300 μm is used, the heating ramp for JSC-1A powder is 10°C/minute and is kept for 30 minutes to 60 minutes at a temperature from 900 °C to 1130 °C. For bronze, a layer thickness of 200 μm is used, the heating ramp is 5°C/minute and the powder is sintered at 780 °C for 30 minutes. Bronze is used to illustrate the capability of making metallic parts.

Experiments show that all sintered parts can be separated easily. The sintered part is separated from the redundant material by the separator coating as seen in Figure 7.a. Some of the S-powder is already brushed away to show the easiness of separation. Lunar simulant JSC-1A is grey before sintering and the grey base material takes a reddish color as a result of oxidation in the ambient environment during the sintering process. The final part achieves the shape as it is designed (Figure 7.b). The white powder on the boundary can be removed with ease, such as by hand. For the tile of this shape, many identical pieces will form the interlocking pad for certain purpose (Figure 7.c). In this project, manufacturing of this tile is meant to produce functional tile, which will be used for building landing pads on the moon or Mars for spacecraft landing. Multiple ceramic parts have been manufactured with JSC-1A as illustrated in Figure 7.d.

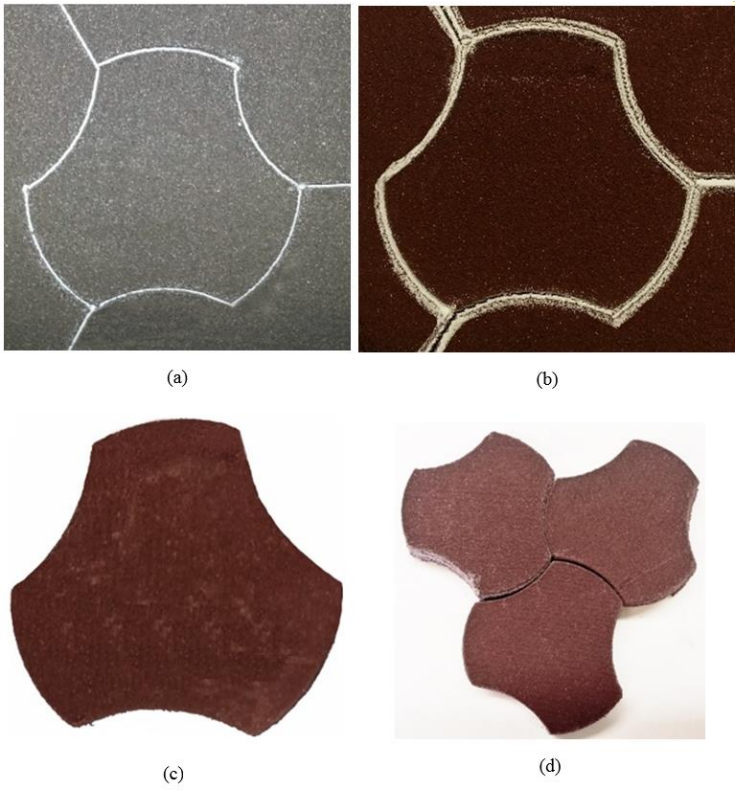

Figure 7 The sintered ceramic inter-locking tiles made of JSC-1A. (a) printed 200 micron wide S-powder inside regolith as B-powder (b) The separated tile unit; (c) Sintered tile, (d) Interlocking tile pattern

Metallic parts have also been fabricated successfully with SSS. A bronze piece of half cone is designed and sintered with spherical alumina powder being the S-powder as illustrated in Figure 8 (a & b). A 2.5D bronze gear is produced with spherical tungsten powder as S-powder. The surface of the parts has been slightly polished.

`

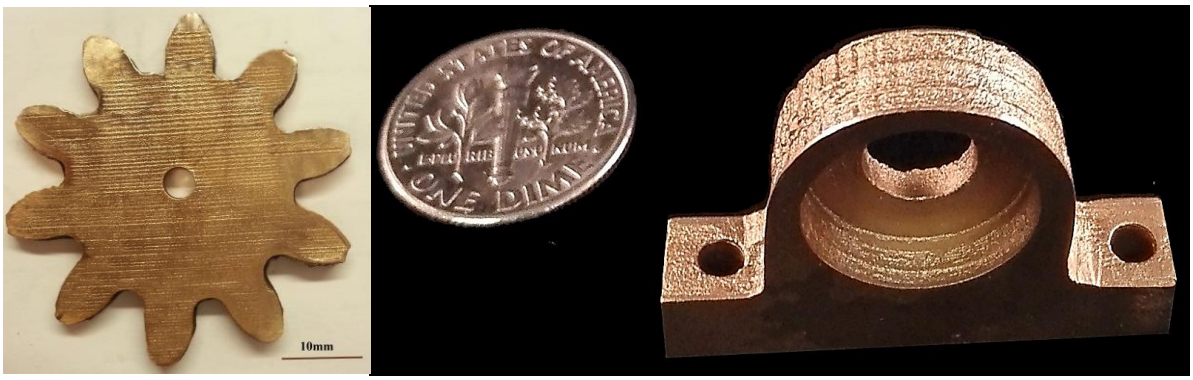

Figure 8. Metallic parts printed with SSS out of bronze powder

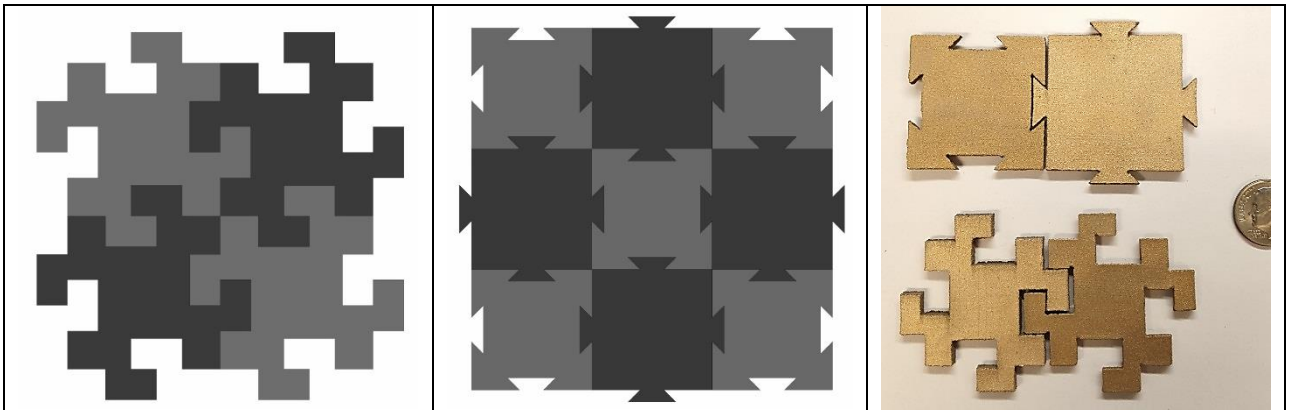

(a) (b) (c)

Interlocking tiles (a) Interlocking pattern 1 (b) Interlocking pattern 2 (c) Printed samples

Figure 9. Inter-locking metallic parts made with SSS

`

Sulfur Concrete for SSS:

On Mars, sufficient supply of sulfur in the regolith can serve as a building agent to prepare a granular material for SSS which will bring down the energy consumption significantly. According to the regolith composition table provided, sulfur concentration on Mars is about 2.2 wt. % and can be obtained as a byproduct where metals are extracted. Sulfur melts at a temperature of 239.4℉ or 115.2℃. To prepare the granular material, 35% wt. of molten sulfur may be uniformly mixed with 65% wt. of Martian regolith at a temperature above sulfur's melting point. When the mixture is cooled down and crushed into small granular form where each grain would contain portions of sulfur and regolith which would be close to the portions of these material in the original mix. The granular material may be crushed further and sifted to arrive at the desirable mesh size. This powder material may now be effectively used as the stock fabrication material by the SSS process because when heated the sulfur portion melts and acts as a strong binder to consolidate the regolith. Any ceramic powder can be used as the separator powder in this case. According to our experiments in sulfur concrete construction using Contour Crafting, we have learned that sulfur concrete can have a compressive strength of about 4000 psi, which is given the Martial gravity this would be equivalent to the strength of a 12000 psi concrete in terrestrial condition. Figure 10 shows a Contour Crafted sulfur concrete object that we have fabricated using Contour Crafting. We have just started our research on application of SSS in construction of sulfur concrete structures and objects such as inter-locking bricks.

Figure 10. Sulfur concrete part made with Contour Crafting.

6. Fabrication without Powder Layering

It should be noted that the SSS can operate without powder layering by inserting its nozzle deep into the base powder and depositing the separation powder for every part layer profile each time raising the nozzle to deposit the succeeding layer. This capability makes the SSS process the only powder based AM method that can be used in zero-gravity. Figure 11 shows a part that has been made with SSS without powder layering.

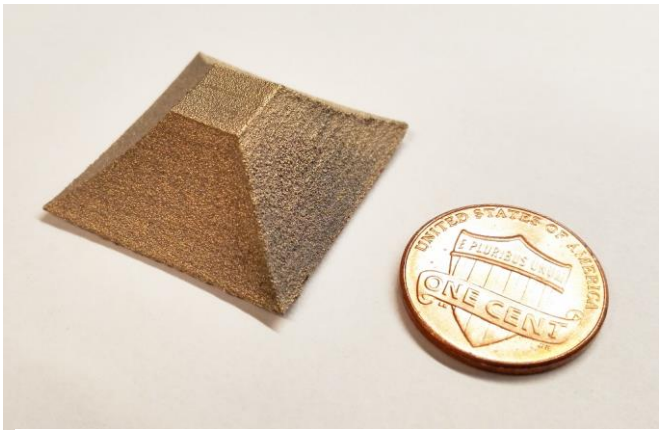

Figure 11. Part built with SSS without powder layering

7. Analysis

SSS enables application of existing knowledge on processing materials. As the operating principle indicates the sintering profile of the B-powder is not affected by the choice of S-powder, provided that S-powder has a high enough sintering temperature compared to B-powder. Therefore, an S-powder with high enough sintering temperature is safe to work with multiple B-powder materials.

`

Transportation and assembly are of low cost. Light weight rails and gantry system can be used as the starting infrastructure. All other materials can be obtained locally. Extra rails and gantry system can be fabricated with SSS technology therefore a self-replication can be done.

The build length is the length of the rails which can be extended at relatively low cost. Using a mobile heating system such as microwave energy or radiation heating, there is not really a limitation on the size that can be sintered. Such capability allows the construction of large parts as whole pieces.

As a 3D printing technology, SSS can be used to fabricate customized parts. Planetary transportation will not allow extra spare parts and complex parts might be needed for unexpected cases. SSS, with the capability of building complex shape, provides more flexibility for fabrication in remote environments using in-situ material.

The speed of SSS fabrication is comparatively higher than other AM technologies. Using the following definitions,

m_{mch}: mass of the machine;

m_{out}: output mass of the machine;

T_h: maximum thickness of one layer;

μ: energy penetration factor of printable thickness;

S: Total length of all edges of a unit block;

v: speed of the deposition;

t: print time;

β: ratio of layer time printing time to separator deposition time;

V_t: printed volume in unit time;

t_{span}: life span of the machine working nonstop;

ρ: density of the regolith;

η: shape factor (as deposition time linearly proportional to the length of the boundary lines, a shape factor is the ratio of the total length of a 2D shape to a square that the 2D shape has the same area of the square)

The time it takes to print one layer is:

$$t = \frac{4S\eta\beta}{v}$$

The volume of each layer is:

$$V_t = \frac{S^2 T_h \mu}{t} = \frac{S T_h \mu v}{4\eta\beta}$$

Some typical values to be used are:

$$T_h = 5\ cm;\ \mu = 10\%;\ \eta = 3;\ \beta = 2; S = 20\ cm;\ v = 2.5\ cm/s$$

`

The volume built per hour is:

$$V_t = 240in^3/hr = 3.9L/hr$$

The machine can be designed such that it could work for 4 months (2,880 hours) before needing maintenance. In this case the overall building volume in the period of operation would be:

$$V = V_t t_{span} = 11326L$$

Take the density of the regolith as $2g/cm^3$

The weight of the structures built in the 4 month period would be almost 22 mT:

$$m_{out} = 22{,}653\ kg$$

The machine weight $m_{mch} = 100\ kg$, as all separator powder will be extracted in-situ; the payload mass equals that of the machine;

The multiplier M is:

$$M = \frac{m_{out}}{m_{mch}} = 226.5$$

As for the energy consumption, to produce 1 kg of useful interlocking unit, the material is heated up to about 1000℃, the specific heat is denoted by C_{sh}, the energy absorption efficiency is denoted by ε.

The energy consumed for 1kg of regolith is:

$$E = m\Delta T C_{sh}/\varepsilon$$

The specific heat for lunar regolith is taken as: $C_{sh} = 1000J/kgK$, $\Delta T = 1000K$, $m = 1kg$,$\varepsilon = 40\%$;

$$E = 2.5MJ = 0.7kWh$$

8. Conclusion

Selective Separation Sintering (SSS) has proven ability to fabricate ceramic and metallic parts at various scales. The building material can be entirely ISRU. Transportation cost of the SSS technology can be low and customized parts and structures may be fabricated in an autonomous way at impressive speed. SSS is a minimally complex but highly capable technology that can effectively assist planetary exploration, utilization and colonization. Figure 12 shows a typical deployment scenario for planetary construction of landing pads and roads using inter-locking tiles made out of in-situ regolith.

`

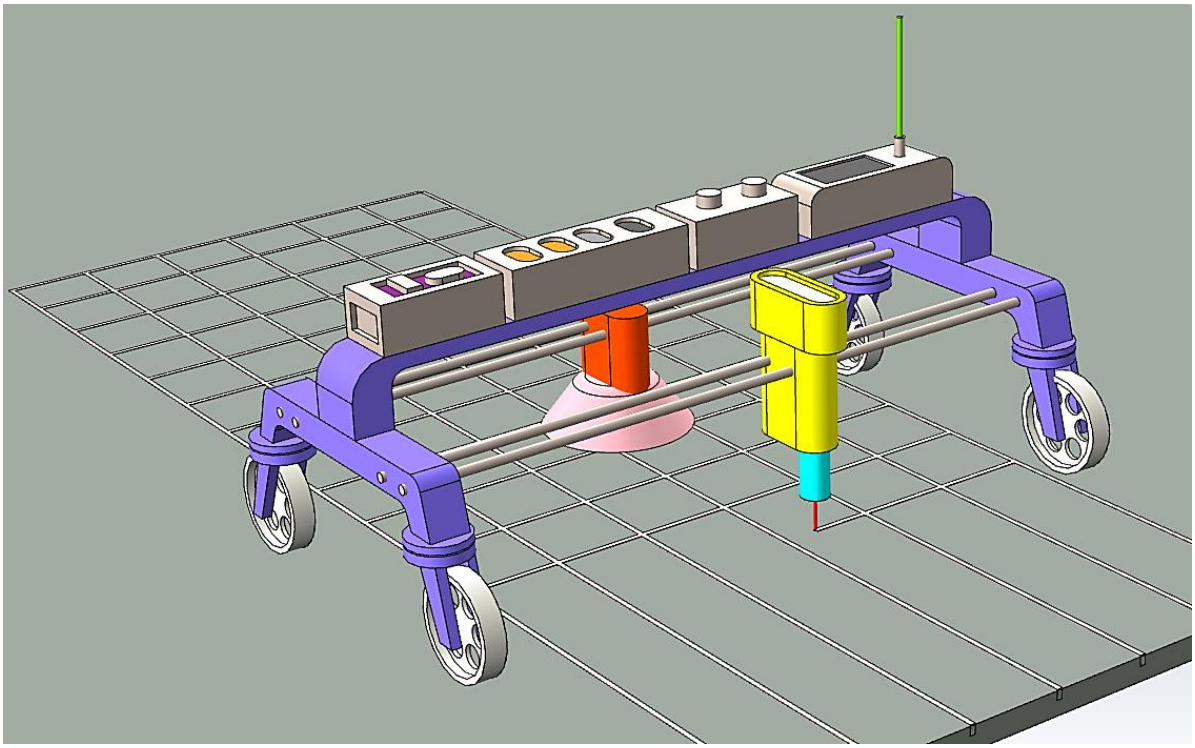

Figure 12. A planetary in-place tiling system using SSS and microwave sintering. Similar arrangement may be made for fabrication of other objects using the non-powder layering mode of SSS

References

[1] T Lin, Concrete for lunar base construction, 1 (1985) 381.

[2] F Horz, Lava tubes-potential shelters for habitats, 1 (1985) 405-412.

[3] M Roberts. Inflatable habitation for the lunar base, LPI Contributions. 652 (1988) 204.

[4] H Benaroya, M Ettouney. Framework for evaluation of lunar base structural concepts, J.Aerospace Eng. 5 (1992) 187-198.

[5] B Khoshnevis, MP Bodiford, KH Burks, E Ethridge, D Tucker, W Kim, et al., Lunar contour crafting—a novel technique for ISRU-based habitat development, (2005) 7397-7409.

[6] B Khoshnevis, M Thangavelu, X Yuan, J Zhang. Advances in Contour Crafting Technology for Extraterrestrial Settlement Infrastructure Buildup, AIAA. 5438 (2013) 10-12.

[7] F Ruess, J Schaenzlin, H Benaroya. Structural design of a lunar habitat, J.Aerospace Eng. 19 (2006) 133-157.

`

[8] D Beike. Mining of Helium-3 on the Moon: Resource, Technology, and Commerciality—A Business Perspective, (2013).

[9] MJ Rhodes. Principles of powder technology, (1990).

[10] Z He, J Ma. Constitutive modeling of alumina sintering: grain-size effect on dominant densification mechanism, Computational Materials Science. 32 (2005) 196-202.

[11] T Vasilos, R Spriggs. Pressure sintering: mechanisms and microstructures for alumina and magnesia, J Am Ceram Soc. 46 (1963) 493-496.

[12] LA Taylor, TT Meek. Microwave sintering of lunar soil: properties, theory, and practice, J.Aerospace Eng. (2005).

[13] C Schwandt, JA Hamilton, DJ Fray, IA Crawford. The production of oxygen and metal from lunar regolith, Planet.Space Sci. 74 (2012) 49-56.

[14] CH Ji, NH Loh, KA Khor, SB Tor. Sintering study of 316L stainless steel metal injection molding parts using Taguchi method: final density, Materials Science and Engineering: A. 311 (2001) 74-82.

[15] G Schaffer, B Hall. The influence of the atmosphere on the sintering of aluminum, Metallurgical and Materials Transactions A. 33 (2002) 3279-3284.

CHAPTER 4

Beneficiation of Lunar and Mars Soils in support of Automated Construction by CC and SIS

Introduction

This report will examine how to obtain native sulfur from the surface of the Moon and Mars. It will also explore how to extract high melting point ingredients from both lunar regolith types (Highlands and Mare) as well as find geologic concentrations of refractory minerals on Mars. It is intended to be a preliminary TRL1-2 examination of mineral beneficiation for providing feedstock for automated lunar and Mars construction using the Contour Crafting (CC) and Selective Inhibition Sintering (SIS) 3D printing techniques.[1]

1.0 Lunar Sulfur & Refractory Minerals Extraction

In-situ construction will be a critical component of the future human settlement of the Moon and Mars. Methods that can leverage local materials will be favored over methods that rely on imports. This is particularly true in the long run as government-based exploration funding is replaced by private financing where economic sustainability is more of an issue.

> *"Sulfur on the Moon may well prove satisfactory replacement for lighter volatile elements and their compounds in some applications. It may even open new possibilities and uses that surpass a mere duplication of what is already done on Earth."* [Vaniman, 1988]

For the Moon, the use of sulfur in making concrete appears to offer an optimum with regard to local availability, physical and chemical characteristics, and especially environmental compatibility. The demonstrated extension of automated 3D printing by Contour Crafting into concrete mixing and casting underscores the value of lunar sulfur. However, there is a concern about stability of sulfur above 140°C. Clearly this will not be a problem on Mars, and the use of a thin blanket of lunar regolith as insulation should offset any liability for construction on the Moon.

> *"Thermal stability is a concern; Crow and Bates (1970) suggest that sulfur concrete be used only in buried structures on the Moon where full-sun thermal exposure will not be a problem."* [Vaniman, 1988]

Another important lunar construction and fabrication technique is possible by using microwave-assisted sintering of agglutinic regolith glasses and a ceramic insulator implemented by the

[1] This section is primarily the contribution of Mr. Brad Blair, NewSpace Analytics LLC, who served as the consultant to this project.

Selective Inhibition Sintering (SIS) technology. By leveraging the difference in physical properties between low melting temperature glassy components that readily couple with microwave energy and high melting temperature refractory materials that are microwave-transparent, the use of 3D printing techniques for lunar manufacturing and construction will be taken to a new level of sophistication. A refractory powder can be used in order to isolate regions of a glass-enriched powder and printed into shapes that are later exposed to microwaves, which will sinter and bind the glassy components but not the refractories. This way the sintered objects can later be separated.

The sections below will examine in more detail how to obtain sulfur for making concrete from lunar materials as well as how to separate both glassy components and refractory materials from lunar regolith feedstock.

1.1 Identifing Candidate Geologic Occurrences for Lunar Sulfur

Sulfur can be found in two primary locations on the lunar surface, depending on location. For equatorial regions the most abundant form is in the mineral Troilite – an iron sulfide associated with basalt which can be concentrated at certain locations on the lunar near side associated with volcanism.

> *"Sulfur is a relatively volatile element that plays a dual role on the Moon: in the gases that drove lunar pyroclastic eruptions, and in the gases released during impact heating. For a planet with a surface otherwise poor in volatile elements, the Moon has a fair amount of sulfur. Lunar mare basalts, for instance, have about twice as much sulfur as do typical terrestrial basalts. On the Moon, this sulfur is present in sulfide (S) minerals; the low oxygen partial pressures in the lunar environment apparently do not permit the formation of sulfate (SO4) minerals."* [Heiken, 1991, p.174]

> *"Troilite (FeS) is the most common sulfide mineral in lunar rocks. Although it almost always forms less than 1% by volume of any lunar rock, troilite is ubiquitous. It is commonly associated with native Fe, ilmenite, and spinel. … The most common occurrence of troilite is as an accessory phase in mare basalts, where it is usually a late-stage crystallization product. ... Secondary troilite forms later, in the solid rocks, in cases where the partial pressure of sulfur increases rapidly and sulfurizes native Fe during the high temperature shock metamorphism produced by meteoroid impacts. … Other sulfide minerals positively identified in lunar rocks include chalcopyrite (CuFeS2), cubanite (CuFe2S3), pentlandite [(Fe,Ni)9S8], mackinawite (Fe1+xS), and sphalerite [(Zn,Fe)S]. All these minerals are so rare as to be only geologic curiosities, and they have only minor applications in determining the origins of the rocks that contain them."* [Heiken, 1991, p.174]

Theory also suggests that due to stability at low temperature, sulfate compounds and potentially even native sulfur could potentially be found at the lunar poles. Evidence from the NASA LCROSS mission affirms some of these conclusions.

1.1.1 High-Titanium Orange Glass and Lunar Pyroclastic Deposits

The high-Titanium orange glass is a pyroclastic deposit sampled during Apollo 17 which represents the highest concentration of sulfur measured during the Apollo missions. Note that this is a real geologic occurrence sampled during the Apollo lunar missions that is well characterized and 100% certain.

> *"Our present knowledge of lunar samples suggests that the best place to collect sulfur on the Moon is from mare soils and rocks. Although sulfur is not so abundant that it is available without effort, it does rank eleventh in weight abundance among the elements in average lunar mare rocks. Gibson and Moore (1974) found that the high-Ti mare basalts, in particular, have high sulfur contents, in the range of 0.16% to 0.27% by weight. These authors also make the important point that lunar basalts actually have more sulfur than terrestrial basalts, which seldom have more than 0.15%."* [Vaniman, 1988]

However, liberating sulfur from the interior of mineral grains will require crushing, a power-intensive operation that may be too complex and costly for early lunar operations. Yet there is a simple solution offered by locating lunar near-side pyroclastic deposits where sulfur has migrated to the surface of mineral grains.

> *"Although the richest known sources of sulfur are the high-Ti mare basalts, extraction of this sulfur would require energy intensive crushing of hard rock. Most of the sulfur in the basalts occurs as sulfide in the mineral troilite (FeS). The easiest source of sulfur is high-Ti mare soils, which need not be crushed prior to processing. In addition to the sulfur in troilite, some surface correlated sulfur can be found in soil samples. In pyroclastic soils, surface-correlated metal sulfides probably occur (Butler and Meyer, 1976; Cirlin and Housley, 1979), but sulfur may also occur as metal sulfates that are readily volatilized to produce SO2 (D. McKay, personal communication, 1988)."* [Vaniman, 1988]

1.1.2 Lunar Polar Volatiles May Contain 1% or More by Weight Sulfur

Polar deposits of native sulfur as well as sulfate minerals may exist in surface layers due to natural enrichment processes. Theory suggests an estimated minimum concentration of 1wt%.

> *"Though the loss mechanisms, their rates, and the delivery rate of sulfur at the lunar poles are not clear, the loss rate of sulfur is less than that of water due to a lower partial pressure, higher atomic mass, and longer photo destruction time. If we neglect the loss mechanisms of sulfur from cold traps, we can estimate the sulfur content to be as high as 2 g cm−2 in regions of sulfur stability with an area of 105 km2. … Then, a 2g/cm2 sulfur content corresponds to about 1wt% in 1m top layer of the regolith."* [Berezhnoy, 2003]

> *"The LCROSS results indicate that a variety of useful substances are present in the polar cold traps. Water is our principal object for future resource extraction, being one of the most valuable and readily available substances for spaceflight imaginable (i.e., a life-support consumable, a medium of energy storage and rocket propellant). However, both ammonia and methane have a variety of industrial uses, as well as being ready sources of nitrogen and carbon, two elements essential for the support of human life.*

Sulfur is also a useful element and appears to be present in fair quantity as both native sulfur and sulfide." [Spudis, 2010]

Compound	Molecules cm^{-2}	% Relative to $H_2O(g)$
H_2O	5.1(1.4)E19	100.00%
H_2S	8.5(0.9)E18	16.75%
NH_3	3.1(1.5)E18	6.03%
SO_2	1.6(0.4)E18	3.19%
C_2H_4	1.6(1.7)E18	3.12%
CO_2	1.1(1.0)E18	2.17%
CH_3OH	7.8(42)E17	1.55%
CH_4	3.3(3.0)E17	0.65%
OH	1.7(0.4)E16	0.03%

Figure 1. Sulfur compound concentration detected by LCROSS at lunar North Pole. [Colaprete, 2010]

"Given the estimated total excavated mass of regolith that reached sunlight, and hence was observable, the concentration of water ice in the regolith at the LCROSS impact site is estimated to be 5.6 +/- 2.9% by mass. In addition to water, spectral bands of a number of other volatile compounds were observed, including light hydrocarbons, sulfur-bearing species, and carbon dioxide." [Colaprete, 2010]

Quick calculation:
5.6*0.1675=0.938% or ~1% H2S
5.6*0.0319=0.179% SO2

Conclusion: the lunar polar sulfur estimate of 1% is largely accurate. Paul Spudis above affirms the possibility of native sulfur, but the evidence for this is not shown in Tony Colaprete's article.

The direct use of beneficiated polar native sulfur might be possible without the need for chemical refining (as described in Sections … above), provided it can be concentrated to the ratio needed for use in concrete using physical or electromagnetic separation methods to increase its relative abundance from 1% to the 12-22% values that would be needed as a binder. This of course presumes it is mixed with other surface materials in an icy regolith that also include natural aggregates, and that volatiles easily separate during the heating process (these volatiles would have high value for propellant, industrial and settlement-related purposes of course). This could be tested in a set of experiments with simulated polar regolith mixtures.

1.2 Candidate Geologic Occurrences of Lunar Refractory Minerals

The lunar Mare is mostly basalt, although refractory imenite does occur and can be somewhat concentrated (this is possible – see Agosto's work below for juicy quotes…). It can clearly be separated from the glass agglutinates.

Highlands is crystalline and made mostly refractory stuff. It can be separated from the glass.

"ASTM C71 defines refractories as "non-metallic materials having those chemical and physical properties that make them applicable for structures, or as components of systems, that are exposed to environments above 538 °C"" ... "The oxides of aluminum (alumina), silicon (silica) and magnesium (magnesia) are the most important materials used in the manufacturing of refractories. Another oxide usually found in refractories is the oxide of calcium (lime). Fire clays are also widely used in the manufacture of refractories." ... "Refractory materials must be chemically and physically stable at high temperatures. Depending on the operating environment, they need to be resistant to thermal shock, be chemically inert, and/or have specific ranges of thermal conductivity and of the coefficient of thermal expansion." [Wikipedia, http://en.wikipedia.org/wiki/Refractory]

Fire clays are weathered feldspar. Feldspars were just found on Mars (see section 2).

1.2.1 The Lunar Highlands Material is Largely Refractory

Lunar highlands soil may be suitable for refractory use as-is depending upon purity requirements and the efficacy of separation methods.

"Olivine is actually a name for a series between two end members, fayalite and forsterite. Fayalite is the iron rich member with a pure formula of Fe2SiO4. Forsterite is the magnesium rich member with a pure formula of Mg2SiO4. The two minerals form a series where the iron and magnesium are substituted for each other without much effect on the crystal structure."
http://www.galleries.com/Olivine

"The pyroxene minerals are inosilicates of the general formula XY(Si, Al)2O6. The X, represents ions such as calcium, sodium, iron+2 and magnesium and more rarely zinc, manganese and lithium. The Y, represents ions of generally smaller sized such as chromium, aluminum, iron+3, magnesium, manganese, scandium, titanium, vanadium and even iron+2."
http://www.galleries.com/Pyroxene_Group

"Amphibole is the name of an important group of generally dark-colored, inosilicate minerals, forming prism or needlelike crystals,[1] composed of double chain SiO4 tetrahedra, linked at the vertices and generally containing ions of iron and/or magnesium in their structures."
http://en.wikipedia.org/wiki/Amphibole

1.3 Terrestrial Separation Methods Currently in Use for Compatible Geology

The term "beneficiation" is used by the mining industry to describe a variety of processes whereby extracted ore is separated into mineral and gangue, the former suitable for further processing or direct use. Primary types of beneficiation include size classification (sorting) and the separation of soil components using screens, gravity, fluids, electrical and magnetic fields. For lunar cases it is assumed that low temperature and low energy processes are preferred.

Flotation has also been successfully used by industry as a method of beneficiating and concentrating Olivine [Wells, 1959]. However, the amount of water required for mineral flotation combined with the difficulty of obtaining water on the Moon make this process unsuitable for lunar uses.

> *"The primary commercial application of mineral electrostatic beneficiation is in processing beach sands and alluvial deposits for titanium minerals. All of the heavy mineral beach sand plants in Australia, and most in the United States (Florida),use electrostatic methods to separate rutile and ilmenite from zircon and monazite (Fraas, 1962; Kelly and Spottiswood, 1982).The most common electrostatic separator designs use a drum or slide configuration. In both designs, a high intensity electric field (several kV/cm) is established by a high voltage electrode spaced a few cm from the grounded drum or slide. Many separators use an additional ionizing electrode above the field electrode to charge the mineral feed with air ions and electrons before it enters the accelerating field (Fraas, 1962; Carpenter, 1970; Moore, 1973)."* [Agosto, 1985]

> *"Minerals falling through the separating field commonly acquire charge by one or some combination of the following mechanisms: (1) Electrostatic induction; (2) Contact charging; (3) Ionic charging."* [Agosto, 1985]

Reagents can also be added to input streams to improve electrostatic process efficiency. One approach used in industry is to add organic coatings to increase the electrical potential of selected minerals.

> *"The present invention relates to the field of separating certain mineral components of an ore from other mineral components of the same ore using electrostatic separation. Specifically, the present invention relates to electrostatic modification reagents and methods of using them in an electrostatic separation process to separate the mineral components within the ore with improved efficiency."* [Ravishankar, 2011]

1.3.1 Terrestrial Sulfur Deposits and Processes

Terrestrial native sulfur deposits are formed at steam vents in some volcanoes such as the Kawah Iljen volcano in Java, Indonesia (see below) with mining of elemental sulfur continuing through today. Today the primary global sulfur production is as a byproduct of petroleum refining, where sulfur removal is used to "sweeten" crude oil.

Figure 2. Sulfur miners at Kawah Iljen Volcano [Wikipedia, http://en.wikipedia.org/wiki/Ijen]

Primary industrial sulfur production is done using the Frasch, Marox and Claus processes. The Frasch process was widely used in the last century to mine sulfur by pumping hot water underground to dissolve native sulfur from salt domes and other sources, then precipitating the sulfur at the surface. To a large degree the process is an industrial analog of the natural processes at work in volcanoes such as Ijen as shown above, although it has largely fallen out of favor as a major source of industrial sulfur. The Merox process (an acronym for mercaptan oxidation – see Sullivan, 2004) uses a proprietary catalytic chemical reaction in oil and natural gas processing to remove mercaptans from liquid or gas input streams by converting them to hydrocarbon disulfides. It is not really suitable for lunar use.

Figure 3. Refinery sulfur generated by the Claus process. [Wikipedia, http://en.wikipedia.org/wiki/Claus_process]

The Claus process

Gases with an H2S content of over 25% are suitable for the recovery of sulfur in straight-through Claus plants while alternate configurations such as a split-flow set up or feed and air preheating can be used to process leaner feeds. Hydrogen sulfide produced, for example, in the hydro-desulfurization of refinery naphthas and other petroleum oils, is converted to sulfur in Claus plants. The overall main reaction equation is:

2 H2S + O2 → S2 + 2 H2O. In fact, the vast majority of the 64,000,000 metric tons of sulfur produced worldwide in 2005 was byproduct sulfur from refineries and other hydrocarbon processing plants. [Wikipedia]

SO2 + 2 H2S → 3 S + 2 H2O

> *"A wide variety of schemes could be proposed for extracting sulfur from lunar rocks and soils, but not all may be cost effective or practical on the Moon. Procedures requiring multiple complex processing steps are probably too cumbersome to be practical - especially if they cannot be automated and run as autonomous systems. Heating lunar feedstocks to over 1100°C is probably one of the simplest of possible extraction procedures. Moreover, this method has already been tested and proven. Gibson (1973) used thermogravimetric-quadrupole mass-spectrometric analysis to determine that Apollo 14 and 15 soil samples release their sulfur as SO2 and H2S on heating to 1000°-1300°C. His experiments were run at vacuum conditions close to those that would be expected on the Moon. These gases arc thus the sulfur products to be anticipated on simple heating of lunar feedstocks."* [Vaniman, 1988]

> *"The catalytic reduction of SO2 to elemental sulfur by methane was studied over ceria-based catalysts. Both La-doped and undoped ceria were found to catalyze the SO2 reduction by CH4 in the temperature range of 550–750C at atmospheric pressure and with feed gases containing a molar ratio of CH4/SO2 = 0.5–3. At temperatures below 550 C, the catalyst surface is capped by SO2. The reaction light-off coincides with the threshold temperature for sulfate decomposition. Various SO2/CH4/H2O gas mixtures were used to study the catalyst activity and selectivity to elemental sulfur."* [Zhu, 1999]

1.3.2 Industrial Analogs for Cryogenic Polar Sulfur Processing

No compatible terrestrial geologic analog exists for cryogenic lunar polar sulfur. However, as low-temperature industrial processing facilities become more common for separation and condensation of liquefied natural gas, lessons learned might benefit future lunar polar mining and processing operations. Analogs might also exist for solids, particularly where physical or electromagnetic properties change as a function of temperature (note: this thread should be explored further should polar sulfur prove itself a viable option).

1.3.3 Refractory Mineral Separation

Processes are common - many analogies exist. An important question arises: How pure do we need the feedstock (sulfur and/or refractory minerals) for our process to work? High purity requirements will add considerable complexity to a mineral processing circuit.

1.4 Preliminary Assessment of Process Suitability for Lunar Surface Use

> *"Electrostatic Concentration: In 1985, I reported designing mineral electrostatic separators based on commercial models. With my separators, I demonstrated the electrostatic concentration of lunar ilmenite in the 90- to 150-micrometer grain size*

fraction of Apollo 11 soil 10084,853 to levels above 60 percent at collection points near the high-voltage electrode after one pass through a slide-type electrostatic separator in a nitrogen environment. Ilmenite behaved like a semiconductor and was separable electrostatically because the other major soil components, including the metal-bearing agglutinates, behaved like nonconductors." [Agosto, 1992]

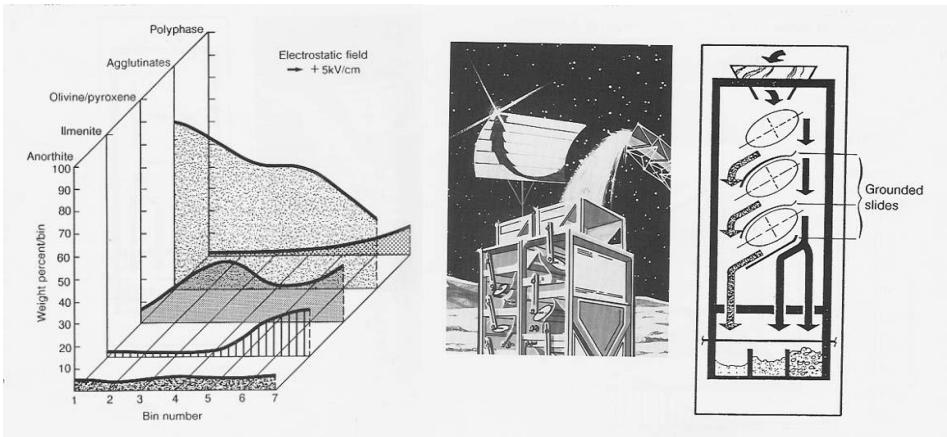

Figure 4. Lunar beneficiation systems analysis. [Agosto, 1992]

1.4.1 Evaluate Suitability of Processes in Low Gravity, Cryogenic and Vacuum Conditions

Sulfur

The heating experiments of Gibson and Moore (1973) on Apollo 15 and 16 samples indicate that 12-30% of the total soil sulfur can be extracted at 750°C, 50-70% of the total sulfur is extracted at 950°C, and 85-95% of the total sulfur is extracted at 1100°C (vacuum conditions, <2 × 10 .6 torr). Gibson and Moore (1974) suggest that the 12-30% of the sulfur extracted at 750°C is surface correlated. Most of the higher temperature sulfur is probably derived from troilite. The sulfur is given off as SO2 and H2S, which Gibson (1973) attributes mainly to reaction between troilite and other phases at high temperatures." [Vaniman, 1988]

"…the sulfur-bearing gases that are liberated from lunar feedstocks can be combined in the Claus reaction to produce pure sulfur and water.

$$SO2 + 2H2S => 2H20 + (3/x)Sx$$

where x varies between 2 and 8. This reaction has been studied intensively and used in the treatment of SO 2 waste gases on Earth (Pfeiffer, 1975). The Claus reaction is of particular interest not only because it uses exactly those sulfur gases expected from lunar feedstock, but also because it produces valuable water." [Vaniman, 1988]

"Coproduction of sulfur during oxygen extraction from ilmenite-rich mare soils could yield sulfur in masses up to 10% of the mass of oxygen produced. Sulfur deserves serious consideration as a lunar resource." [Vaniman, 1988]

"Multistage electrostatic separation systems like those used in all commercial electrostatic mineral concentrators should raise grades and recoveries to 90%+ levels (e.g.,Kelly and Spottiswood, 1982), provided the soil ilmenite is sufficiently liberated. Even without additional liberation, lunar soil ilmenite grades in the size range tested could reach the high 70s because combined glass and polyphase soil components that reported along with ilmenite to the conductor bins and beyond were comparable to ilmenite in abundance (Table 3) and are about half ilmenite in composition. Agglutinates are the major component of ilmenite bearing mare soils (Papike et al., 1982),and their divergent electrical behavior to ilmenite is an indication that the two components are separable electrostatically. This work suggests that the best sequence for concentrating lunar soil ilmenite would be magnetic extraction of the ferromagnetic agglutinates followed by electrostatic concentration of ilmenite in the non-ferromagnetic soil fraction." [Agosto, 1985]

"Electrostatic separators offer the advantages of low power consumption and mass and efficient high voltage generation in a vacuum environment such as the lunar surface." [Agosto, 1985]

Refractories

Highlands material has lots of refractories - electrostatics can separate the glassy agglutinates from the refractory particles easy enough - most of the nanophase iron is in the glass. Two piles of material will be resulted - one that couples with microwaves and one that is a high temp insulator. Some real Apollo 17 soil from JSC would be suitable for testing this process.

One has to make a choice regarding process complexity and purity of feedstock. The simple approach of proving the process with experiments using highlands soil returned from Apollo 16 or 17 is recommended.

In general it is observed that the granular lunar highlands breccias are mostly made of refractory minerals, with the space weathering process adding glass and nanophase iron due to reduction.

Refractory minerals resist high temperatures and are used in industrial ceramics as insulators and crucibles. The melting temperature of a random mixture of bulk and especially trace minerals is difficult to predict from first principles due to complex interactions and fluxing. While extensive literature exists showing phase diagrams for melting points of silicate and oxide minerals as a function of pressure (this research has been underway for many decades, and was originally done to understand the crystallization processes for mantle and crustal materials), most of the research has been limited to purified materials and simplified mixtures, mapping the effects of pressure and temperature on crystallization. A more experimental approach is used in industrial and artistic ceramics, where empirical relationships can be directly measured between kiln temperature and the melting of mixtures of clay and glaze from various sources. For the lunar materials a similar approach is recommended – get some real soil, beneficiate it using simple means, then measure the melting temp of the products. Simulants of sufficient quality are available today that could be used to approximate this process (e.g., ones with refractory, glass

and nanophase iron components). It is also suggested to bring a nanophase iron expert such as Larry Taylor in as a consultant. [Shen, Guoyin, and Peter Lazor], and following sources:

http://www.hpcat.aps.anl.gov/shen/publication/Shen-JGR95.pdf
http://www.gly.uga.edu/railsback/Fundamentals/HardnessMeltingPlot06.pdf
http://hyperphysics.phy-astr.gsu.edu/hbase/geophys/meltrock.html
http://curator.jsc.nasa.gov/lunar/lsc/15415.pdf

Periclase (the mineral version of MgO) is a relatively minor component of the lunar highlands soil, although it does sit at the highest temperature end of the refractory spectrum. Other refractories that are much more available include Olivene, Forsterite, Anorthite and Pyroxene. A simple electrostatic circuit will concentrate these four and separate the glassy, nanophase iron-rich agglutinates.

> *"The silicate minerals, especially pyroxene, plagioclase feldspar, and olivine, are the most abundant minerals in rocks of the lunar crust and mantle. These silicate minerals, along with other minerals and glasses, make up the various mare basaltic lavas and the more complex suite of highland rocks (melt rocks, breccias, and plutonic rocks) discussed in Chapter 6."* Lunar Source Book p. 123

TABLE 5.1. Modal proportions (vol.%) of minerals and glasses in soils from the Apollo (A) and Luna (L) sampling sites (90–20 μm fraction, not including fused-soil and rock fragments).

	A-	A-	A-14	A- (H)	A- (M)	A-16	A- (H)	A- (M)	L-16	L-20	L-
Plagioclase	21.4	23.2	31.8	34.1	12.9	69.1	39.3	34.1	14.2	52.1	20.9
Pyroxene	44.9	38.2	31.9	38.0	61.1	8.5	27.7	30.1	57.3	27.0	51.6
Olivine	2.1	5.4	6.7	5.9	5.3	3.9	11.6	0.2	10.0	6.6	17.5
Silica	0.7	1.1	0.7	0.9	-	0.0	0.1	-	0.0	0.5	1.7
Ilmenite	6.5	2.7	1.3	0.4	0.8	0.4	3.7	12.8	1.8	0.0	1.0
Mare Glass	16.0	15.1	2.6	15.9	6.7	0.9	9.0	17.2	5.5	0.9	3.4
Highland Glass	8.3	14.2	25.0	4.8	10.9	17.1	8.5	4.7	11.2	12.8	3.8
Others	-	-	-	-	2.3	-	-	0.7	-	-	
Total	99.9	99.9	100.0	100.0	100.0	99.9	99.9	99.8	100.0	99.9	99.9

Data from *Papike et al.* (1982), *Simon et al.* (1982), *Laul et al.* (1978a), and Papike and Simon (unpublished). (H) Denotes highland. (M) Denotes mare.

> *"The other two types of common monomict highland rocks, ferroan anorthosites and Mg-rich rocks, are (or have been) derived from large igneous bodies rich in plagioclase feldspar. Earlier workers (e.g., Kell et al., 1972) tended to combine them on the basis of mineral composition, with plagioclase-rich polymict rocks into a single category "ANT" (for Anorthosite-Norite-Troctolite rocks)."* Lunar Source Book p. 214

The following definitions come from Wikipedia

- **Norite**, also known as orthopyroxene gabbro, is a mafic intrusive igneous rock composed largely of the calcium-rich plagioclase labradorite, orthopyroxene, and olivine.
- **Troctolite** is a mafic intrusive rock type. It consists essentially of major but variable amounts of olivine and calcic plagioclase along with minor pyroxene. It is an olivine-rich anorthosite, or a pyroxene-depleted relative of gabbro.

- **Anorthosite** is a phaneritic, intrusive igneous rock characterized by a predominance of plagioclase feldspar, and a minimal mafic component. Pyroxene, ilmenite, magnetite, and olivine are the mafic minerals most commonly present.

2.0 Mars Sulfur & Refractory Minerals Extraction

2.1 Identify Candidate Geologic Occurrences for Mars Sulfur

2.1.1 Sulfur is Ubiquitous on the Surface of Mars

> *"After seven years of orbital measurements, the Mars Odyssey Gamma Ray Spectrometer (GRS) has obtained sufficient data to produce a statistically useful map of S distributions in the Martian near surface for low- to mid-latitudes (i.e., excluding high-latitude areas with H-enrichment: the so-called H-mask). The surface of Mars is characterized by elevated S, but varying from <1% to >3%, and with highest concentrations being found at low latitudes. Global average S content is approximately 2%, similar to average Martian soils analyzed to date."* [McLennan, 2009]

> *"For low latitudes, where occurrence of near surface ice is least likely (30°N to 30°S) the slope of the hydrogen - sulfur linear correlation can be interpreted as reflecting structural and/or bound water in near-surface minerals. The average slope thus is equivalent to an average hydration state of approximately 2 for divalent cation sulfates (e.g., Ca-, Mg-, Fe(II)-sulfates), a value broadly consistent with expected thermodynamic stability in these regions."* [McLennan, 2009]

Note that the average sulfur on Mars is the high-grade sulfur on the Moon. While sulfate minerals are common, elemental or native sulfur is rare. A process will be needed to refine the sulfur.

2.1.2 Review of Geologic Concentrations of Mars Sulfate Deposits (including aqueous and aeolean pathways)

Figure 6. Homestake Vein – a sulfate mineral deposit on Mars. [Webster, 2011]

The following news peaces are fairly recent:

“NASA's Mars Exploration Rover Opportunity has found bright veins of a mineral, apparently gypsum, deposited by water”.

“Researchers used the Microscopic Imager and Alpha Particle X-ray Spectrometer on the rover's arm and multiple filters of the Panoramic Camera on the rover's mast to examine the vein, which is informally named "Homestake." The spectrometer identified plentiful calcium and sulfur, in a ratio pointing to relatively pure calcium sulfate. Calcium sulfate can exist in many forms, varying by how much water is bound into the minerals' crystalline structure. The multi-filter data from the camera suggest gypsum, a hydrated calcium sulfate. On Earth, gypsum is used for making drywall and plaster of Paris”

Guy Webster, “NASA Mars Rover Finds Mineral Vein Deposited by Water”, press release, NASA Jet Propulsion Laboratory, Pasadena, Calif., December 07, 2011

2.2 Candidate Geologic Occurrences for Mars Refractory Minerals

2.2.1 Known Sources Include Newly Discovered Granites

Figure 7. Evidence for Granitic mineral separation on Mars. [Fuller-Wright, 2013]

“While the vast majority of Mars is indeed basaltic, "a percent or two or three" is made of these granite-like rocks, plus another 10 percent or so with an intermediate composition.”

“Chemically speaking, it's easy to make a basalt magma. Just heat up the inside of a planet, and the first thing that melts will be (more or less) basalt. Making a granite magma is much more complicated.”

“"If you've ever seen feldspar, it's very light, often white, and really, really hard to detect," explains Briony Horgon, a planetary science professor at Purdue University who reviewed

Wray's paper for the journal Nature Geoscience. "The fact that they were able to see distinct signatures of this mineral means that there's a ton of it there, maybe 80 to 90 percent feldspar in these areas.""

2.3 Terrestrial Separation Methods Currently in Use for Compatible Geology

> *"Electrostatic separation in accordance with the present invention can be used to separate a variety of mineral systems. These systems include, but are not limited to, mineral sand, ilmenite/staurolite, ilmenite/monazite, rutile/zircon, zircon/leucoxene, iron ore/silicate, hard rock ilmenite, hard rock rutile, metal recycling, kyanite/zircon, cromite/garnet, and* ***celestite/gypsum****."* [emphasis added - Ravishankar, 2011]

> *"Investigations were conducted by the lndiana Geological Survey for some dry methods of bene-ficiating low-grade gypsum ore. Seventy-two batch and continuous flow tests were performed with a roller mill, rod mill, pebble mill, electronic color sorter, electrostatic separator, and an air separator. Approximately 650 size analyses and 550 chemical analyses were performed during the investigation." ... "The low-grade material used in these investigations was obtained from the waste pile of the National Gypsum Co.'s plant at Shoals. The waste ore averaged about 67.4% gypsum and was contaminated by various amounts of shale, dolomite, and limestone. All the material had been previously crushed and screened to minus 1 1/4 to plus 3/8 in. X-ray analyses of powdered, sedimentated, gly-colated, and heat-treated samples of the shale showed that it was composed of slightly structurally disordered illite, Fe-rich chlorite, and very finegrained disseminated silt. The clays and silt were partly cemented with carbonate material. Light-gray argillaceous limestone and gray or brown porous dolomite made up most of the carbonate rock contamination." ... "The data obtained from the tests (see Table I) illustrate that the relatively hard carbonate rock allows appreciable beneficiation (13.6 to 18%), but the low strength gypsum and shale allows only minimal separation (3.1 to 7.5%)."* [French, 1966]

2.3.1 Sulfate Phase Separation & Concentration

Sulfate mineral concentrations have been proven to exist on the surface of Mars. It may be possible to find industrial quantities through exploration. A vein of what appears to be gypsum has been found by the Opportunity rover – the so-called "Homestake" vein, named after the Homestake gold mine in South Dakota. "NASA's Mars Exploration Rover Opportunity has found bright veins of a mineral, apparently gypsum, deposited by water" [Webster, 2011].

Finding industrial quantities of gypsum or other sulfate salts on the surface of Mars would start with making a list of the geologic characteristics of environments suitable for their formation and concentration. A global exploration program of identifying suitable environments would be followed up by searching remote sensing data for likely candidates, then finally by sending exploration rovers to the best targets to find and prove the existence of mineral resources. The rovers would require suitable instrumentation to certify the deposit type, chemistry and quality. One site that looks promising is a depression in Noctis Labyrinthus (10.4S, 98.6W on Mars)

which may hold an "inner pit partially filled with several hundred meters of stratified material" [Thollot, 2012].

> *"Three categories of sulfates can roughly be distinguished spectrally: (1) polyhydrated sulfates (i.e., with more than one water molecule per mineral formula, such as hexahydrite MgSO4.6H2O) typically feature both 1.9–2.0 mm and 2.4 mm broad bands, (2) monohydrated sulfates (i.e., with one water molecule per mineral formula, such as kieserite MgSO4.H2O) usually display a broad 2.1 mm band, (3) hydroxylated sulfates (i.e., with hydroxyl (OH) but no water in the mineral formula – notwithstanding the presence of water adsorbed on the mineral surface, such as jarosite* $KFe_3^{3+}(SO4)2(OH)6$ *have distinctive spectra with variable features."* [Thollot, 2012]

2.3.2 Extraction / Refining of Sulfur from Sulfate Minerals

Once suitable deposits of relatively pure Martian sulfate minerals have been identified, the basic chemistry of extracting elemental Sulfur from them should be a straightforward extension of known terrestrial processes. The primary industrial processes for terrestrial Sulfur refining will be summarized below. Research about the direct conversion of gypsum to sulfur will also be presented.

Frasch process

The Frasch process is a method of extracting sulfur from underground elemental sulfur deposits. Most terrestrial sulfur was obtained using the Frasch process until late in the 20th century, when sulfur recovered from petroleum and natural gas became more commonplace [http://en.wikipedia.org/wiki/Frasch_process]. The Frasch process pumps superheated water into the elemental sulfur deposit, which puts the sulfur into solution so it can be extracted. The Frasch process is capable of producing high purity sulfur.

Merox process

The Merox process was introduced to the refining industry more than 40 years ago, and is characterized by the catalytic oxidation of mercaptans to disulfides in an alkaline or basic environment [Sullivan, 2004]. It is primarily used to remove sulfur from a stream of hydrocarbons in a refinery, but requires Hydrogen Sulfide gas to be removed before it can function. Separation of gas from a liquid stream is straightforward, facilitating this process.

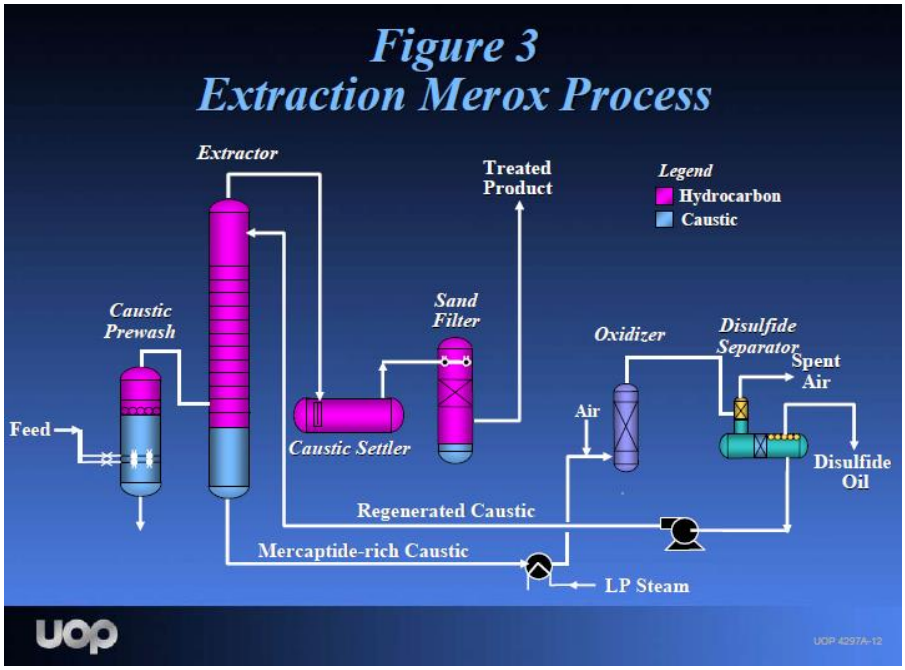

Claus process

The Claus process can recover elemental sulfur by desulfurizing a natural gas stream, and has been utilized since 1883. The multi-step process can recover elemental sulfur from gaseous hydrogen sulfide associated with natural gas, crude oil and other industrial feedstocks. In the thermal step hydrogen sulfide gas reacts at temperatures above 850 °C such that elemental sulfur precipitates process gas cooler [http://en.wikipedia.org/wiki/Claus_process].

Conversion of Gypsum to Sulfur

While not a mainstream industrial process, the direct conversion of gypsum to elemental Sulfur has been studied by the US Bureau of Mines [Rice, 1990]. The basic two-step process combines thermal and hydrometallurgical elements as follows:

> *"…the conversion of phosphogypsum to sulfur is being investigated. The proposed process incorporates the thermal reduction of phosphogypsum to calcium sulfide and a hydrometallurgical treatment to convert calcium sulfide to sulfur. The research described herein is focused on the latter half of the process. It was demonstrated that calcium sulfide could be converted to ammonium bisulfide, and that ammonium bisulfide could be oxidized by air in the presence of a catalyst, to elemental sulfur, which was adsorbed on the catalyst. Two methods for recovering sulfur from the catalyst were developed: (1) thermal treatment to volatilize sulfur, and (2) leaching the sulfur from the catalyst with liquid anhydrous ammonia. Over 90 pct of the sulfur adsorbed on activated carbon (the catalyst) was recovered by both methods. Based upon the encouraging laboratory investigations, a hydrometallurgical scheme was proposed for the overall conversion of calcium sulfide to elemental sulfur."* [Rice, 1990]

2.3.3 Refractory Mineral Separation Processes - Terrestrial Analogies

Separation of sulfates from granular media is currently done terrestrially using gravity, hydrometallurgical and electrostatic methods.

> *"Investigations were conducted by the lndiana Geological Survey for some dry methods of beneficiating low-grade gypsum ore. Seventy-two batch and continuous flow tests were performed with a roller mill, rod mill, pebble mill, electronic color sorter,* electrostatic separator*, and an air separator. Approximately 650 size analyses and 550 chemical analyses were performed during the investigation. Batch samples were tested by the Survey, and most of the continuous flow tests were handled by commercial laboratories."* [French, 1967]

Electrostatic methods in particular are sensitive to humidity and temperature. The addition of reagents can offset some of these problems, enhancing separation efficiency.

> *"Heavy minerals separation processes use extensive physical separation technologies such as gravity, magnetic and electrostatic separations. Particularly, electrostatic separation suffers from separation efficiency issues owing to sensitive variables such as humidity, surface contamination, temperature, particle sizes of the feed and other equipment parameters. The variations in the process conditions during separation result in production rate losses and product quality issues suggesting a need for robust technology. Cytec Industries has developed chemical enhancement technologies for physical separation especially for electrostatic and magnetic separation. This paper will discuss chemically enhanced electrostatic separation of rutile and zircon using feed from various parts of the world. The major advantage of our technology is its bolt-on nature to the existing electrostatic and magnetic separation technology. The separation efficiency was increased from 8–11% with the problematic feeds that are not easily amenable to conventional electrostatic separation without reagents. The increase in separation efficiency reduced the recycle load and saved energy."*[Ravishankar, 2009]

The use of reagents for enhancing electrostatic separation processes has been studied for its effectiveness in gypsum separation and show promise.

> *"The chemical enhancement of electrostatic technology can be applied to avariety of mineral separation including: (a) mineral sand, (b) ilmenite/staurolite, (c) ilmenite/monazite, (d) rutile/zircon, (e) zircon/leucoxene, (f) iron ore—silicate removal, (g) hard rock ilmenite or rutile, (h) metal-plastics recycling, (i) kyanite/zircon, (j) cromite/garnet, and (k) celestite/gypsum."* [Ravishankar, 2009]

2.4 Preliminary Assessment of Process Suitability for Mars Use

A critical step in feasibility assessment for the production of refined Sulfur on Mars is to evaluate the suitability of candidate processes given the anticipated environmental conditions on

Mars. Processes that can leverage the unique environmental characteristics available there should be given favor.

2.4.1 Evaluation of refining process suitability

The Frasch process requires native sulfur as an input feedstock, and is unsuitable for use on Mars until native sulfur deposits are found. The Merox process may have limited applicability for Martian use due to process complexity and feedstock chemistry, and also because no hydrocarbon streams with sulfur contamination have been identified on Mars to date. The Claus process would be a suitable process should sources of hydrogen sulfide gas be found, or provided a high temperature process be used to generate hydrogen sulfide by heating Martian soil. Perhaps the most suitable process was identified by Rice [1990], mainly because gypsum deposits have been identified on Mars, making direct conversion using the proposed methods useful.

2.4.2 Evaluation of extraction and separation process suitability

Separation may not be required if high-grade Martian sulfate deposits can be found. However, should it be required for lower grade deposits, electrostatic gypsum separation and concentration methods used on Earth may be applicable to cases for Mars sulfates. Evaluation of the suitability of candidate processes in low gravity, low pressure and CO2 atmospheric conditions would be an important step in developing enabling technology for Mars sulfur extraction and refining. The dry, low-pressure Mars atmosphere and relative cold temperatures could favor electrostatic separation methods, in locations where separation or ore concentration would be beneficial.

3. Recommendations

Investigating the electrical and magnetic properties of sulfur and refractory minerals could yield novel strategies for separation and production that exploit environmental differences (particularly vacuum and cold).

Separation using electrostatic means should be investigated for vacuum and low gravity conditions, extending work done in nitrogen, etc.

4.0 References

Alexey A. Berezhnoy, Nobuyuki Hasebe, Takuji Hiramoto, and Boris A. Klumov, “Possibility of the Presence of S, SO2, and CO2 at the Poles of the Moon,” PASJ: Publ. Astron. Soc. Japan 55, 859–870, 2003 August 25, http://pasj.oxfordjournals.org/content/55/4/859.full.pdf+html

Paul D. Spudis, “Strange Lunar Brew,” Smithsonian Air and Space Magazine, October 22, 2010, http://www.airspacemag.com/daily-planet/strange-lunar-brew-156444303/

Paul Spudis ""Regolith, the “Other” Lunar Resource," January 5, 2011, Smithsonian Air & Space Magazine, http://www.airspacemag.com/daily-planet/regolith-the-other-lunar-resource-156943194/

Anthony Colaprete, et al., “Detection of Water in the LCROSS Ejecta Plume,” Science 330, 463 (2010); DOI: 10.1126/science.1186986, ftp://cai.igpp.ucla.edu/PHW-F/temp/Lunar%20HOTTIE%20refs/Volatile%20refs/Colaprete%20et%20al-2010-Science-Detection%20of%20water%20in%20the%20LCROSS%20ejecta%20plume.pdf

D. Vaniman, D. Pettit, and G. Heiken, “USES OF LUNAR SULFUR,” 2nd Conference on Lunar Bases and Space Activities, 1988, http://www.nss.org/settlement/moon/library/lunar2.htm

Grant Heiken, David Vaniman and Bevan French, Lunar Sourcebook: A User's Guide to the Moon, Cambridge University Press, 1991, 736 pages, http://cosmochemists.igpp.ucla.edu/lunarsourcebook_searchable.pdf

H Toutanji, Becca Glenn-Loper, Beth Schrayshuen, "Strength and Durability Performance of Waterless Lunar Concrete," MSSP-3: In-Situ Resource Utilization and Space Manufacturing, 43RD AIAA AEROSPACE SCIENCES MEETING AND EXHIBIT, 10 - 13 January 2005

W.G. Wells, Jr., “Olivine Uses and Beneficiation Methods,” Minerals Research Laboratory Bulletin, Vol. 1, No. 2, August 1959, http://mrl.ies.ncsu.edu/reports/1959_Oliv_Uses_Benef.pdf

W.N. Agosto, “Lunar Beneficiation”, in *SPACE RESOURCES Volume 3 - Materials*, NASA Special Publication 509, Editors Mary Fae McKay, David S. McKay, and Michael B. Duke, Lyndon B. Johnson Space Center, Houston, Texas 1992, http://www.nss.org/settlement/nasa/spaceresvol3/toc.html

Sathanjheri Ravishankar, Harsha Kolla, Bing Wang, “Process for enhancing electrostatic separation in the beneficiation of ores,” European Patent EP2342020A1 (WO2010051201A1), Publication date Jul 13, 2011 http://www.google.com/patents/EP2342020A1?cl=en

Dennis Sullivan, “The Role of the Merox Process in the Era of Ultra Low Sulfur Transportation Fuels,” 5th EMEA Catalyst Technology Conference, 3 & 4 March 2004, http://www.uop.com/?document=uop-the-role-of-the-merox-process-in-ultra-low-sulfur-transport-fuels-production-tech-paper

Tianli Zhu, Andreas Dreher, Maria Flytzani-Stephanopoulos, “Direct reduction of SO2 to elemental sulfur by methane over ceria-based catalysts,” Applied Catalysis B: Environmental 21 (1999) 103–120, 3 February 1999, http://ase.tufts.edu/nano-cel/publications/directReductionSO2.pdf

Agosto, W. N., “Electrostatic Concentration of Lunar Soil Minerals,” Lunar Bases and Space Activities of the 21st Century, Houston, TX, Lunar and Planetary Institute, edited by W. W. Mendell, 1985, p.453-464.

Shen, Guoyin, and Peter Lazor. "Measurement of melting temperatures of some minerals under lower mantle pressures." *Journal of Geophysical Research: Solid Earth* (1978–2012) 100.B9 (1995): 17699-17713.

McLennan, S. M.; Boynton, W. V.; Hahn, B. C.; Karunatillake, S.; Taylor, J., "Sulfur Distribution on the Martian Surface Determined by Mars Odyssey Gamma Ray Spectroscopy," American Geophysical Union, Fall Meeting 2009, abstract #P12A-04, http://adsabs.harvard.edu/abs/2009AGUFM.P12A..04M

Liz Fuller-Wright, "Granite on Mars? Scientists find 'highly evolved' rocks on Martian surface." Christian Science Monitor, November 19, 2013 http://www.csmonitor.com/Science/2013/1119/Granite-on-Mars-Scientists-find-highly-evolved-rocks-on-Martian-surface

French, RR, "Dry Beneficiation of Gypsum," AIME Transactions, 1966, Vol. 235, pp. 157-161. http://www.onemine.org/search/summary.cfm/Industrial-Minerals--Dry-Beneficiation-of-Gypsum?d=638C73B4864030E81FFDC2F24C0492F114907F848DADE278CFEF0DC79343F99227027

Patrick Thollot, Nicolas Mangold, Véronique Ansan, Stéphane Le Mouélic, Ralph E. Milliken, Janice L. Bishop, Catherine M. Weitz, Leah H. Roach, John F. Mustard, and Scott L. Murchie, "Most Mars minerals in a nutshell: Various alteration phases formed in a single environment in Noctis Labyrinthus," JOURNAL OF GEOPHYSICAL RESEARCH, VOL. 117, E00J06, published 21 April 2012, http://planetary.brown.edu/pdfs/4380.pdf

[Sullivan, 2004] Dennis Sullivan, "The Role of the Merox™ Process in the Era of Ultra Low Sulfur Transportation Fuels," 5th EMEA Catalyst Technology Conference, 3 & 4 March 2004, http://www.uop.com/?document=uop-the-role-of-the-merox-process-in-ultra-low-sulfur-transport-fuels-production-tech-paper&download=1

[Rice, 1990] David A. Rice, Olice C. Carter, Jr., Alexander May, Margaret M. Ragin, and Robert G. Swanton, "Recovery of Sulfur From Phosphogypsum: Conversion of Calcium Sulfide to Sulfur," US Bureau of Mines Report of Investigations 9297, UNITED STATES DEPARTMENT OF THE INTERIOR, 1990, http://stacks.cdc.gov/view/cdc/10671/cdc_10671_DS1.pdf

[French, 1967] French, R. R., "Industrial Minerals - Dry Beneficiation of Gypsum," AIME Transactions, 1967, http://www.onemine.org/search/summary.cfm/Industrial-Minerals--Dry-Beneficiation-of-Gypsum?d=25B3BCDDE59889EDDE3167DED21EA786F6477C9B0AB15980F3F51EE51758072627027

[Ravishankar, 2009] Ravishankar, S.A. and Kolla, H., "Chemically enhanced electrostatic separation," The 7th International Heavy Minerals Conference, The Southern African Institute of Mining and Metallurgy, 2009, http://www.saimm.co.za/Conferences/HMC2009/203-206_Ravishankar.pdf

---

Web Links:

lunar mars sulfur & aluminum:

http://en.wikipedia.org/wiki/Lunarcrete
http://ntrs.nasa.gov/archive/nasa/casi.ntrs.nasa.gov/19980001900_1997093192.pdf

sulfur in lunar polar volatiles:
http://selena.sai.msu.ru/ber/publications/pasj2449modified.pdf

"mars geology sulfur concentration mechanism"
http://hal.archives-ouvertes.fr/docs/00/80/18/10/PDF/Gaillard_et_al-revised-SPAC917R2.pdf

search "mars crustal granites"; search "mars refractory mineral deposits":
http://www.nss.org/settlement/moon/library/LB2-518-LunarConcreteForConstruction.pdf
http://www.lpi.usra.edu/publications/books/lunar_bases/LSBchapter06.pdf
http://www.lpi.usra.edu/publications/books/lunar_bases/LSBchapter07.pdf

http://arc.aiaa.org/doi/abs/10.2514/6.2005-1436

beneficiation guides (mining)
http://www.csiro.au/Organisation-Structure/Divisions/Process-Science-and-Engineering/mineral-processing-agglomeration/Mineral-beneficiation.aspx
http://www.fipr.state.fl.us/research-area-mining.htm
http://met-solvelabs.com/mineral-beneficiation/
http://www.outotec.com/en/About-us/Our-technologies/Ore-beneficiation/

fluorine beneficiation
http://www.sepfluor.co.za/our-business/beneficiation
http://www.nma.org/pdf/HardrockEMSGuide.pdf
http://www.sgs.com/~/media/Global/Documents/Flyers%20and%20Leaflets/SGS-MIN-WA054-Beneficiation-EN-11.pdf

http://xbmagneticseparator.yolasite.com/
http://www.epa.gov/osw/nonhaz/industrial/special/mining/techdocs/gold.pdf
http://www.whitecase.com/alerts/022014/domestic-mineral-processing-and-beneficiation-in-indonesian-mining-sector/
http://www.whitecase.com/files/Publication/4f1cf976-74ec-49ca-b575-b6ac7b159c20/Presentation/PublicationAttachment/59ca4cb0-404c-4c38-a9f3-7346f3148972/white-case-md-and-partners-alert-domestic-mineral-processing-and-benefi.pdf

http://www.bullion.org.za/documents/COM%20presentation%20on%20Beneficiation%2022%20May%202012%20handout.pdf

slag beneficiation - a useful analogy (esp glass)
http://charah.com/case-studies/igcc-slag-beneficiation-2/
http://www.vtcorpindia.com/iron-ore-pellet-plant-division/
http://www.permanent.com/space-industry-electrostatic-beneficiation.html

http://ntrs.nasa.gov/archive/nasa/casi.ntrs.nasa.gov/20110016173.pdf

Part 6: Lunar Construction (2.5 MB)
T. D. Lin, "Concrete for Lunar Base Construction,"
J. Francis Young, "Concrete and Other Cement-Based Composites for Lunar Base Construction,"
http://www.lpi.usra.edu/publications/books/lunar_bases/LSBchapter06.pdf

Part 8: Oxygen: Predude to Lunar Industrialization (3 MB)
James L. Carter, "Lunar Regolith Fines: A Source of Hydrogen,"
http://www.lpi.usra.edu/publications/books/lunar_bases/LSBchapter08.pdf

http://isru.msfc.nasa.gov/lib/Documents/BenefWksp2010/abstracts/Moats.pdf
http://web.utk.edu/~lataylor/pub-list/microwave1.pdf
library.queensu.ca/ojs/index.php/PCEEA/.../3992?

beneficiation magnesium - SBM Home
plant.psjsale.com/dolomite_crush/beneficiation-magnesium_3461.html?
http://www.onemine.org/search/index.cfm?fullText=Olivine%20Beneficiation&start=120
http://www.planetary.brown.edu/pdfs/3962.pdf

search "beneficiation of lunar regolith"
http://www.onemine.org/search/index.cfm?fullText=Olivine%20Beneficiation&start=120

search "sulfur concrete" and "thiocrete"

search "thiocrete beneficiation" and "sulphur concrete beneficiation requirements"
http://en.wikipedia.org/wiki/Lunarcrete

http://www.lpi.usra.edu/meetings/lpsc97/pdf/1483.PDF
http://ntrs.nasa.gov/archive/nasa/casi.ntrs.nasa.gov/20080022947.pdf
https://journals.uair.arizona.edu/index.php/maps/article/viewFile/14780/14751

CHAPTER 5

Structure Design for Lunar and Martian Infrastructures

INTRODUCTION

We have identified the structures we will investigate and have developed a framework for finite element analysis (FEA) of these structures. Landing pads, roadways, blast walls and storage structures are the basic infrastructure that would be necessary for larger exploratory and research missions that would require multiple landings to the same site. For the landing pad and apron, boundary conditions and loadings include lander thrust, fuel heat, solar energy, and robotic construction interface with lunar soil or rock. Our focus so far has been on identifying the various properties of construction materials and methods as well as the range of environmental loading that will govern the design of each infrastructural element type. We will use the extension of the project to investigate extra-terrestrial specific issues for each infrastructure element with multi-physics finite element analyses.

For landing pads and aprons, analysis will include repeated heating and thrust from multiple landings, ejecta from fuel and dust, hard landings, micrometeorites, and buckling or cracking potential of the pad surface from the extreme environment. High impact loading and thermal stresses coupled with low tensile strength will influence construction joint pattern and frequency.

For blast wall design, our finite element model will again look at rocket fuel heat and thrust, ejecta from fuel and dust, and the robotic construction interface with lunar soil. The intent of the blast wall is to protect nearby storage or facilities and protect distant settlements from lander-induced high speed clouds of lunar dust. We intend to do a shape optimization study of the wall to minimize all of the following: ejecta reflection to the lander, deposition on storage and settlements, and deterioration.

For the roadways, we will investigate solar energy, rover loading and soil/structure interaction considering maximum payload, traction and buckling and cracking potential from high temperature or load gradients. For storage hangars, boundary conditions and loadings include self weight, solar energy, micrometeorites and soil/structure interaction. Issues to be assessed include thermal stress/strain, stability, crack propagation and radiation protection. A study on the impact of temperature gradients on hangar design is included in this report. Constructability and sequence will also influence our recommendations for hangar overall size and shape.

An extensive literature search on properties of sulfur-based, melted, or sintered materials similar to lunar or martian regolith has shown that we do not currently have accurate or precise information about the strength, thermal and other mechanical properties of these potential construction materials for the moon and Mars. Consideration of the variability and lower expected values of strength properties will have a large impact on the reliability and cost of extraterrestrial infrastructure construction. Early missions in extraterrestrial developments should include in situ testing of robotically fabricated construction materials to improve the statistical

confidence of their true properties to give us the opportunity to redesign more reliable and cost-effective structures.

DESIGN VALIDATION

Structural Design and Analysis

We have identified the main structures that would be required to develop a feasible infrastructure design for lunar or Martian research and development. The parameters influencing the design of the proposed infrastructure to be constructed in situ are described in this section.

Landing pad and apron

For the landing pad and apron, boundary conditions and loadings include lander thrust, engine plume exhaust heat and associated rapid thermal cycling, ambient solar energy, and robotic construction interface with lunar or Martian soil or rock. A lunar polar location currently being studied by NASA is used as reference (NASA 2012). The issues required to be investigated with a multi-physics finite element model include repeated heating and thrust from multiple landings, ejecta from fuel and dust, hard landings, micrometeorites, and buckling or cracking potential of the pad surface from the extreme environment. High impact loading and thermal stresses coupled with low tensile strength will influence construction joint pattern and frequency.

Landing pad and apron parameters include:

- Two dimensional surface structure that requires strength and durability to resist the enormous thrust, heat and ballistic ejecta from rocket engine blasting.
- Boundary conditions and loadings include lander thrust, engine exhaust heat, solar energy, and material interface with lunar soil or rock.
- The issues to be investigated with a multi-physics model include repeated heating and thrust from multiple landings, ejecta from fuel and dust, hard landings, micrometeorites, and buckling or cracking potential of the pad surface from the extreme environment posed by repeated Altair reference class heavy lander touchdowns as well as ambient lunar diurnal thermal cycling.
- High impact loading and thermal stresses coupled with low tensile strength will influence construction joint pattern and frequency.
- The structure – regolith interface considering the friction angle, cohesion, regolith density, and any site specific knowledge of the soil formation, soil mechanics, and structure.

Blast wall

For blast wall design, loading and boundary conditions also include lander rocket engine plume heat and thrust, potential ejecta from lander exhaust and dust, and the robotic construction interface with lunar or martian soil. The intent of the blast wall is to protect nearby storage or facilities and protect distant settlements from lander-induced high speed clouds of lunar dust. A shape optimization study of the wall could determine the shape best suited to minimize all of the following: ejecta reflection to the lander, deposition on storage and settlements, and deterioration. Alternatively, designs that avoid the need for elevated structures in the immediate proximity of the landing pad need more in depth investigation since such elements can be a hazard for landers with clustered engines, especially during the deep throttling touch down phase before main engine cutoff.

Blast wall parameters include:

- Rocket plume heat and thrust, ejecta from fuel and dust, and the material interface with lunar soil.
- We intend to do a shape optimization study of the wall to minimize all of the following: ejecta reflection to the lander, deposition on storage and settlements, and deterioration.
- The structure – regolith interface considering the friction angle, cohesion, regolith density, and any site specific knowledge of the soil mechanics and subsurface structure.
- Site preparation will also include some subsurface stabilization and grading before CC machine activity (Thangavelu 2009).

Roadways

For sensitive equipment and material processing operations and other research done at distance from the landing pad, roadways leading to mining sites and hangar or storage structures must also be constructed. For the roadways, loading and boundary conditions include thermal expansion from diurnal solar energy fluctuations and rover loading and soil/structure interaction. Parameters affecting this are maximum payload, traction, and buckling or cracking potential from high temperature differentials or load gradients. Sintered regolith would be more stable than sulfur concrete for roadways as sintered regolith does not change its properties over a wide temperature range (Lee et al 2012). Tamping the surface is one method to stabilize the roadway before topping with sintering or CC machine layering, as it helps to consolidate and strengthen the regolith subsurface (Schrunk et al 2007).

Roadway parameters include:

- One-dimensional extrusion of a flat wide element.
- Surface traction for lunar or martian gravity and regolith and anticipated vehicle mass.
- Investigate solar energy, rover loading and soil/structure interaction considering maximum payload, traction, and buckling and cracking potential from high temperature or load gradients.
- The large diurnal temperature swings on the Moon and Mars will cause expansion and contraction at levels far exceeding construction on earth requiring a different quantity, size and frequency of expansion joints to avoid cracking or buckling of roadways.
- Expansive materials like asphaltic concrete will not be available, so an approach more similar to sidewalk paving of tiled construction will need to be considered.
- Limiting dust on the roadways will influence the approach to expansion joints.

Unpressurized Hangars or Storage Structures

For hangars, boundary conditions and loadings include self-weight, solar energy, micrometeorites and soil/structure interaction. Issues to be assessed include thermal stress/strain, stability, crack propagation and radiation protection. Constructability and sequence would also influence recommendations for hangar overall size and shape.

Hangar or storage parameters include:

- Boundary conditions and loadings include self-weight, solar energy, micrometeorites and soil/structure interaction.
- Self-weight needs to include an additional weight of 3 meters of regolith cover to provide radiation shielding (Benaroya 2010), micrometeorite impact protection (Jolly, Happel and

Sture 1994) and regulating temperatures to which the concrete is subjected (Vaniman et. al 1991).
- Thermal stress/strain, stability, crack-propagation and radiation protection.
- Constructability and sequence will also influence overall size and shape.

If gantry or related moving or point load structures are prescribed to assist in payload movements within these structures, or to help in transfer of payloads from lander to hangar and vise versa, hooks and scars for hard points and load distribution will need to be incorporated with adequate reinforcements and will require further study and recommendations.

LUNAR CONSTRUCTION STRUCTURAL AND ENVIRONMENTAL ISSUES

Infrastructure:
Initial requirements for infrastructure will be landing pads, landing aprons and blast walls for protection of equipment or resources close to the landing sites. Research stations or settlements will need to be further away from the landing path to avoid damage from rocket ejecta and regolith projectiles. This will require construction of roads, dust-free platforms, shade walls, equipment storage hangars and radiation and meteorite protection shelters. All of the above infrastructure can be built from regolith and other ISRU materials utilizing several methods of robotic fabrication investigated in this proposed study. Maximizing ISRU using robotic construction technology as an enabler is the prime driver for this architecture.
Several construction tasks will be necessary to achieve safe and productive conditions for extended human presence at extraterrestrial sites (Mueller and King, 2007):

- Provide hard-surfaced landing pads to reduce, curtail or eliminate the generation of abrasive rocket engine blast ejecta at landing sites.
- Build blast shields to deflect residual ejecta away from personnel and equipment.
- Provide smooth-surfaced utility roads with enhanced traction topping to increase the efficiency of vehicular transport.
- Build level and secure foundations for civil engineering structures
- Provide surface stabilization to mitigate the effects of regolith dust degradation of equipment
- Install thermal, micrometeoric and bulk radiation shielding and emergency shelters for personnel in excess of that which can be affordably launched from Earth.
- Construct equipment storage and servicing hangars in a dust free environment.

Focusing on the Moon as an initial test bed for infrastructure buildup, the lunar surface is scattered with minerals and compounds that may be readily accessed to produce metals, glass, bricks, paints and other materials that are necessary for the construction of permanent settlements and infrastructure. There are two primary approaches considered in this study for construction of bulk infrastructure materials (Lunar or Martian concrete). Sintering or melting of regolith requires high working temperatures and energy but will create more durable concrete for the harsh environment. Sulfur has also been proposed as a binder for waterless construction and will be investigated because of its much lower melting temperature relative to sintered regolith. This

would be appropriate for infrastructure in colder regions of the moon or Mars. We have already conducted experiments creating small samples of sulfur based concrete with regolith stimulant. With either approach, we will also investigate the possibility of using ISRU extracted metals to reintroduce as finite elements or into the regolith mix as a binding matrix to develop tensile strength in the materials. We will first see how much infrastructure can be built without tensile reinforcement to avoid the complexity of requiring metals processing for initial infrastructure.

Material Properties:
The proposed layered deposition of in situ processed materials requires a compression-based structure due to possible lack of in situ materials or early stage processing to reinforce regolith concrete with sufficient tensile strength (although basalt fiber reinforcement could be a possibility). Forms must be developed to ensure a compressive load path or that require a minimal amount of tensile reinforcement of Earth based materials such as the lightweight carbon fiber composites. However, as we have demonstrated by improving tensile strength of structures made by molten regolith mixed with metal powder, with parallel advancements in material extraction, metals from regolith could be reintroduced to the sintering or melting of the regolith to create a composite matrix that would have more substantial tensile properties which could reduce the material and time required for construction.

In-situ processes of molten regolith for robotic deposition require careful investigation of melt chemistry, flow properties, and the cooling process to yield structures sufficiently strong to withstand tensile forces that the different infrastructure forms may be subjected to under thermal gradient and/or blast loading.

Sulfur Concrete:
It should be noted that sulfur concrete is unstable at extreme temperatures. Sulfur starts melting at 119°C but volume changes are noticed at a lower temperature of 96°C. Sulfur concrete also suffers from de-bonding at lower temperatures, but this is debatable. HA Toutanji and Grugel (2008) suggest there is a massive drop in strength when concrete is subjected to repeated freeze-thaw tests (cycling between 21°C to -191°C), whereas H Toutanji, Fiske, and Bodiford (2006) state there is no drop in strength when concrete is cycled from 21°C to -180°C. Further research needs to be done here, as batching of sulfur concrete occurs at 130°C and would be subject to low temperatures the moment it is extruded from the machine for likely lunar development sites in polar regions. Construction could be limited by diurnal cycles or extended through preheating by redirecting solar energy into craters that only experience darkness but otherwise are beneficial locations for development. Alternatively, recently discovered lunar and martian lava tubes may offer the steady temperatures and ambient environment for CC machine sulfur concrete structures.

There is a significant difference in the range of compressive strengths of sulfur concrete reported by different tests. A conservative value has been recommended in this report. The table below shows some testing done with sulfur-based concrete using JSC-1 lunar simulant for the sand and aggregate.

SULFUR CONCRETE		
(JSC-1 : S = 65:35)		
Property	**Value**	**Reference Source**
Modulus of Rupture	8.3MPa	Happel 1993
Compressive Strength	20MPa	HA Toutanji, Evans, and Grugel 2010
Tensile Strength	3.44MPa	H Toutanji, Fiske, and Bodiford 2006
Modulus of Elasticity	20700MPa	Fontana, Farrell, and Yuan 1998
Poisson Ratio	0.24	Hammons, Smith, and Wilson 1993
Impact Test	Refer to the appendix	HA Toutanji, Evans, and Grugel 2010
Thermal Expansion Coefficient	$5.4x10^{-6}$ cm/cm/C	Happel 1993

Table 1: Properties of Sulfur Concrete

Sintered Regolith:

Sintered regolith is relatively stable over a wide range of temperatures (Lee et al. 2012), but its mechanical properties are not understood very well. Apart from compression tests and thermal expansion checks, not much is known about this material. Future tests need to be done to understand the behavior of sintered regolith when it comes to impact loads.

SINTERED REGOLITH		
Property	**Value**	**Reference Source**
Modulus of Rupture	9-18MPa	Happel 1993
Compressive Strength	9-18MPa	Happel 1993
Thermal Conductivity	0.9 to 1.6 W/m K	Mottaghi and Benaroya 2014

Table 2: Properties of Sintered Regolith

Lunar Soil:

The bulk density of regolith ranges from 0.9 to 1.1 g/cm^3 near the surface and significantly increases to 1.9 g/cm^3 at a depth of 20 cm. The average is taken to be 1.7 g/cm^3 (Ruess, Schaenzlin, and Benaroya 2006). This increase can be attributed to the frequent meteorite impacts on the moon's surface. The meteorite impact breaks and loosens up the upper portions of the soil, but causes a tamping effect on the lower portions thereby increasing density. Bedrock is found at a depth of 8-12 m in the highland regions and at a depth of 3-10 m in the mare regions (Brown and Rix 1992). The jump in density at relatively shallow depths will allow for construction of roadways and structures with minimal excavation.

The geotechnical properties of lunar soil are shown in the table below.

LUNAR SOIL		
Property	**Value**	**Reference Source**
Cohesion	1.0 kN/m^2	Mitchell and Houston 1972
Friction Angle	50°	Mitchell and Houston 1972

Bulk Density	1.7 g/cm^3	Ruess, Schaenzlin, and Benaroya 2006
Modulus of Subgrade Reaction	1000 kN/m^2/m	
Porosity	45 (at the surface)	
Compressibility	C_c = 0.3 (loose regolith)	
	C_c = 0.05 (dense regolith)	

Table 3: Properties of lunar soil

It is interesting to note that because of the low lunar gravity, trenches with vertical walls can be excavated to a depth of 3m. Boreholes remain stable at that depth too (D. Carrier 2005). Further study on using robotic construction to make subsurface structures should be explored to benefit from reduced impact from micrometeorites, reduced direct galactic radiation, reduced construction time, and reduced thermal variation. In this respect, lava tubes mentioned earlier may offer natural protection from the harsh extraterrestrial surface environment to build and commission permanent structures.

Environmental Factors:

Dust is a primary concern and architectural designs must address this concern directly. Meteorites, radiation and light intensity can also be a problem. The regolith concrete must form the desired inhabited and uninhabited spaces as well as resist and provide durability against meteorites, radiation, thermal loading and direct sunlight. An optimal solution should be sought that takes advantage of increased buckling strength to minimize the material but still resist meteorites and provide a barrier for radiation.

Severe temperature differences exist between stark daylight and shadow, and even more severe surface temperature differences can be found in the diurnal thermal cycling. Fixed structures induce internal stresses based on thermal gradients and temperature differences from initial construction temperatures. A structure that is partially shaded can develop large unbalanced thermal stresses. Uniformly heated or cooled structures can be designed more readily to accommodate thermal expansion and contraction and minimize the unbalanced stresses that may introduce tension and cracking. Severe temperature differences may also arise based on sun angle. Sunlight can be harvested and if consideration is being made for developments near the lunar south pole, this will be necessary to reduce heating demands for habitation and for fluidity of the concrete regolith during construction.

Solar intensity will influence both architectural and structural design. To avoid extreme variation, forms need to be sought with similar sun exposure throughout their exposed surface. Particular attention will therefore need to be paid to the geometry and behavior of the sun with regard to the solar envelope. Layout of Moon development should carefully consider the long shadows that will occur at a polar development to ensure equal exposure. Shading walls can assist in maintaining a smaller range of temperature variation and can be slender due to increased buckling capacity with lower gravity and also due to lower wind and seismic lateral loadings. Thermal blankets will need to be deployed extensively, especially on dynamic structures, surface vehicles and systems that are subject to rapid temperature swings as they execute their missions.

The exterior surfaces of permanently located structures should also be form-found to counter the thermal gradient of the exposed side to the shaded side to minimize development of tension on any surface. A double wall system could be used to heat gases or fluids that could be used for any development needs including conditioning air and water for human use or for irrigation of moon farming. It could also be used as a geothermal heat pump to increase temperatures above the low below surface levels to temperatures within the space required for experiment or temporary habitation. Incidentally, water is also a very good material for radiation shielding. 30cm thick water or ice is sufficient protection, and if methods can be devised to mine and use lunar water for this purpose, this procedure could substitute for a much thicker 3.5m coat of lunar regolith that is recommended for the same radiation shielding effectiveness.

Thus, to summarize, the major environmental problems from a structural analysis point of view are: dust, micrometeorites, radiation and thermal issues which can cause stresses in structures. Since none of these structures are meant to be 'habitable', pressurizing them is not going to be a requirement and thus will not be considered. These factors, along with other factors like lander plume exhaust thrust, etc. are quantified below.

Thermal issues:

Temperatures on the moon have drastic swings, with a drop of 5°C per hour (Sherwood and Toups 1992). Equatorial temperatures range from 374k during lunar noon to 120k during the night. Polar temperatures range from 160k during the lunar noon to 120k at night (Heiken, Vaniman, and French 1991). Since 30 cm of regolith cover is enough to dampen the fluctuations in temperature by 280K (Vaniman et al, 1991), providing 3-3.5m regolith cover for radiation protection is more than enough to dampen the swings effectively.

The thermal coefficient values of various asphalt mixtures for roadway construction on earth in one report ranged between 2.046 and 6.321 x 10^{-5} cm/cm/°C (Mamlouk, Witczak, and Kaloush). Sulfur-based concrete has a thermal coefficient of 5.4 x 10^{-6} cm/cm/°C, one order of magnitude smaller. This means temperature swings ten times larger than what we see here on earth would be required to create the same extent of cracking or buckling of roadways.

Dust:

The particle size ranges from 1-100 micrometer (Morris et al. 2012) with an average of 70 μm. During landing, these particles can speed up to 3000 m/s and travel at an angle of about 3° to the horizontal (Susante 2012). These particles require a blast wall which can protect any equipment and personnel near the landing pad from the spray. Walls around 20m away from the site tend to work most effectively (Morris et al. 2012).

Micrometeorites:

Micrometeorite weights can be taken as 1 gm and their speeds range from 10-15 km/s (Benaroya 2010). These micrometeorites can be stopped by 3-4 m regolith cover on top of the structure (Jolly, Happel, and Sture 1994).

Radiation:

Radiation consists of solar photons and galactic cosmic rays. The radiation can be brought down to acceptable levels with about 3.5 m regolith cover or 30cm thick water or ice can do the same once methods can be devised to create lunar water.

Clearly, storage hangars will benefit from a 3.5 m regolith cover. This will protect the hangar and its contents from temperature swings, radiation, and micrometeorites.

Vehicular Loading:
Other major conditions include the landing of the craft, and the weight of the rovers on the road. The lander thrust is about 50 metric tonnes on a 10 m^2 area, or approximately 49 kPa. This thrust along with the actual weight exerted by the craft onto the landing pad are the major compressive stresses experienced by the pad. Other infrastructure design forces include the weight of the rover on roads made of sintered regolith, but with a maximum weight of 2300 kg (Spudis and Lavoie 2010), and considering the moon's gravity is only $1/6^{th}$ of the Earth's, this should not be the critical case.

The following calculations show that sintered regolith has enough compressive strength (Lee et al. 2012). Considering a payload of 765 kg and a lander with 4 legs, each leg supports a weight of 191.25 kg, which is reduced to 31.875 kg considering moon's gravity ($1/6^{th}$). The compression stress under the lander foot measuring 30 cm would be 4.42 kPa. Another case would be a SELENE-2 in JAXA with a weight of 520 kg, which translates to a weight of 21.67 kg per leg. For this lander, the foot diameter is only 25 cm, which yields a compressive stress of 4.33 kPa. These pressures are one tenth of the lander thrust pressures and sintered concrete has a compressive strength of 9-18 MPa, which is more than 100 times stronger than the thrust pressures. These loads are very small considering the compressive strength of sintered regolith. Hence, it can be used to construct a landing pad surface.

However, for emplacing large payloads on the Moon, the landing pads need to be designed for repeated sorties of a heavy lander such as an Altair class reference lander, see image below.

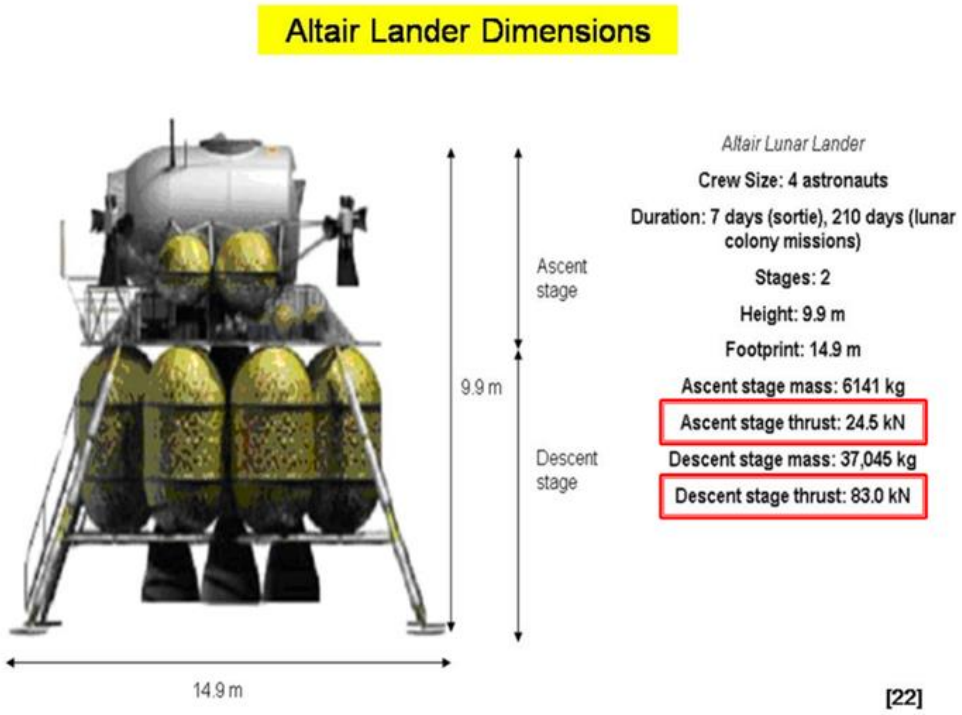

Figure 1. *Altair Lunar Lander properties affecting infrastructure design.* [Credit: NASA JSC]

There is not much information present on the hard landing of the spacecraft on the pad. Impact tests need to be done on sintered regolith slabs to find out the effect of impact and crack lengths.

The heat of the plume can also be an issue, and the landing pad could experience temperatures of about 1000-1500°C. This however, is not a problem as the vacuum and the lack of atmosphere cuts out the heat given by the spacecraft until the last few seconds, where it does not have a severe effect on the landing pad. However, further research needs to be done to understand the fatigue effects of repeated heating and cooling off on the landing pad. If refractory tiles are proposed, thermal spalling will be an issue that needs to be addressed.

Optimal Design:

We have investigated a process to assist in finding the optimal solutions for multi-objective constraints. Optimal designs will consider the following:

- Form optimization to minimize materials
- Form optimization to minimize construction time
- Form optimization to minimize risk to desired performance level
- Layout optimization for same parameters above

Transport, deployment, performance, endurance/maintenance and expansion cost will be common bases for assessing both the robotic techniques and the different infrastructure elements assessed.

Lunar Construction of Protective Hangar:
Optimal design of hangar geometry to minimize tensile stresses for ambient conditions has been investigated. Geometries for completed hangars have been analyzed considering extreme temperature differential between sunlit and shaded surfaces to determine the optimal shape. An optimization algorithm that is being used in the construction industry by structural engineers and architects was used and this work was done in conjunction with architecture students interested in "informed form." We used a Rhino 3D modeling plugin named Galapagos, a genetic algorithm optimization routine native to the Rhino software that can import and export to structural analysis software. The algorithm randomly chooses from a number of defined variables to create a generation of results. The "fitnesses" of the results are compared to the desired optimization function and another generation is created. "Mutations" are used to ensure that the entire solution space is being explored instead of narrowing in on a local best fitness.

A funicular shape definition was used to find the best set of parameters that would provide the necessary shelter volume with the lowest peak tensile stress. Non-ductile materials like concrete, ceramic and glass can sustain some tension without tensile reinforcement while have much more strength in compression. Like the Roman arch, we need to discover the shape for lunar conditions that will minimize our need to use tensile reinforcement that would require great costs to transport or process.

The solution space to be searched using the genetic algorithm is derived from the following variables:

- Ratio of arc length to base width
- Height of structure
- Thickness of walls
- Clearance (constant values that must be exceeded)

The structure is analyzed for moon gravity and a temperature increase of 200 K on one side of the enclosure representing conditions near the south pole with low horizon angles of sunlight. The results shown in the figures below are just 16 samples from hundreds of analyses showing a range of "fitness values" for minimizing the peak tension stress while meeting clearance requirements. The results show that a few variations of the shape and thicknesses actually reduce the peak stress down into the range of terrestrial concrete rupture stresses. Further studies will refine the analysis for expected material properties of sulfur-based or sintered concrete.

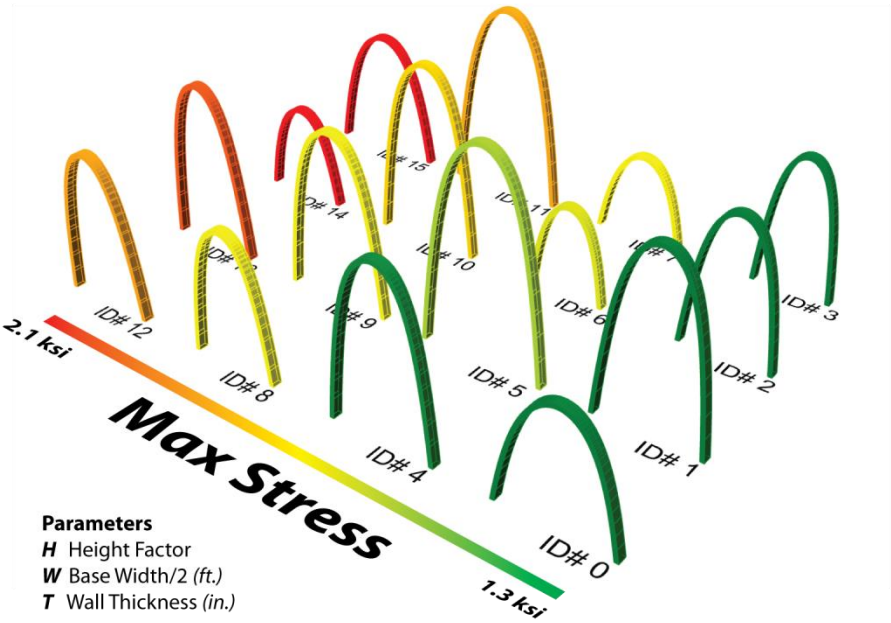

Figure 2. *Peak stresses in several variations of the shelter optimization.*

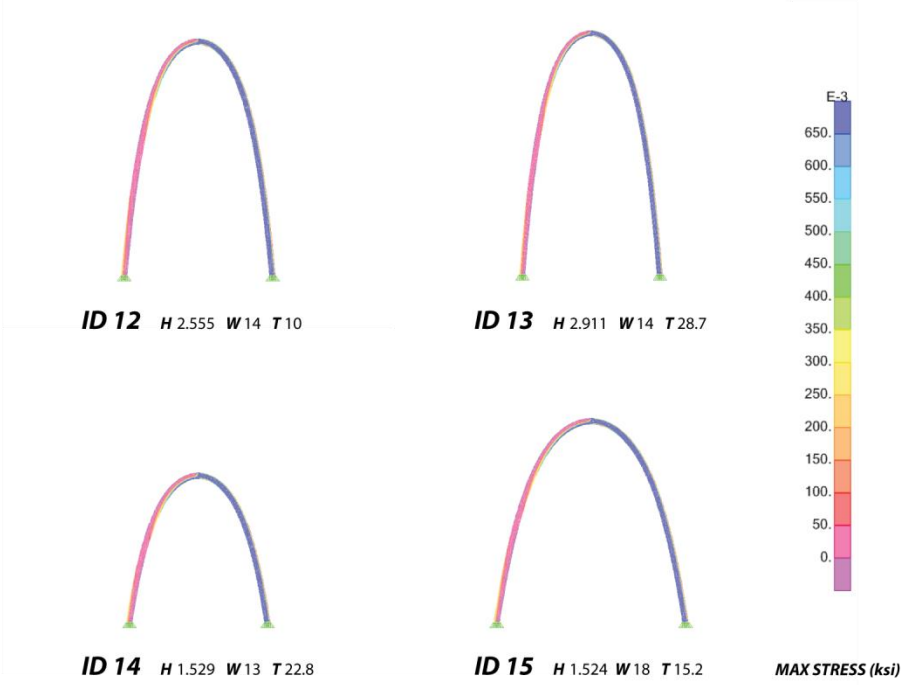

Figure 3. *Results with higher peak tensile stresses for low-horizon sunlight from the left. Note that in each of these examples nearly half the structure exceeds 600psi, a common rupture tensile strength for terrestrial concrete.*

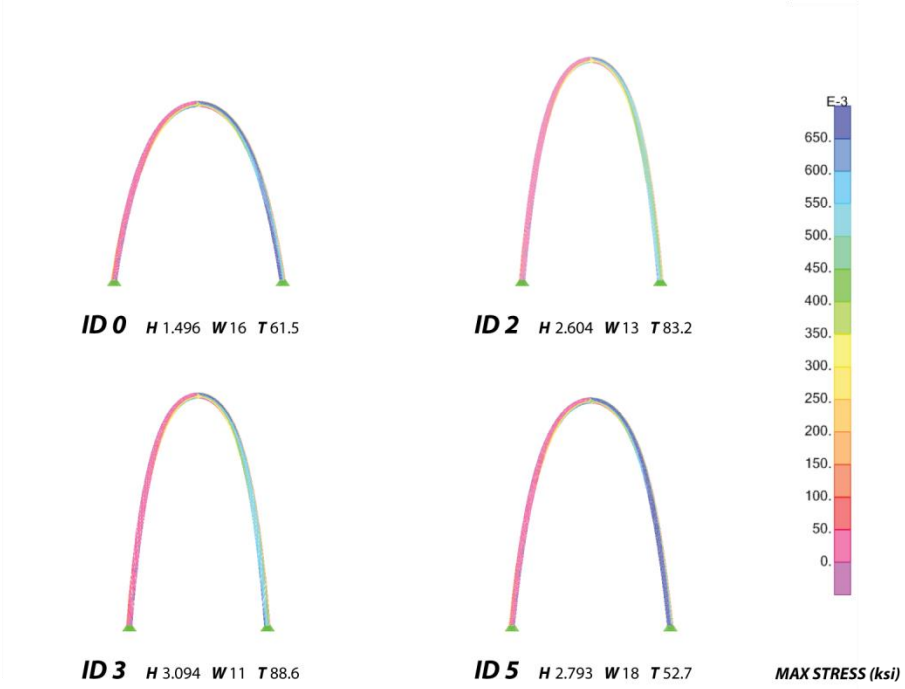

Figure 4. *Results with low peak tensile stresses for low-horizon sunlight from the left. Note in example ID 2 that only a small portion exceeds 600psi, a common rupture tensile strength for terrestrial concrete.*

Material Processing Performance:
Performance metrics will include strength, hermeticity, durability under lunar thermal cycles, and adhesion to underlying base layers. Additional metrics apply to processability, including melt temperature, viscosity, heat capacity, and resistance to thermal shock. The technical approach will aim at assessing suitable mineral formulations and grit sizes for robotic construction that are being developed concurrently at Kennedy Space Center, and demonstrating performance metrics through simulation and testing of small samples made in USC laboratories. Additives (available in situ) will be selected to adjust melt viscosity and flow characteristics. Predictive modeling using FEA, fluid dynamics, and thermal equations will support the materials effort. These models (calibrated to fit our experimental results) will help guide the necessary layer thicknesses, rheology, build speed, and reinforcement architecture.

Evaluation of the Radiation-Shielding Efficacy of Structures and Designs:
The hazards of space radiation and their effective mitigation strategies continue to pose special science and technology challenges to NASA. The NRC identifies radiation protection/mitigation as the number one challenge facing human spaceflight and places it among its top 16 recommended technology priorities in a recent 2012 study[1].

Plagued with largely unpredictable radiation environment and uncertain radiobiological effects, current radiation exposure and risk estimates for extended (> few months) and deep (beyond the confines of the Earth's magnetosphere) space exploration suggest that shielding will be inevitable. It is widely accepted now by the space radiation community that shielding space

[1] http://www.nap.edu/catalog.php?record_id=13354

vehicles and structures will have to rely on new and innovative materials since aluminum, and all other metals for that matter, are known to be poor shields against the particulate and highly ionizing nature of space radiation. At the same it is accepted that shielding materials alone, within realistic volume and mass, are not able to perfectly shield against the deeply penetrating energetic particles of space radiation.

As a result, current shielding solutions – motivated and constrained by power and mass limitations – couple this realization with the emerging trend (and eventual) requirement towards "multi-functionality," both in design concept as well as material function and composition. Multi-functionality usually implies that a radiation shielding material, a new polymer-based composite, for example, in addition to its shielding function, must also be able to provide non-radiation functions like structural support or other system or mission support in general.

Shielding efficacy of a structure is both material and geometry dependent. Smart structures combine multi-functionality with optimized geometry. This optimization adds to the complexity in both design (3D) and choice of materials and their functions. Hence, evaluation of the shielding efficacy of such structures is necessarily an iterative and intensive 3D radiation-transport problem.

NASA MSFC through various recent space radiation and radiation-protection related programs and projects has developed a core experience in Geant4-based radiation-transport simulations. Geant4 is a powerful tool-kit originally designed by CERN, http://geant4.cern.ch/, to help design and validate sophisticated particle detectors for use in high-energy particle physics research. It is an open source with strong support network worldwide. Geant4 is an inherently 3D simulation suite covering an extremely wide range of energy as well as physics of radiation-matter interactions. Today, Geant4 is used for various 3D radiation-transport applications ranging from medical to space, in addition to its intended nuclear and particle physics applications.

Using standard CAD or similar format files of generated designs or structures we will perform Geant4 radiation-transport simulations and analyses for them. Evaluation of their shielding efficacy will be done under various space-radiation environments and for various material and geometry combinations, validating their radiation-smart design. This portion of research will be conducted by our MSFC collaborator under MSFC support and at minimal cost to the proposed Phase II project.

MARTIAN CONSTRUCTION STRUCTURAL AND ENVIRONMENTAL ISSUES

Environmental Factors:

Thermal Issues:

From a structural point of view, the thermal conditions on Mars are a lot more hospitable as compared to the moon. Surface temperatures range from -87°C to -5°C with an average of -63°C, as compared to the moon where the swings are to the order of 250°C. The lower average temperature is due to Mars' greater distance from the Sun. The lower range of temperatures can be attributed to the atmosphere on Mars, which also keeps micrometeorites at bay. The existence of an atmosphere, while limited in comparison to the Earth's, means that the regolith cover on

top of structures can be reduced to just 1m of cover to protect just against radiation instead of being required for temperature swings and micrometeorites.

Dust:
The presence of an atmosphere greatly reduces particle velocities to acceptable limits. However, dust storms are a huge problem. They can take weeks to subside, which means solar power can no longer be considered a reliable source for energy. Mars receives less than half the specific solar flux the Earth and Moon does, and the elliptical orbit causes a 39% annual insolation variation (Benaroya 2010). Particle size distribution of martian regolith ranges from 0.07 to 0.8mm. Thus the dust is very fine and has the consistency of smoke (Alshibli and Alsaleh 2004).

Wind:
Wind speeds are generally very high on Mars (to the order of 100m/s) but it does not have a major structural impact because the atmosphere is thin (0.6KPa, as compared to 101.3KPa on the Earth) (Benaroya 2010).

Frost:
Permafrost occurs through most of the Martian surface apart from the equatorial belt, thus foundations require special thermal management designs (Benaroya 2010). Much like construction in Northern climates on Earth, foundations would need to be excavated deeper into the ground to get below the depth of dry ice / water ice into sturdy bedrock. This minimizes heaving and cracking of the structure with seasonal or other temperature swings in and out of ice, liquid and gas states. Thickness of dry ice ranges from 1m at the north pole to 8m at the southern pole (Byrne and Ingersoll 2003). Water ice has a thickness ranging from 5-18 cm at some polar locations (Smith et al 2009).

Radiation:
Radiation consists of solar photons and galactic cosmic rays, but it won't be as big an issue as on the moon due to presence of an atmosphere. One meter of regolith cover or 30cm thick of water or ice should suffice (Simonsen et al 1991).

Gravity:
Gravity is 3/8g, or 3.67m/s^2. While lighter than on Earth, weights are 2.25 times larger than on the moon. Consider the maximum possible payload of a craft on mars to be around 20000kg (Braun and Manning 2007). For a craft with 4 legs / tires, each one supports a mass of 5000kg (49.0kN), which is reduced to 18.4kN considering Mars' gravity, which can be taken up by cast basalt (Compressive strength of 300MPa).

Material Properties:

Martian Regolith holds about 1-3% water content and has a density of about 1150-1600 kg/m^3, and can be compressed into bricks by just cold pressing it. These ‘bricks’ have a compressive strength of around 5MPa (Badescu 2009). These cold-pressed blocks are also known as ‘Duricrete’ (Boyd 1989).

Another method would be to form martian basalt by melting and slowly cooling regolith to avoid crystallization. Though martian basalt is much stronger, Duricrete requires minimal energy. The properties of martian basalt and regolith are given below.

Martian Regolith		
Avg Bulk Density	1.52 g/cm^3	Alshibli and Alsaleh 2004
Specific Gravity	2.62 g/cm^3	Alshibli and Alsaleh 2004
Thermal Conductivity	0.105 W/m^{0}K at 210K	Zent and Hudson 2009
Cohesion	0.238 KPa	Beegle et al 2007
Friction Angle	36.6°	Beegle et al 2007

Table 4: Properties of martian soil

Cast Basalt		
Specific Gravity	2.9-3.0 g/cm^3	Benaroya 2010
Compressive Strength	300MPa	Duke, Benaroya, and Bernold 1998
Bending Strength	40MPa	Benaroya 2010
Tensile Strength	10MPa	Benaroya 2010
Thermal Conductivity	0.7KCal/m^2/Hg°C	Benaroya 2010
Thermal Expansion	77-86 x 10-7 / °C	Benaroya 2010

Table 5: Properties of temperature-controlled basalt bricks

LUNAR AND MARTIAN CONSTRUCTION SUMMARY

Summary of parameters influencing infrastructure design:
We have reviewed information that will assist in determining a figure of merit for the Contour Crafting construction of infrastructure on the moon and mars. We have also developed a process to assist in finding the optimal solutions for multi-objective constraints. The main parameters influencing constructability and structural performance include:

Materials

- Regolith binding agents
- Mechanically hewn and shaped lunar rock
- Crushed lunar aggregates in a range of shapes and sizes
- Powders and other fines for extensive use in paints and markers
- Extracted metals
- Regolith with extracted metal matrix
- A range of fiber glass materials – fibers to fabrics
- Structural properties

Construction

- Tele-operated
- Some human supervision – co-robotics
- Sintered
- Dry packing
- Other deposition techniques

Structures

- Landing pads
- Roadways
- Equipment shelters
- Shade walls
- Tensile Fabric structures
- Thermal blankets
- Platforms
- Other infrastructure (solar panels / communication equipment)

Environmental Factors

- Dust
- Micrometeorites
- Radiation
- Thermal issues (shade vs. sunlit, diurnal, regional variation)

Severe temperature differences

- Fixed structures induce internal stresses based on thermal gradients and temperature differences from initial construction temperatures.
- A structure that is partially shaded can develop large unbalanced thermal stresses.
- To avoid extreme variation, forms need to be sought with similar sun exposure throughout their exposed surface.
- Particular attention will therefore need to be paid to the geometry and behavior of the sun with regard to the solar envelope.
- Cooling rates of sintered regolith

Economics

- Form optimization accounting for crew and robot safety issues during buildup and over the lifecycle of structures
- Form optimization to minimize materials and tools
- Form optimization to minimize construction time
- Energy economics
- Form optimization to minimize risk to desired performance level
- Layout optimization for same parameters above

Note that Contour Crafting is an enabling technology. Parameters listed above affect a whole range of extra-terrestrial materials, systems and construction methods, and we are currently studying how to utilize Contour Crafting in the most effective way, applying synergies with existing and proposed NASA tools, systems and strategies.

Transport, deployment, performance, endurance/maintenance and expansion cost will be common bases for assessing both the robotic or co-robotic techniques and the different infrastructure elements assessed.

Summary of Material Properties:
While some research has been done to test different in-situ construction techniques using Martian and lunar simulants, many more mechanical property tests should be performed to gain confidence in the reliability of extra-terrestrial fabricated materials. The experiments that have been performed suggest that Martian and lunar construction materials could have similar properties to our Portland cement based concrete here on earth, which is promising for developing infrastructure required for future research and development. Since tensile reinforcement is exorbitantly expensive to import, future testing should focus on tensile strength and fatigue of these materials to predict the durability and reliability of the different infrastructural forms.

Strength and Density Comparison of Construction Materials					
	Mars - Cast Basalt	Mars - Consolidated bricks	Moon - Sintered	Moon - Sulfur Concrete	Earth
Density	2.9-3.0 g/cm^3	2.6 g/cm^3	> 1.9 g/cm^3	1.7 g/cm^3	1.4 - 2.4 g/cm^3
Compressive Strength	300MPa	5MPa	9-18MPa	20MPa	15-60MPa
Tensile Strength	10MPa	-	-	3.44MPa	2.5-5.5MPa
Thermal Expansion	7.7-8.6x10^{-6} /°C	-	-	5.4x10^{-6} /°C	12x10^{-6} /°C

Table 6: Comparison of properties for different construction materials

WHAT IS ANTICIPATED AFTER PHASE II

After Phase II, we anticipate NASA and the Army Corps of Engineers to fund Phase III of the project to further the development of these promising technologies and the structures they can produce. As an initial next step beyond Phase II, samples of infrastructure elements subject to lunar and Martian environmental loadings would be made using robotic construction technology (TRL-4). This will help validate FEA simulations and the feedback may influence refinements to the infrastructure designs. After that, samples of infrastructure elements would be made with robotic construction methods in an environment similar to the Moon or Mars and subject to Lunar and Martian environmental loadings (TRL-5). This will also help validate FEA simulations and the feedback may influence refinements to the infrastructure designs. Further maturity of the robotic construction technology and structures it can make would lead to full scale prototypes of infrastructure components built in vacuum or Martian-like atmosphere and be subjected to thermal and blast loading (TRL-6). This test performance will be used to demonstrate agreement with FEA simulation predictions.

In addition to research that will advance the maturity of this architecture, we anticipate other divisions of NASA to be interested in expanding the robotic construction methods to build other types of ISRU based components beyond basic infrastructure. Robotic construction technologies could build tools, other robots, scientific equipment and many other objects that can be formed from excavated and processed extraterrestrial materials. We also anticipate major contributions by robotics researchers at NASA divisions to integrate our proven fabrication technologies with space-worthy advanced class of NASA robotics hardware and intelligent software. Once such integration materializes exciting demonstrations at sites like D-RATS could be performed and following successful demonstration and refinement the ultimate dream of actual Lunar and Martian settlement construction will be materialized.

Automated building technologies will revolutionize the way structures are built on Earth, in dense urban environments, in difficult-to-build and difficult-to-service sites, or in remote and hostile regions of the globe. The technologies under development by our group have the potential to simplify construction logistics, reduce the need for hard physical labor by assigning humans to a strictly supervisory role, eliminate issues relating to human safety, and produce intricate and aesthetically refined designs and structures at significantly reduced construction cost. Space architecture in general and Lunar and Martian structures in particular will also provide a rich new aesthetic vocabulary for architects to employ in the design and creation of buildings that employ high technology and building information modeling that is vital for optimizing use of materials and energy that is critical to building economics. We anticipate this NIAC initiated endeavor to ultimately lead to revolutionizing construction on our planet and significantly impacting the quality of life for billions of people and improving the state of the earth environment.

S CONCRETE DATA

Paper	Authors	Specimen Details	Mix Details	Compressive Strength
Investigation of Molten Sulfur Concrete as a Structural Material	US Army Corps of Engineers	4 x 8 Cylinder	>45.9% CA, 34.6% FA, 11.5% S Cement, 8% Class F flyash >Mixing done in trucks at 132°C	54.7MPa (mean)
Production of lunar concrete using molten sulfur	Dr. Husam A Omar	2' cubes (S + JSC-1 used in diff proportions)	>S + JSC-1 used in different proportions. % of S = 25,30,35...70 >Metal and glass fibers used >Metal Fibers added at 2% by weight and glass fibers added at 0.35% and 0.5% by weight	24.0MPa (for 30% S) 33.8MPa (for 35% S) 24.4MPa (for 30% S, reinforced) 43.0MPa (for 35% S, reinforced)
Performance of "waterless concrete"	Toutanji, Steve Evans, Grugel	2' cubes	>35% S and 65% JSC-1 >Silica-Sulfur binder + JSC-1 specimens also prepared >Mixed at 140°C-150°C	22MPa
Structural Design of a Lunar Habitat	Ruess, Schaenzlin, Benaroya	--	Water has been used here, not sulfur	39-75.7MPa
Mechanical Properties and Durability Performance of "waterless concrete"	Toutanji, Grugel	2' cubes for almost all the tests 1' cubes for the severe freeze-thaw test	35% S and 65% JSC-1 25% S, 20% Silica, 55% JSC - 1 2 types of cycles : >21°C to -27°C (Light freeze-thaw) >21°C to -191°C (Severe freeze-thaw)	S+JSC-1: 17.3MPa S+JSC-1+SiO2: 22MPa Light Freeze Thaw S+JSC-1: 17.3MPa Light Freeze Thaw S+JSC-1+SiO2: 19.4MPa S+JSC-1: 15.51MPa (at constant -27°C) S+JSC-1+SiO2: 19.4MPa (at constant -27°C)
Analysis of lunar-habitat structure using waterless concrete and tension glass fibers	Toutanji, Meyers	2' cubes	35% S and 65% JSC-1	--
Guidiing for mixing and placing sulfur concrete in construction	ACI 548.2R-93, Reapproved 1998		Not explicitly given	27.6MPa
Experimental Study of waterless concrete for lunar construction	Won Koh, Yoo,	5cm cube	Not explicitly given	10.3MPa
Sulfur Concrete - A viable alternative for lunar construction	Gracia, Casanova		Not explicitly given	34MPa
Development and application of lunar concrete for habitats	Toutanji, Fiske, Bodiford	2' cubes	35% S and 65% JSC-1	Not explicitly given
Manufacture and properties of sufur mortar for lunar applications	Roqueta, Casanova	4x4x16mm casts	S + JSC -1 used, with S% = 25,30,35,40	25% = 26.0+-3.0MPa 30% = 39.3+-6.1 (sample a) 30% = 41.7+-8.0 (sample b) 30% = 38.3+-11.6 (sample c) 30% = 27.9+-3.0 (sample d, poorly compacted) 35% = 46.6+-1.2MPa 40% = 54.6+-1.2MPa 100% = 12.2.+-2.2MPa

Paper	Tensile Strength	Other Test Results	Other data in the paper
Investigation of Molten Sulfur Concrete as a Structural Material	2.4MPa (splitting tensile test, mean) (Splitting tensile test = 4.5% of the compressive strength)	**Modulus of Elasticity :** 32400MPa (mean)	Compressive creep tests Freeze and Thaw durability, test conducted on beams Bond Tests Beam Tests
Production of lunar concrete using molten sulfur	>No tensile test results given >Glass Fibers weaken the Comp Str by 27% and tensile strength by 20%		Data on workability was given. Sulfur needs to be higher than 30% in the mix ratio for smooth workability
Performance of "waterless concrete"	Not given	**Impact Test :** > 1mm diameter aluminum projectile @> 5.85km/s >Hole had a 3.1mm central depth. Crack exceeds to 1cm into the sample below the crater	
Structural Design of a Lunar Habitat	Not given	**Thermal Expansion Coeff :** 5.4 x 10^-6 cm/cm/°C **Modulus of Elasticity :** 21400MPa	
Mechanical Properties and Durability Performance of "waterless concrete"	>Fiberglass used here for testing >Sample w/o fiberglass : 5.8MPa >With long drawn fibers : 9.27MPa >With short drawn fibers : 9MPa (mixed 1% by mass)	Continuation of the compressive test results : >The average maximum compression strength for the non-cycled samples was 35MPa >It was 7MPa for the cycled ones (severe freeze-thaw test)	>Here, freeze and thaw experiments were also conducted >Silica improves compressive strength by around 26% but it reduces workability, and causes a more brittle failure >There was no difference in samples cycled between 21°C to -101°C >Mentions the use of fiberglass
Analysis of lunar-habitat structure using waterless concrete and tension glass fibers	Tensile Str of S+JSC-1 concrete is 500psi		>Silica improves compressive strength by around 26% >Here it says that there is no change in strength when subjected to a long duration of freeze and thaw exposure which is from -30°C to 21°C
Guidiing for mixing and placing sulfur concrete in construction	4.1MPa	**Thermal Expansion Coeff :** 15x10^-6/°C **Modulus of Elasticity :** 20700MPa – 27600MPa **Flexural Strength :** 5.2MPa	
Experimental Study of waterless concrete for lunar construction	7.13MPa		
Sulfur Concrete - A viable alternative for lunar construction			>Monthly variations should not exceed 114°C (to prevent melting of Sulfur) >Temperature should also be lower than 96°C to prevent volume change in the concrete
Development and application of lunar concrete for habitats	Tensile Str of S+JSC-1 concrete is 500psi		>Silica improves compressive strength by around 26% >Monthly variations should not exceed 114°C (to prevent melting of Sulfur) >Temperature should also be lower than 96°C to prevent volume change in the concrete >Here it says that there is no change in strength of S+Silica concrete when subjected to severe freeze and thaw exposure which is from -180°C to 21°C
Manufacture and properties of sufur mortar for lunar applications	4.8MPa 7.1MPa 6.1MPa 7.0MPa 4.2MPa 9.6MPa 8.6MPa 1.6MPa	Tensile Strength Values = 15% of Compressive Strength Values	The amounts of S used in the preparation of mortars with JSC-1 are substantially higher than in the case of commercial Sulfur concrete, where the mix proportions are b/w 10-20%. This is because the JSC-1 has a higher surface area with respect to the conventional, coarse grained aggregates so we need more cement to coat the aggregate surface.

Paper	Additional Notes
Investigation of Molten Sulfur Concrete as a Structural Material	
Production of lunar concrete using molten sulfur	Here, the paper says that the fiberglass fibers reduce the strength, and only metal fibers are used to increase the strength
Performance of "waterless concrete"	Huge difference in the values between this paper and the previous one even though the specimen, and the test appears to be the same
Structural Design of a Lunar Habitat	
Mechanical Properties and Durability Performance of "waterless concrete"	>Here, it says fiberglass is used to IMPROVE the tensile and flexural strength, contrary to the second paper >The results were very unfavorable for samples cycled between 21°C to -191°C
Analysis of lunar-habitat structure using waterless concrete and tension glass fibers	>Here it says fiberglass significantly improves the strength of the material
Guidiing for mixing and placing sulfur concrete in construction	
Experimental Study of waterless concrete for lunar construction	
Sulfur Concrete - A viable alternative for lunar construction	
Development and application of lunar concrete for habitats	
Manufacture and properties of sufur mortar for lunar applications	

References

Allen, CC, KM Jager, and RV Morris. 1998. “JSC Mars-1: A Martian Soil Simulant.” *Proceedings of Space 98*: 469–476.

Alshibli, KA, and MI Alsaleh. 2004. “Numerical and Experimental Study of Strength Properties of Martian Regolith.” *Engineering, Construction, and Operations in Challenging Environments*: 1–8.

Al-Tayyib, AHJ, MF Tewfik, and MS Khan. 1991. “Strength and Durability of Sulfur Mortar.” *Journal of Materials in Civil Engineering* 3 (2): 154–164.

Badescu, V. 2009. *Mars: Prospective Energy and Material Resources*. Edited by Springer.

Beegle, LW, GH Peters, GS Mungas, GH Bearman, JA Smith, and RC Anderson. 2007. “Mojave Martian Simulant: A New Martian Soil Simulant.” *Lunar and Planetary Science XXXVIII*.

Benaroya, Haym. 2010. *Turning Dust to Gold: Building a Future on the Moon and Mars*. Springer.

Braun, RD, and RM Manning. 2007. “Mars Exploration Entry, Descent, and Landing Challenges.” *Journal of Spacecraft and Rockets*: 1–32.

Brooks, Ron. 2012. “Rock, Rubble, and Regolith.” *MMM-INDIA QUARTERLY* #13 (JANUARY): 20–29.

Brown, By Dan A, and Glenn Rix. 1992. “Geotechnical Investigation Strategies for Lunar Base.” *Journal of Aerospace Engineering* 5 (2): 199–213.

Carrier, D. 2005. “The Four Things You Need to Know about the Geotechnical Properties of Lunar Soil.” *Lunar Geotechnical Institute* (September).

Carrier, WD. 1991. “Physical Properties of the Lunar Surface.” In *Lunar Sourcebook*, 475–594.

Chua, KM, and SW Johnson. 1998. “Martian Soil Mechanics Considerations.” *Proceedings of Space 98*: 515–532.

Duke, M, H Benaroya, and L Bernold. 1998. “Workshop on Using in-Situ Resources for Construction of Planetary Outposts.” *Proceedings of Space 98*.

Dundas, CM, S Byrne, and A S Mcewen. 2014. “Clean Ground Ice on Mars: Evidence from Spacecraft, Fresh Craters and Thermokarst.” *Eighth International Conference on Mars (2014)*: 26–27.

Fontana, JJ, LJ Farrell, and RL Yuan. 1998. “ACI 548.2R-93 Guide for Mixing and Placing Sulfur Concrete in Construction Reported by ACI Committee 548”. Vol. 93.

Gosau, Jan-Michael. 2012. “Regolith Stabilization and Building Materials for the Lunar Surface.” *Earth and Space 2012* (April 17): 243–249.

Gracia, V, and I Casanova. 1998. “Sulfur Concrete: A Viable Alternative for Lunar Construction.” *Proceedings of Space 98*.

Hammons, Michael, Donald Smith, and Dan Wilson. 1993. “Investigation of Modified Sulfur Concrete as a Structural Material.” *U.S. Army Corps of Engineers*.

Happel, John A. 1993. “Indigenous Materials for Lunar Construction.” *Applied Mechanics Review* 46 (6): 313–325.

Heiken, G, D Vaniman, and BM French. 1991. *Lunar Sourcebook: A User’s Guide to the Moon*. Cambridge University Press.

Jolly, SD, J Happel, and S Sture. 1994. “Design and Construction of Shielded Lunar Outpost.” *Journal of Aerospace Engineering* 7 (4): 417–434.

Khoshnevis, Behrokh, and MP Bodiford. 2005. “Lunar Contour Crafting—a Novel Technique for ISRU-Based Habitat Development.” *43rd AIAA Conference* (January): 1–12.

Kozicki, J., and J. Kozicka. 2011. “Human Friendly Architectural Design for a Small Martian Base.” *Advances in Space Research* 48 (12) (December): 1997–2004.

Koh, Sung Won, Jaemin Yoo, Leonhard E. Bernold, and Tai Sik Lee. 2010. “Experimental Study of Waterless Concrete for Lunar Construction.” In *Earth and Space 2010*, 1098–1102. Reston, VA: American Society of Civil Engineers.

Lee, Jaeho, Byung Chul Chang, Sangah Lee, and Tai Sik Lee. 2012. “Feasibility Study on Lunar Concrete Landing Pad.” In *Earth and Space 2012*, 128–134. Reston, VA: American Society of Civil Engineers.

Mamlouk, By Mike, Matthew Witczak, and Kamil Kaloush. “Thermal Properties of Asphalt Mixtures.” https://schoolofsustainability.asu.edu/docs/smartWebArticles/mat_thermprop.pdf.

McKay, DS, and CC Allen. 1996. “Concrete—A Practical Construction Material for Mars.” *Engineering, Construction, and Operations in Space V*: 566–570.

Mendell, WW. 1985. *Lunar Bases and Space Activities of the 21st Century*. *Lunar Bases and Space Activities of the 21st Century*. NASA Astrophysics Data System.

Meyers, C, and H Toutanji. 2007. “Analysis of Lunar-Habitat Structure Using Waterless Concrete and Tension Glass Fibers.” *Journal of Aerospace Engineering* (October): 220–226.

Mitchell, JK, and WN Houston. 1972. “Mechanical Properties of Lunar Soil: Density, Porosity, Cohesion and Angle of Internal Friction.” *Proceedings of the Third Lunar Science Conference*.

Morris, A. B., D. B. Goldstein, P. L. Varghese, and L. M. Trafton. 2012. “Modeling the Interaction between a Rocket Plume, Scoured Regolith, and a Plume Deflection Fence.” *Earth and Space 2012* (April 17): 189–198.

Mottaghi, Sohrob, and Haym Benaroya. 2014. “Design of a Lunar Surface Structure. I: Design Configuration and Thermal Analysis.” *Journal of Aerospace Engineering* (12): 1–12.

Omar, HA, and M Issa. 1994. “Production of Lunar Concrete Using Molten Sulfur.” In *Engineering, Construction, and Operations in Space IV*.

Roqueta, J, and I Casanova. 2014. “Manufacture and Properties of Sulfur Mortar for Lunar Applications.” *Space 2000*: 851–855.

Ruess, F, J Schaenzlin, and H Benaroya. 2006. “Structural Design of a Lunar Habitat.” *Journal of Aerospace Engineering* (July): 133–157.

Scheerbaum, G. 2000. “In-Situ Manufacture of Martian Construction Materials.” *SPACE 2000*: 934–940.

Sherwood, Brent, and Larry Toups. 1992. “Technical Issues for Lunar Base Structures.” *Journal of Aerospace Engineering* 5 (2) (April): 175–186.

Spudis, PD, and Tony Lavoie. 2010. “Mission and Implementation of an Affordable Lunar Return.” *Proc. of Space Manufacturing*: 1–30.

Stoker, CR, JL Gooding, T Roush, A Banin, D Burt, BC Clark, G Flynn, and O Gwynne. 1993. “The Physical and Chemical Properties and Resource Potential of Martian Surface Soils.” *Resources of Near-Earth Space*: 659–706. University of Arizona Press.

Sture, S. 2006. “A Review of Geotechnical Properties of Lunar Regolith Simulants.” *Earth & Space* (303): 1–6.

Susante, PJ van. 2012. “Landing Pad Construction Rover Attachment Development.” *Earth and Space 2012*: 165–174.

Toutanji, H, MR Fiske, and MP Bodiford. 2006. “Development and Application of Lunar ‘Concrete’ for Habitats.” In *2006 Proc. ASCE Conf. on Earth & Space*.

Toutanji, H, and RN Grugel. 2008. “Mechanical Properties and Durability Performance of ‘Waterless Concrete.’” In *Earth & Space 2008*, 1–8. Reston, VA: American Society of Civil Engineers.

Toutanji, HA, S Evans, and RN Grugel. 2010. “Performance of ‘Waterless Concrete.’” In *ICPIC 2010 – 13th International Congress on Polymers in Concrete*, 1–8.

Zent, AP, and TL Hudson. 2009. “Mars Regolith Thermal and Electrical Properties: Initial Results of the Phoenix Thermal and Electrical Conductivity Probe (TECP).” In *Lunar and Planetary Science XL*.

CHAPTER 6

An Outline for Overall Architecture

Introduction

The team has been spending time accessing how to integrate the various technological advancements achieved so far with CC and SIS for lunar/Mars application as well as looking at the limitations of this robotic technology for extraterrestrial infrastructure development.

In order to present our technologies for lunar/Martian applications we address the overall architecture and propose the various elements that make up alternative configurations for both a high fidelity simulation on Earth as well as potential architecture concepts for viable lunar settlement, employing CC and SIS in the best possible modes for safe and economic infrastructure establishment. To that end, we are monitoring ongoing projects, accumulating and evaluating data to see how we might best apply our technologies for this purpose.

LRO Mission Data

We are following LRO mission progress and refined data sets from LRO are being studied to identify location of surface facilities in the polar regions of the Moon. Since current interest hovers around the lunar south polar region, we have access to the high resolution images of those regions, especially the Mons Malalpert and Shackleton areas. These sites hold promise for early lunar return and as potential locations for initial settlements (please see Figures 1-9).

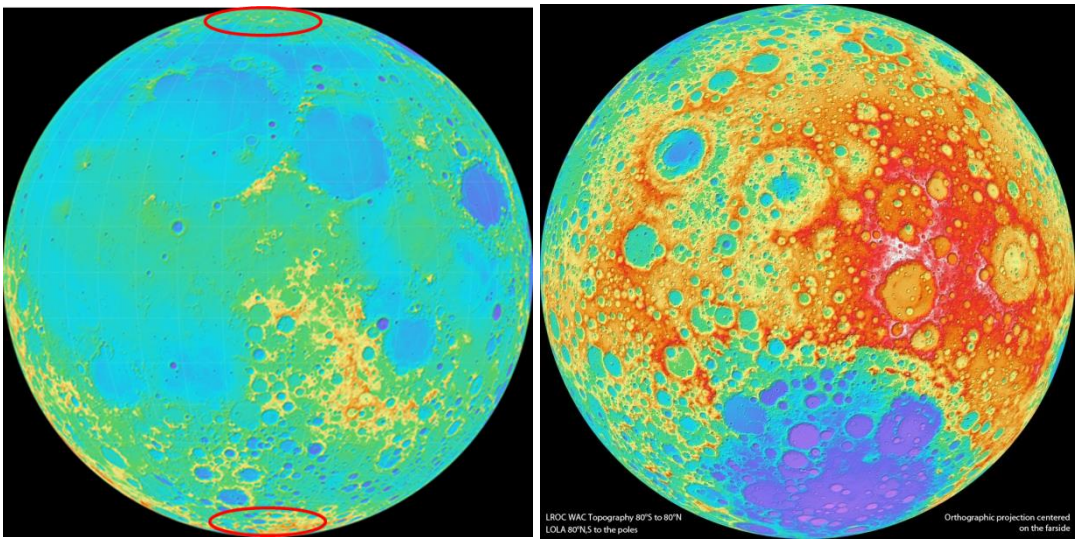

Figure 1. The ongoing LRO mission is mapping the lunar terrain in unprecedented detail. The polar regions(red ovals) in these false color images hold promise for initial lunar settlement

establishment because they offer continuous access to sunlight as well as cold traps that are rich in water and volatiles.[Credit:NASA LRO/LROC, LOLA, MIT]

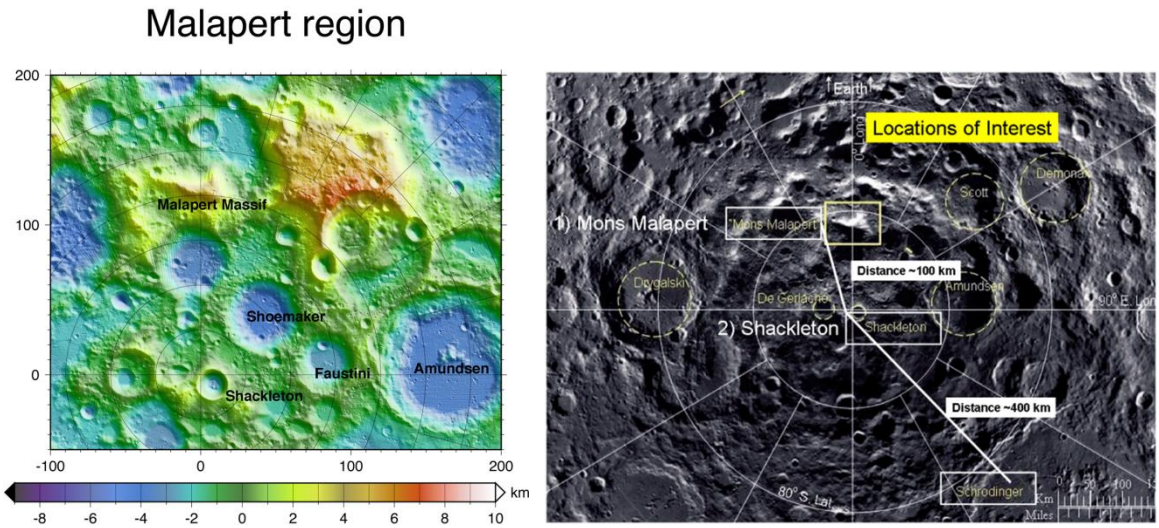

Figure 2. The polar regions of the Moon have attracted interest for further exploration to locate the first lunar settlement. The Malapert mountains in the south polar region and Shackleton crater at the south pole are candidate sites for early return to the moon in recent literature. [Credit NASA LRO, Schrunk etal.]

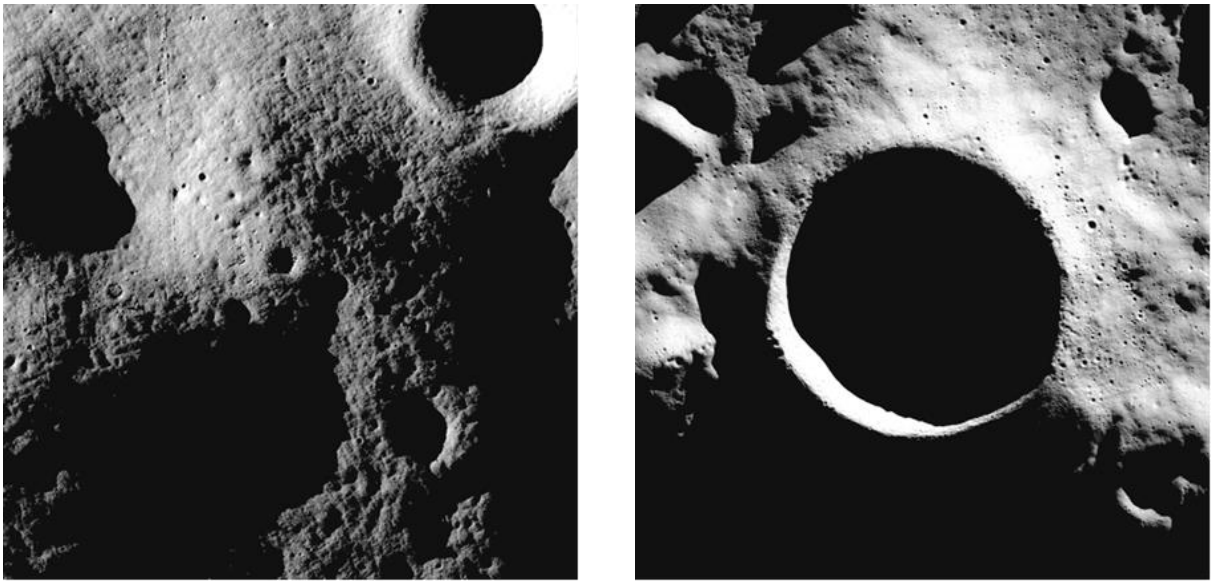

Figure 3. Hi res images of Malapert and Shackleton are further enhanced using data from the Lunar Reconnaissance Orbiter(LRO). The Malapert image on the left covers an area 4096 m x 4096m. Shackleton Crater on the right is 21 kilometers, or 13 miles, in diameter. [Figure credit: D.Wettergreen, Carnegie Mellon U – 2014]

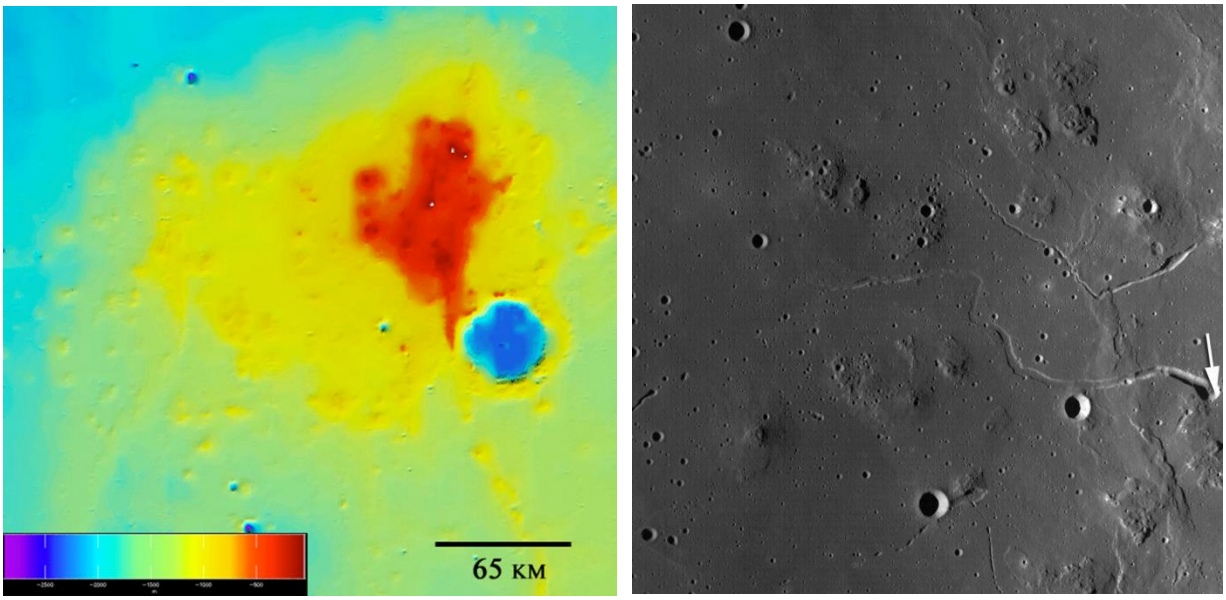

Figure 4. Marius Hills, a volcanic shield region located on the equatorial region of the Moon could be a potential site for a lunar settlement. [Credit NASA LRO, ASU]

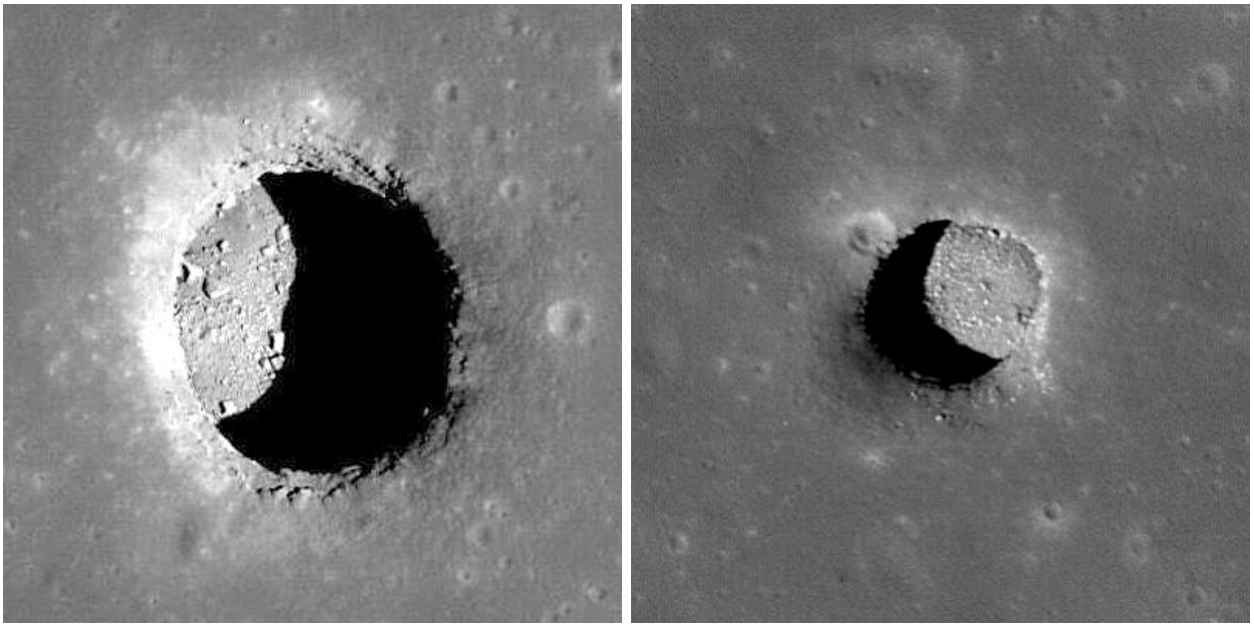

Figure 5. Spectacular high sun view of the Mare Tranquillitatis pit crater on left, about 70m diameter, revealing boulders on an otherwise smooth floor. Marius Hills piton the right has a sunlight incidence angle of 25° that illuminates about three-quarters of the floor. The Marius pit is about 34 meters deep and 65 by 90 meters wide. [Credit NASA LRO, ASU]

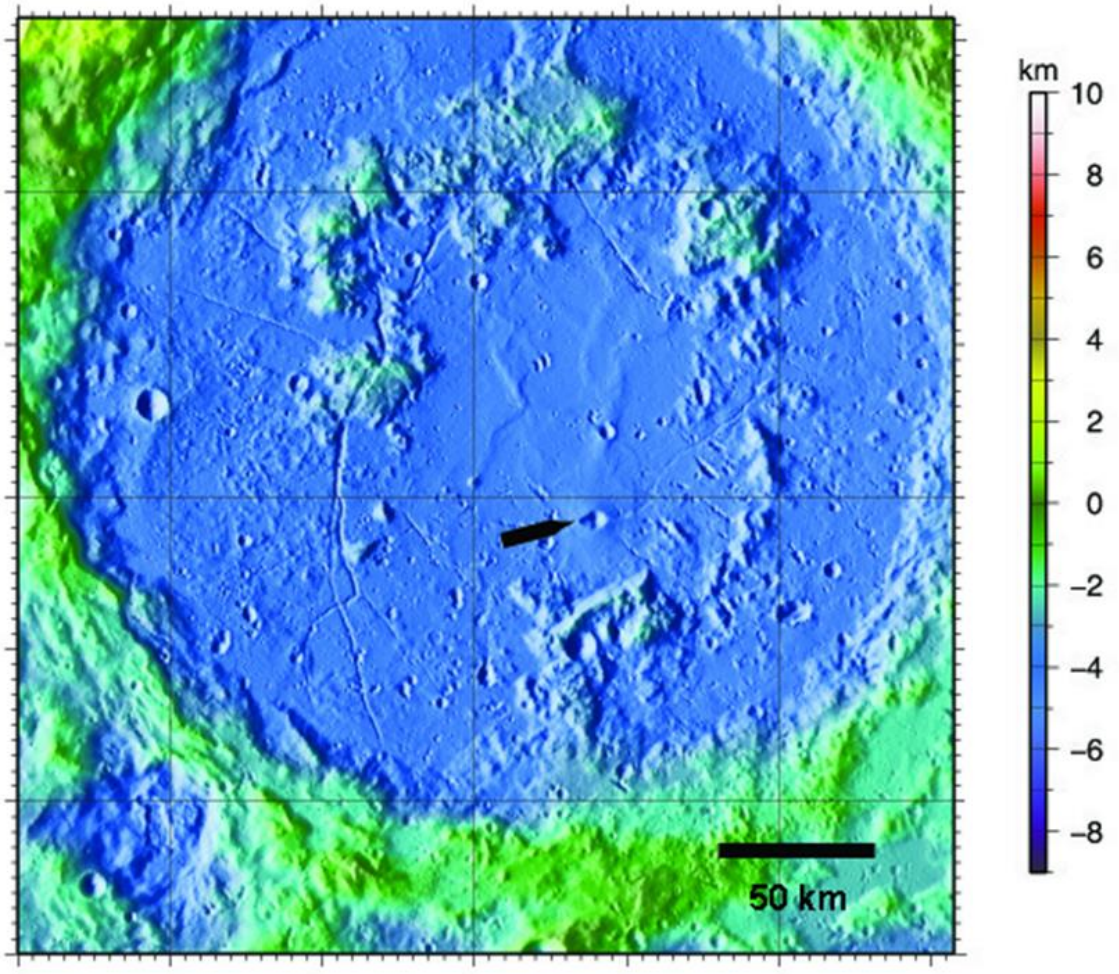

Figure 6. Schrodinger Crater on the south polar farside of the Moon offers a region that shows recent volcanism and is of interest to the science community. Without the Earth on the horizon, a facility built here would also allow crew to experience deep isolation phenomena and develop skills to cope with it.

Habitable lava tubes may also be present there, that could become the site for permanent settlements, naturally protected from the extreme lunar surface environment. [Credit NASA LRO]

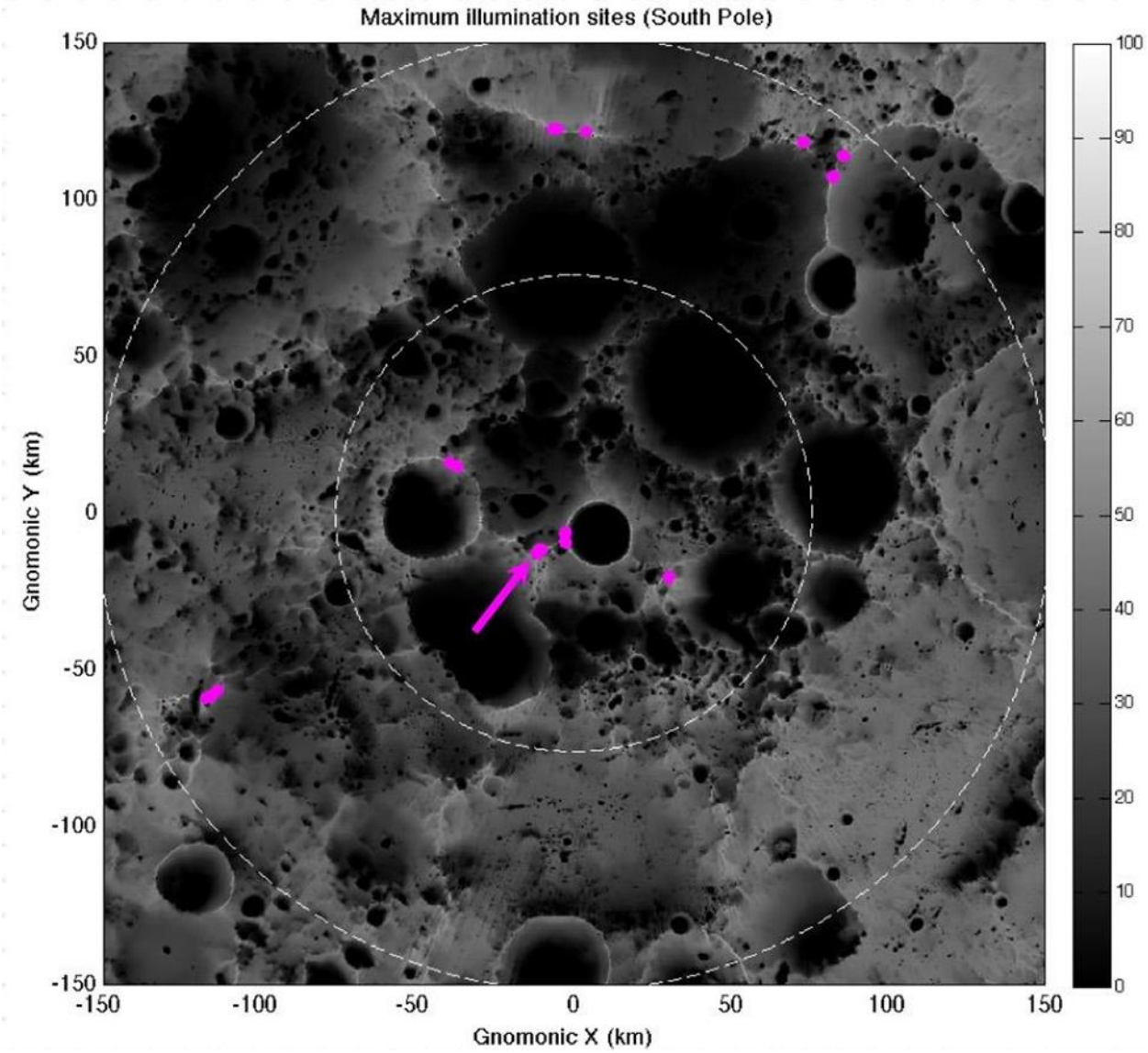

Figure 7. Since the lunar spin axis is almost orthogonal to the ecliptic, the Moon does not experience seasons. In this gnomonic projection of the south polar region, certain elevated peaks show regions where the sun shines throughout the year. Such regions are perhaps the ideal locations to build lunar landing pads with round the clock service capability as well as sites for establishing early permanent settlements. Being very close to permanently shaded regions, the solar power may be used to extract volatiles like water to sustain the settlement. [Credit NASA LRO, ASU]

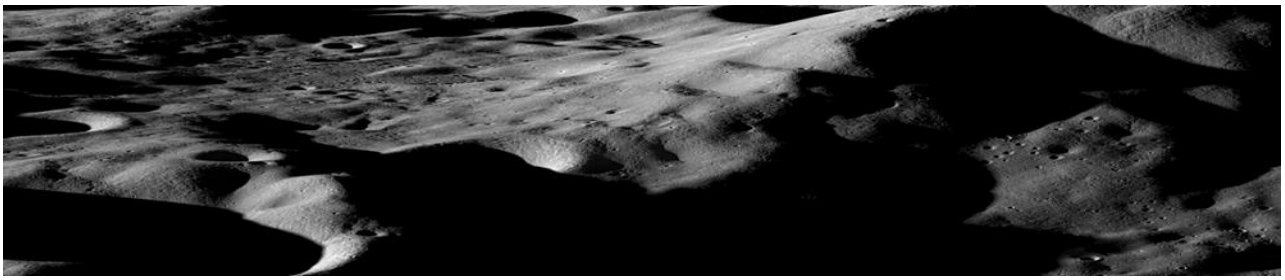

Figure 8. An oblique elevation view of the lunar south polar region shows the rugged highland terrain. This is the view(note the long shadows) a lunar lander pilot might expect to see as the vehicle approaches the lunar landing pad minutes before touchdown, at the south polar lunar settlement. Since the sun angles are very shallow, the ambient lighting conditions are not bright with large patches of shadow, and some craters are in permanent solar shade.[Credit:NASA LRO, ASU]

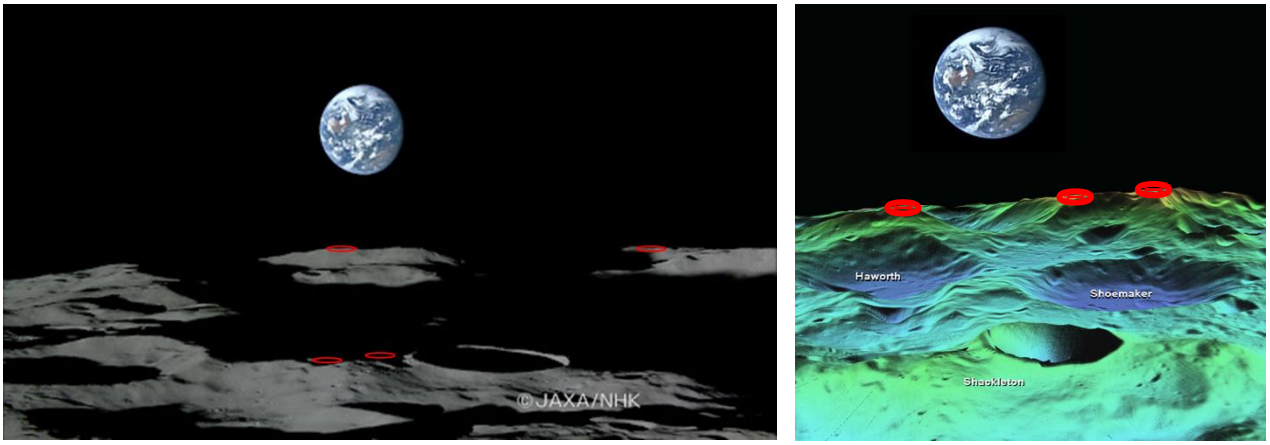

Figure 9. From the lunar lander pilot's visual flight rules view, the upper higher elevation spots on Mons Malapert and Leibnitz Massif may be a better site for lander operations because the peaks are well lit landmarks compared to the lower sites near Shackleton crater. Higher altitude landing pads would save fuel during early sorties. A better line of sight Earth-Moon laser communications link may be established from the upper sites and relays could be employed to extend the network to Shackleton and environs.

High Fidelity Simulation at Lunar Settlement Analog/Test Sites – PISCES, D-RATS and NASA

We are following the work at the Pacific International Space Center for Exploration Systems PISCES in Hawaii. NASA has had several demonstrations including telerobotic activity employing satellite links to this site on the slopes of the Mauna Kea (Figure 10,11). We see the potential for testing lunar CC and SIS systems using local materials that compare favorably with lunar simulants. We are exploring the possibility to use other sites as well including the NASA

D-RATS test site at Black Point Lava Flow in Arizona (Figure 12) and also the simulation testbeds at JPL, KSC, JSC and Ames.

The proposed simulation exercise is being executed in phases. In the first phase, the construction machines will be fully assembled and tested at USC labs. Slabs and tiles built by the SIS machine are being studied under the current NIAC Phase II award. Work is planned on perfecting a portable, lightweight CC machine in collaboration with NASA MSFC as Phase III of the project. The new robot can be collapsed for compact packaging and transport to simulation sites such as those NASA has already used for simulations. In the third phase, the portable CC machine will be packed, transported to and deployed at the preferred NASA site. Using a command and control center at a NASA center, the CC and SIS machines will then be operated telerobotically to build a landing pad prototype using local resources to produce feedstock for the CC machine.

Figure 10. Panoramic View of lunar analog site from Puli rover. Recent activity at the Mauna Kea site include the successful Hungarian Team PULI rover simulation exercise that is attempting to win the Google Lunar X Prize. [Credit: Google Lunar XPrize]

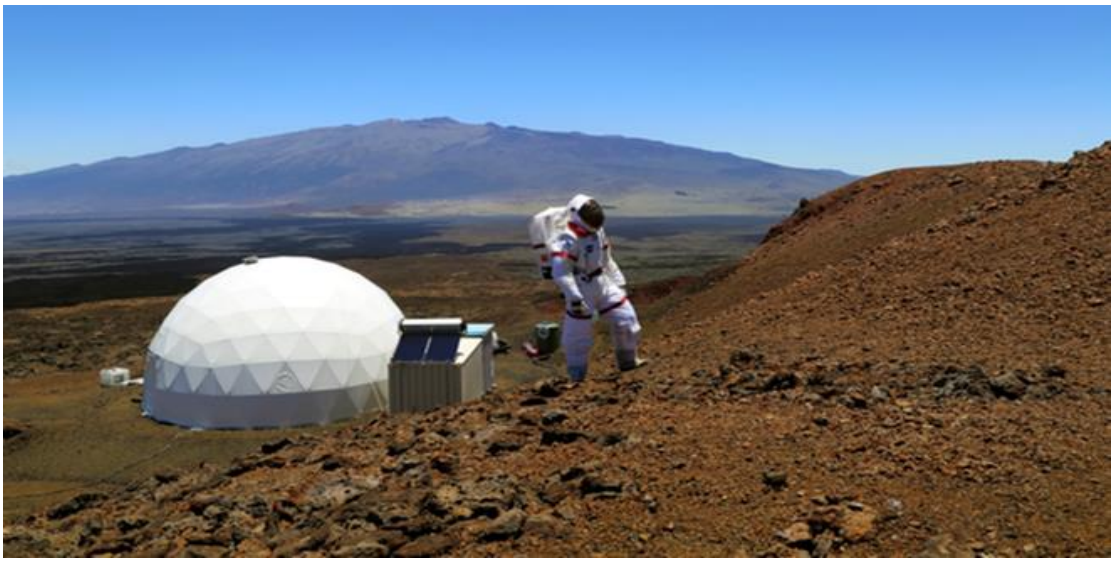

Figure 11. Simulation exercises are being conducted both with astronauts and robotic vehicles.

Figure 12. Alternative simulation sites include the Black Rock Lava Flow region of northern Arizona where NASA has already conducted extensive Desert Research and Technology Studies(D-RATS)[Credit :USGS]

Lander Trajectory Profile and Critical Implications for Lunar Landing Pad Design

Ejecta suppression is the first priority at lander touchdown since it can have severe to lethal consequences for habitats and crew in EVA, as well as for all other exposed high value assets in the vicinity of lander operations.

We have been looking at the problem of how to eliminate, curtail or suppress lander ejecta and this critical issue has been at the core of the lunar/Mars application we proposed in Phase 1. The recent landing of the small Curiosity rover (1000kg) shows how debris from unprepared surface can adversely affect lander components like lander legs, chassis and even the payload (Figure 13).

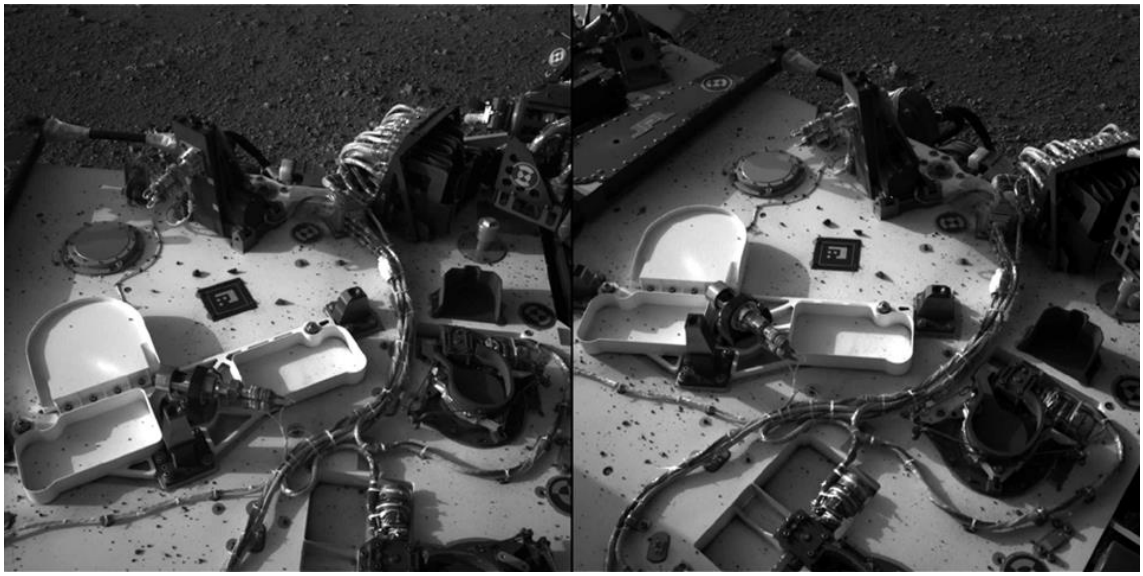

Figure 13. The view through Curiosity's left (A) and right (A) Navcams, looking down on the deck of the rover just after touchdown shows martian soil strewn all over the payload platform. The energy imparted by energetically scattered debris was sufficient to damage an exposed anemometer on the rover.[Credit: NASA/JPL-Caltech]

This issue has been studied in enough detail that we now feel it is time to look at alternative lander trajectories in order to avoid this lethal problem, especially for large landers with heavy payloads (45,000kg).

In an effort to conserve fuel, the reference Apollo lunar excursion modules (LEM 14,000kg) generated large debris clouds because of the shallow approach angle. We cannot safely propose this strategy for repeated sorties of heavy crew and cargo landers because the various elements of the permanent settlement, especially those exposed assets, will be blasted by high energy debris (Figures 14, 15).

One trajectory that we are exploring proposes that the lander hover directly over the landing pad at a TBD altitude that does not agitate loose surface regolith material, and then gently descend vertically to touchdown on the landing pad. The approach proposes to cut the horizontal velocity of the lander to zero, just high enough above the lunar or Mars surface to avoid ejecta generation, initiate a hover maneuver, and then throttle down the engines for a vertical descent and touchdown (Figure 16, 17).

A fuel penalty is inevitable, but such an approach would minimize the landing pad dimensions and stabilized soil surfaces surrounding the landing pad for an Altair reference class lander considerably, that is essential to avoid high energy ejecta production.(Figure 18, 19) A concept for a landing pad in the lunar south polar highlands is depicted and salient features described in Figure 20. The SIS machine will use the maximum ISRU materials to build the landing pad. Sites that need further study include the Malpert Massif and the Leibnitz Massif as they offer

highly visible solar illuminated landmarks for the pilot during all phases of approach from deorbit to touchdown. Sites around Shackleton at the South Pole may not offer such visibility all year round that is critical for safe lander operation.

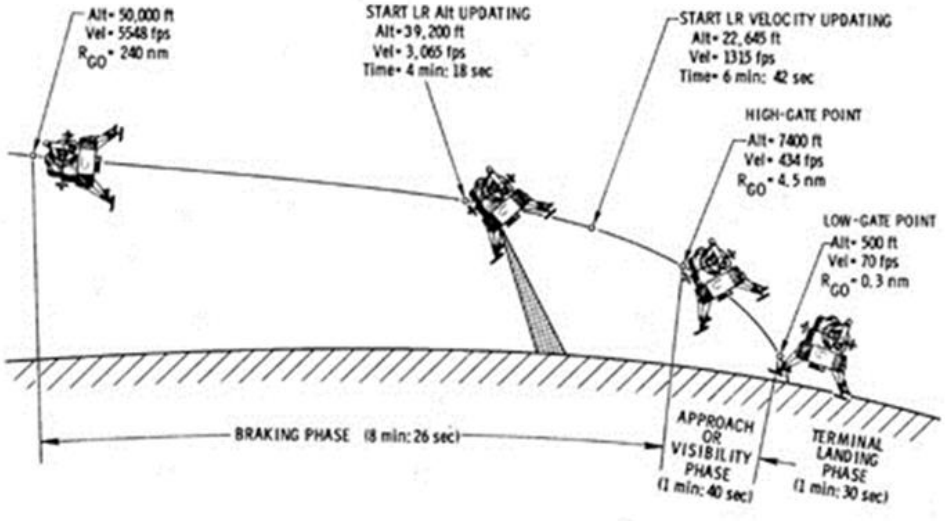

Figure 14. In the Apollo era, the lander fired retro engines, braking for about 8min to dissipate much of the orbital energy from an altitude of 100km. The pilot then had approximately 1-1/2 min for target acquisition, followed by another 1-1/2 minutes for touchdown. [Credit: Apollo Lunar Surface Journals NASA]

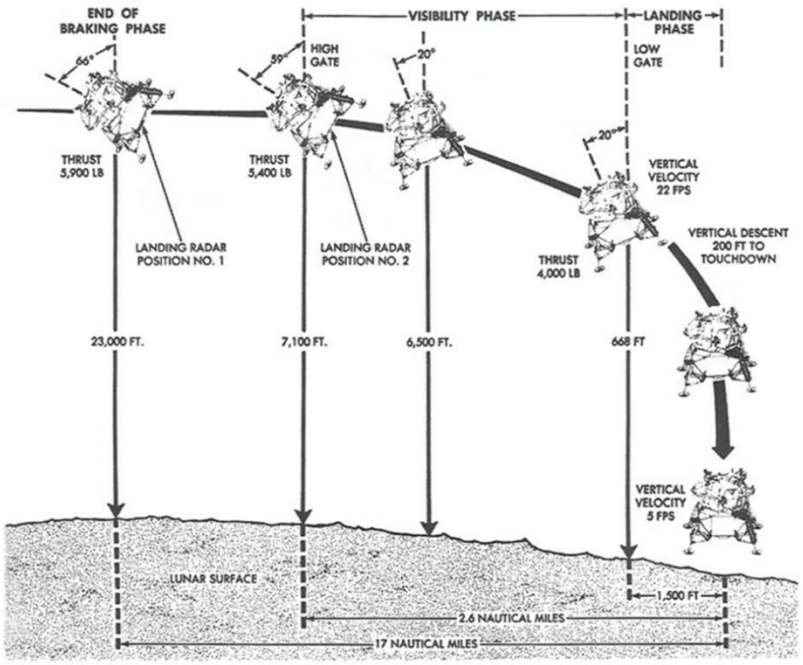

Nominal Descent Trajectory from High Gate to Touchdown

Figure 15. The Apollo lander pilot had to visually acquire landing target at around 7000ft and at a distance of 2-1/2 miles from target, approximately 3min before touchdown. Note the awkward tilt of the lander necessitated by the non-gimballed engine. Also note shallow angle of descent at touchdown(not to scale in this image) [Credit: Apollo Lunar Surface Journals NASA]

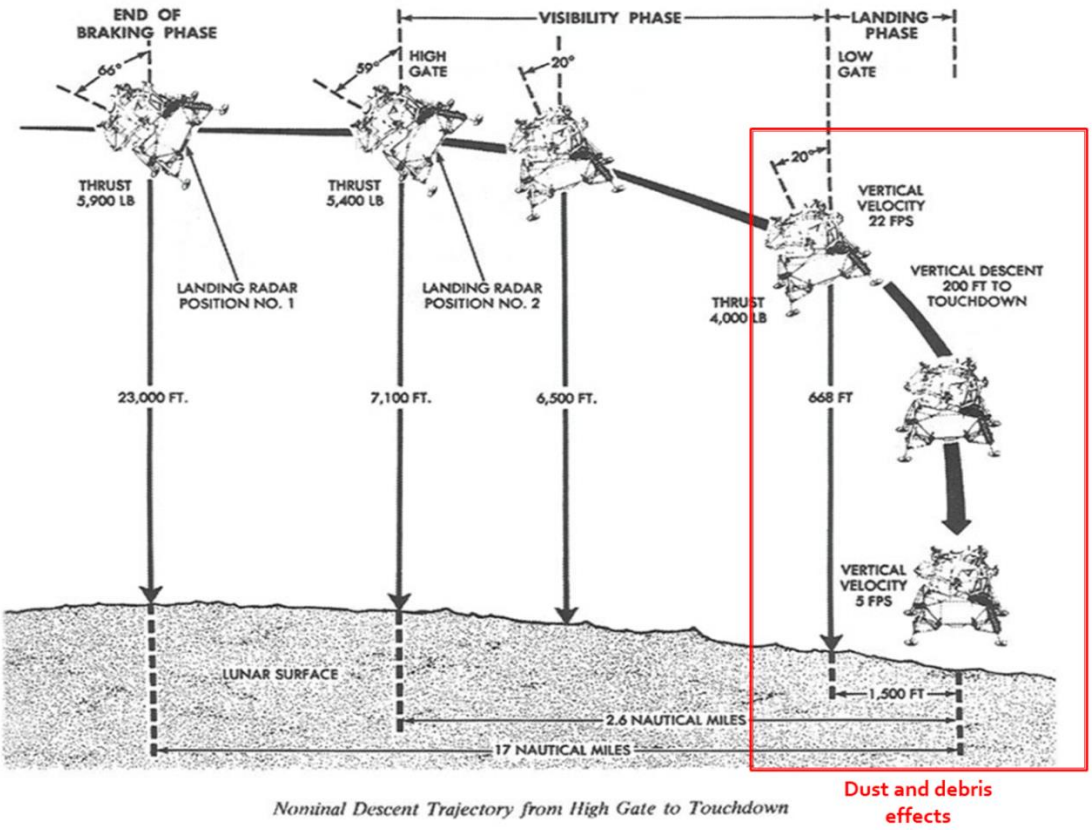

Figure 16. Severe dust and debris effects will pose extreme hazard to crew and high value assets that are exposed on the lunar or martian surface in the vicinity of large landers attempting touchdown on pristine, unstabilized terrain. [Credit Apollo Lunar Surface Journals NASA]

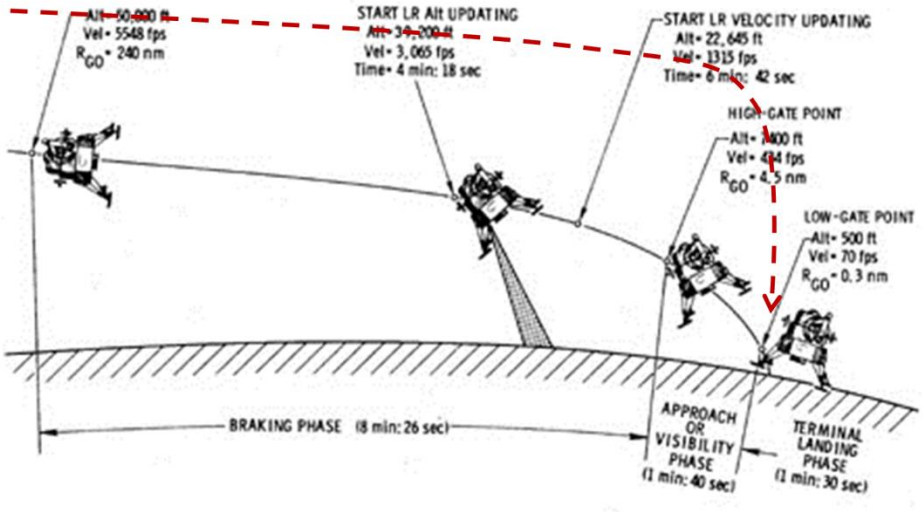

Figure 17. A steeper, more vertical lander descent profile from a higher altitude would reduce the landing pad stabilization area. However, a 10% propellant penalty is inevitable and further trades are warranted.

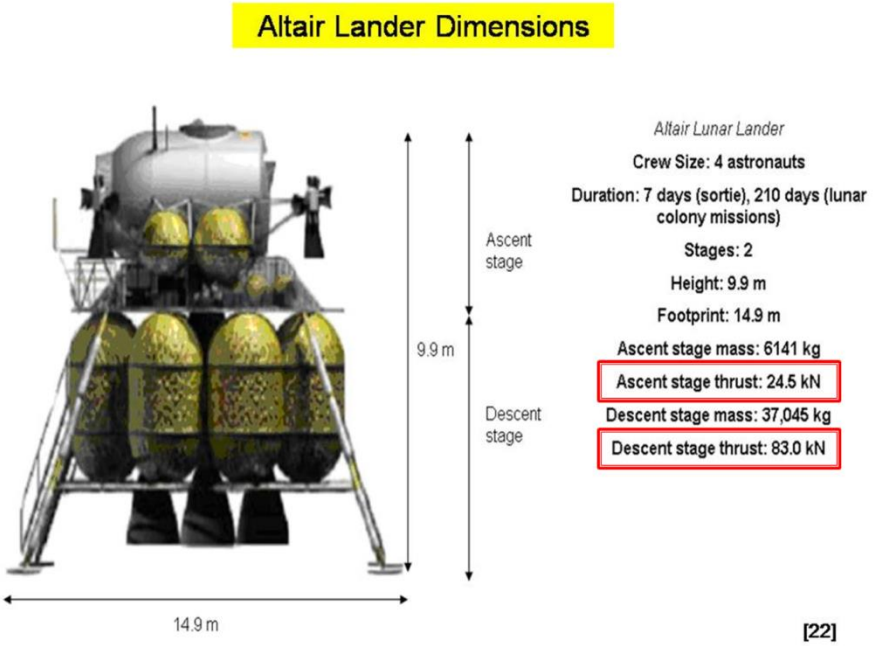

Figure 18. The Altair reference lander descent stage thrust will produce hypersonic dust and debris ejecta that can have lethal effects on crew and assets strewn over the lunar surface. Since lunar gravity is 1/6th the Earth's, loose rocks and boulders may be carried several kilometers in all directions from the landing site in ballistic trajectories.[Credit NASA]

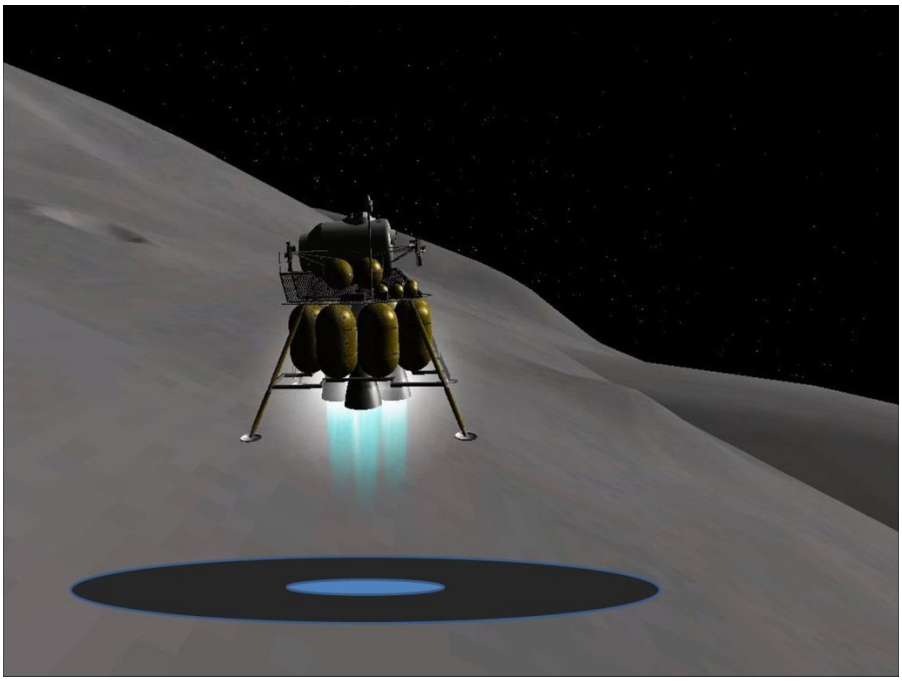

Figure 19. A stabilized landing pad 30m diameter with a 8m diameter refractory tiled center built using CC technology would service over 100 sorties of a reference class Altair heavy crew or cargo lander during the 20 year commissioned life cycle of such a facility.

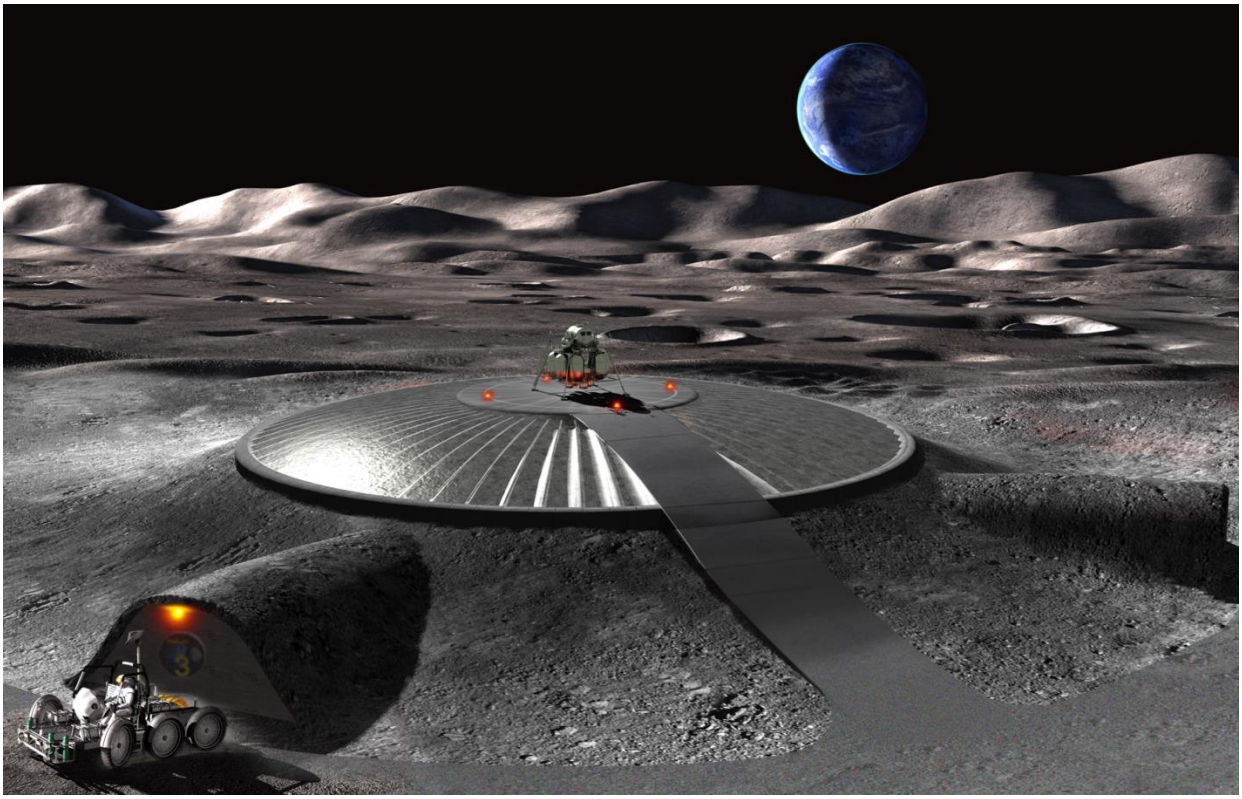

Figure 20. An alternative concept for a lunar landing pad in the south polar region of the Moon. The circular pad will allow round-the-clock landing and liftoff including emergency landings, and may accommodate most abort mission scenarios. A hillock site that is at an elevated location on Malapert or Leibnitz massif is preferred to lower less solar illuminated sites at Shackleton because the site has much better direct line of sight all the way from deorbit phase to touchdown allowing the pilot to approach the landing pad employing visual landmarks and flight rules. This is important because the pilot can land with confidence in case of instrumental flight system error or failure. Once the site has been cleared of rocks and tamped and stabilized using precursory equipment, the construction machines will be programmed to extrude layer by layer of the concrete to create the landing pad. The center of the pad will then be tiled with refractory material that may also be manufactured separately by the SIS machine and locked and screwed into place in order to avoid thermally induced spalling of refractory tiles. A slight convex camber is suggested to keep an errant shallow lander from tipping over on approach. All services are located below landing pad elevation (no blast wall necessary) to allow maximum lander safety in case of engine failure during throttle down operations just before touchdown and engine cutoff. Collapsible aprons not shown.

Site Plan for Lunar Polar Surface Facility

Schematic site plans have been proposed for Shackleton rim and Malapert and several other schematic layouts are being studied. The NASA NIAC O'Handley study based on the NASA Space Exploration Initiative (SEI 1989) is being considered as well to see what infrastructure elements would be best suited for lunar construction case (see Figure 22-23).

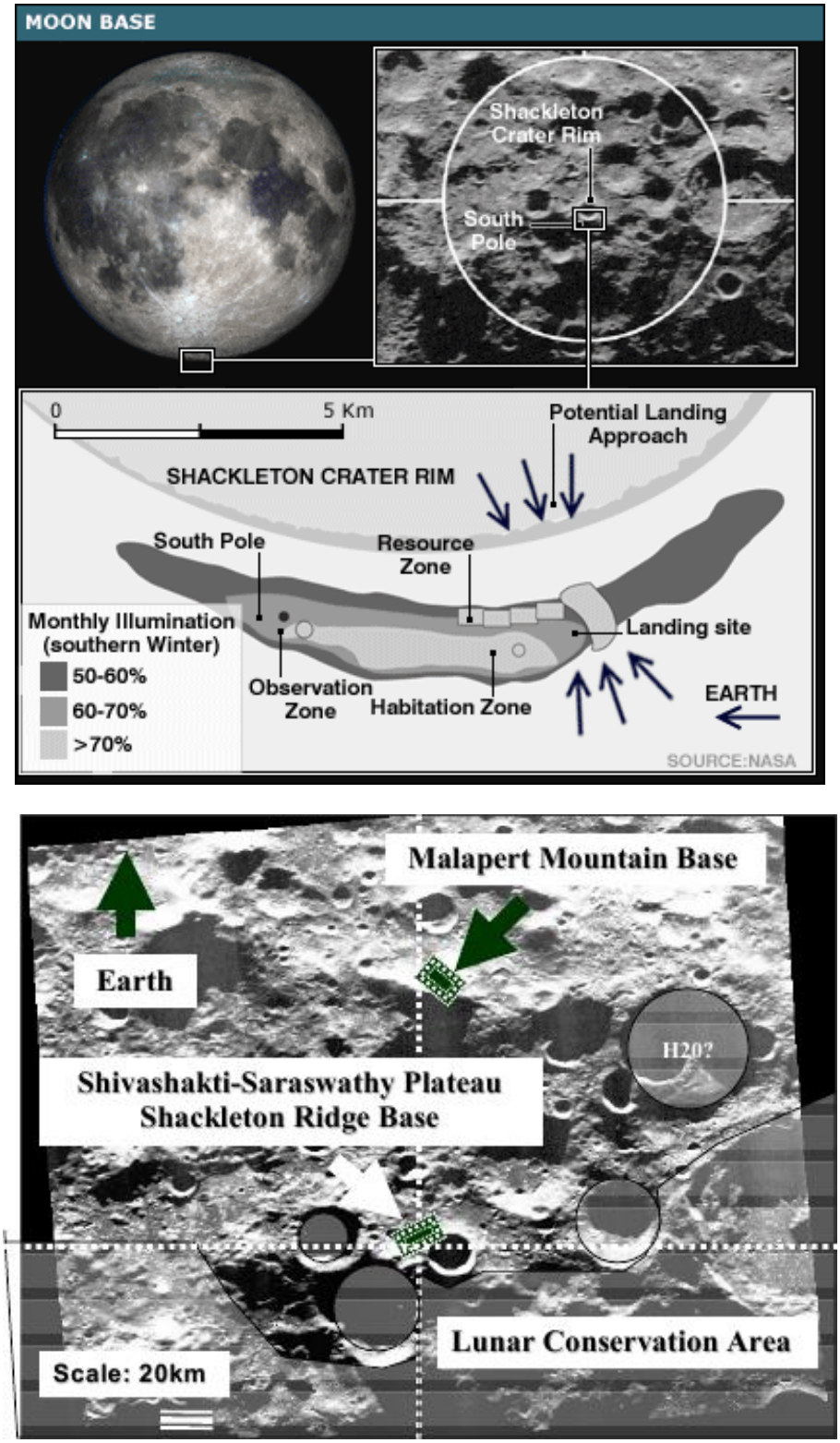

Figure 21. Several schematic site plans are being studied to appreciate which infrastructure elements might be best suited for lunar CC and SIS applications. [Credit NASA(top) and USC School of Architecture(bottom).]

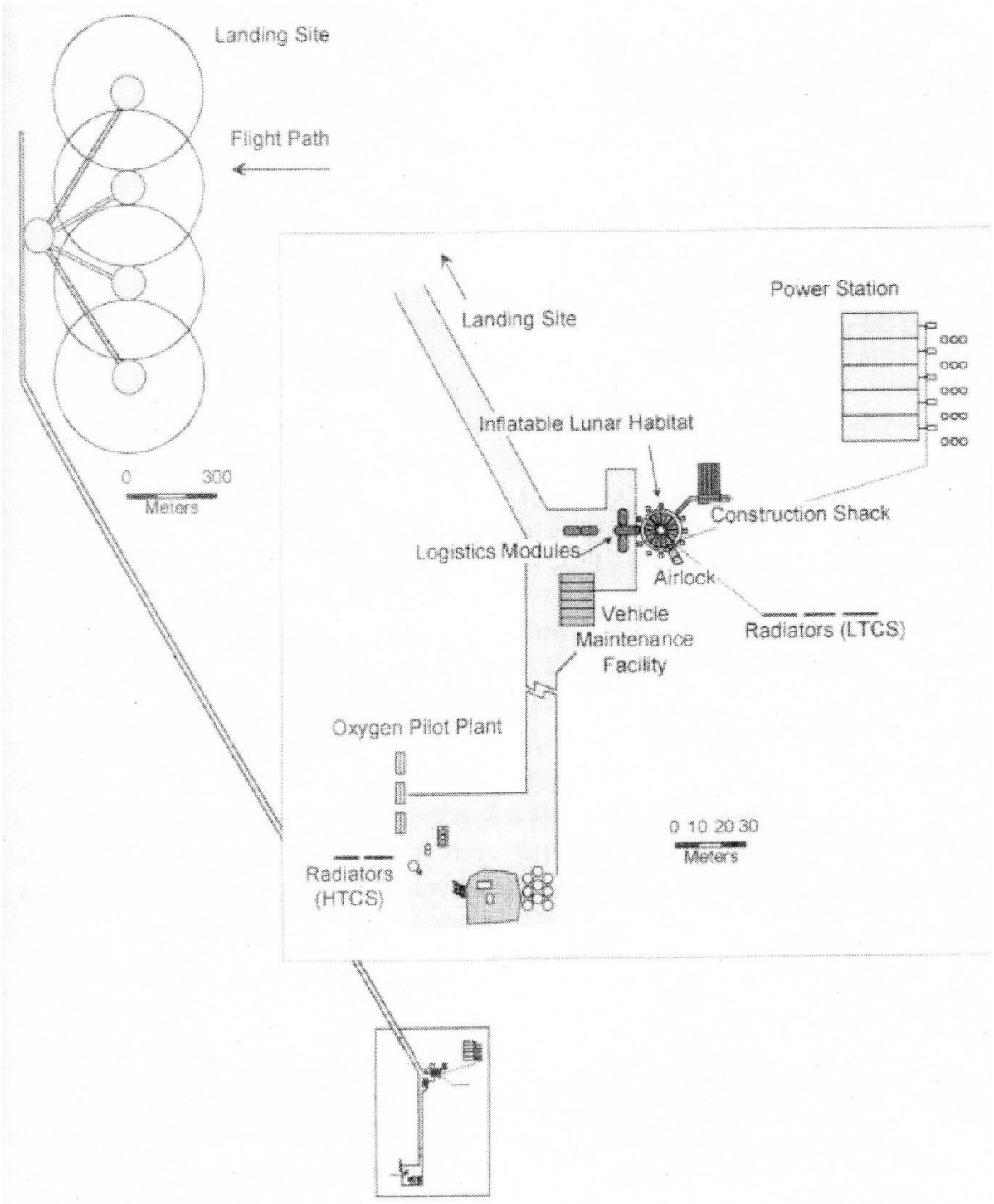

Figure 3. A Lunar Base Layout Developed During the Space Exploration Initiative in 1989-1990 [Alred, et al., 1989]

Figure 22. The O'Handley lunar base referenced an earlier NASA study done during the Space Exploration Initiative (SEI) is being looked at to see what infrastructure elements would be best

suited for lunar CC and SIS applications. [Credit NASA JSC Aldred etal 1989, O'Handley Orbitec NASA NIAC Report 2000]

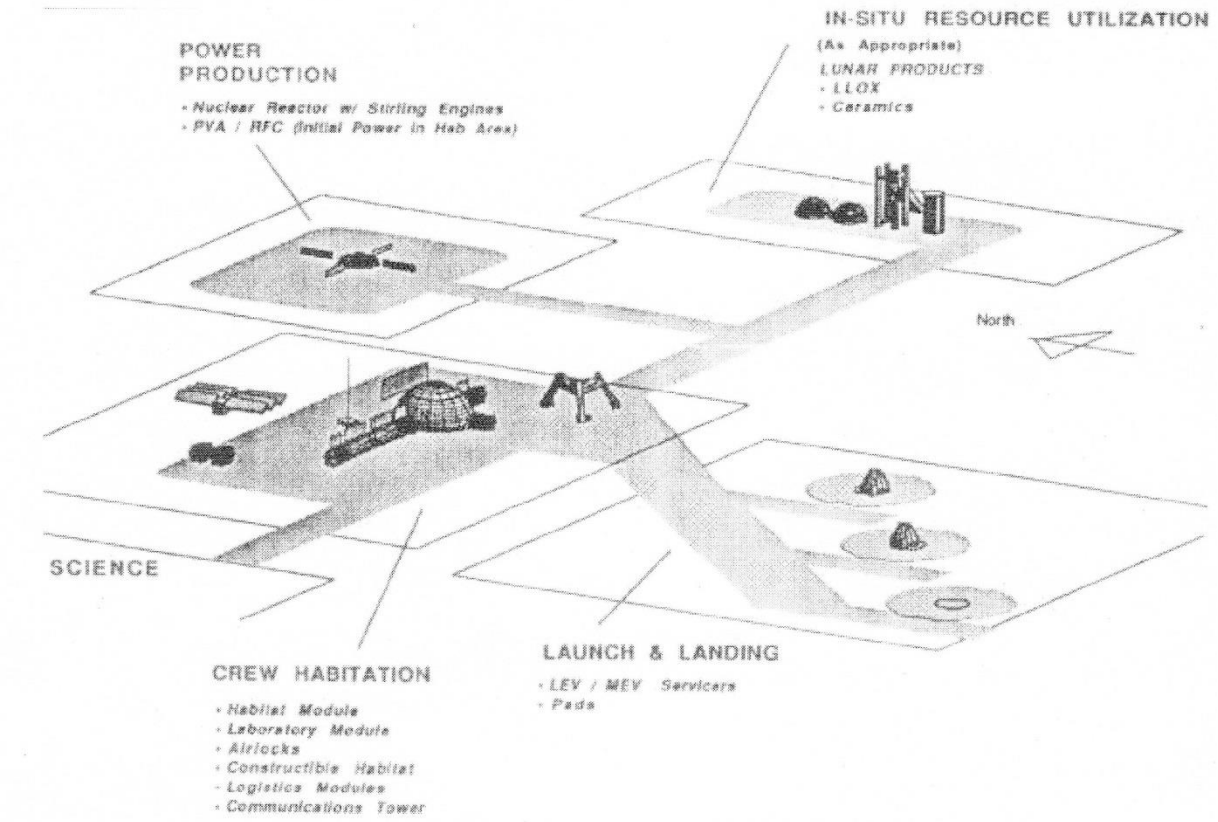

Figure 4. Architecture from the Space Exploration Initiative 90 Day Report [90 Day Report, NASA 1989]

Figure 23. Bird's eye view of the NASA SEI lunar base show the schematic layout of an early lunar base. [*Credit NASA JSC Alred etal.,1989, O'Handley Orbitec NASA NIAC Report 2000]*

CC Communications Command and Control – NASA LADEE Laser Link

For Lunar application of our technologies to be effective, we foresee the need for supervision. Timely supervision will require careful choreography of tasks, sequencing and monitoring during execution. Along with software expressly developed for CC, several systems and protocols already routinely used in automation and manufacture industry may be adapted for lunar CC application.

Depending on the mode of operation deemed most appropriate for lunar construction a telerobotic strategy would be tailored that is most effective for the specific task to be accomplished.

Since these lunar buildup tasks are complex, needing supervision and prompt anomaly resolution as required, the lunar construction system will use broadband communications to cope with the number of channels of high resolution visual data and machine status monitoring via sensors on the machine employing feedback links.

The recent success of the cislunar lunar laser communication demonstration(LLCD) link that was carried on the LADEE mission suggest that access to necessary bandwidth for CC may not be difficult to achieve for Earth based lunar teleoperations. If lunar surface based teleoperations is adopted, then the latency associated with roundtrip signal time delay may be overcome, allowing the operator to react more quickly to unseen or unrehearsed situations or anomalies, as they arise.[Figure 24]

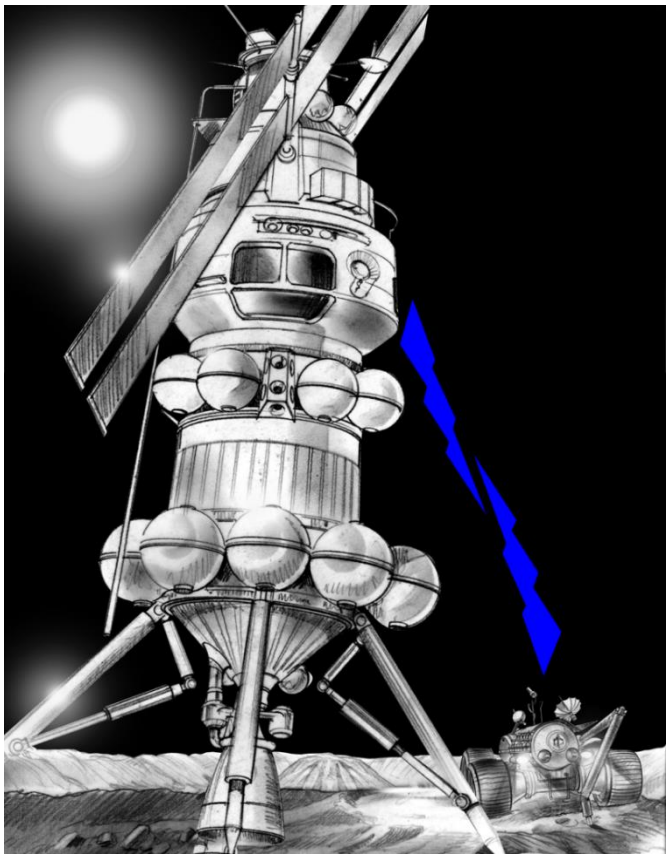

Figure 24. If real time teleoperations is adopted, then crew can operate the construction machines to build a lunar landing pad and associated infrastructure from within the lander cabin. A cabin for teleoperations (C-TOPS) has been proposed for such activity. This strategy would allow the crew to quickly resolve both machine and works site anomalies through EVA.

In a typical CC setup, the instruction file set for complex building shapes are small, ranging from several hundred Mb to a few Gb. Several high definition cameras ranging from panoramic wide angle to those able to see detail of the end effector will be placed on the machine and in the vicinity of the task area. Mobile cameras on booms that can monitor, for example, CC machine

critical component function and examine the CC extrusion in real time will provide continuous footage of activity. Nominal telemetry, typical of spacecraft, will have minimal impact on CC communications. LADEE was able to transmit at 622Mbps (Figure 25). A lunar CC machine may use up to 4Gbps lasercom bandwidth while operating all cameras and sensors. Such a network will employ lunar surface based lasers to C-TOPS on the lunar surface, or to command and control station in lunar orbit or ground station at mission control on Earth (Figure 26).

Figure 25. The lunar laser communication demonstration(LLCD) experiment carried on the LADEE mission proved that low power lasers can provide high bandwidth communications over cislunar distances.[Credit NASA Ames, MIT Lincoln Labs and MDA-SSL]

Telerobotic Strategies – Earth based Orbit based and Lunar surface based command and control

Telerobotic systems have evolved rapidly in the last decade, especially with respect to space systems applications. Robots have been operating over long distance satellite links via and recent demonstrations in telemedicine and the K10 rover operations controlled from the International Space Station and Robonaut 2 manipulation from mission control to ISS all hold promise for extending these systems to the lunar CC application (Figure 27).

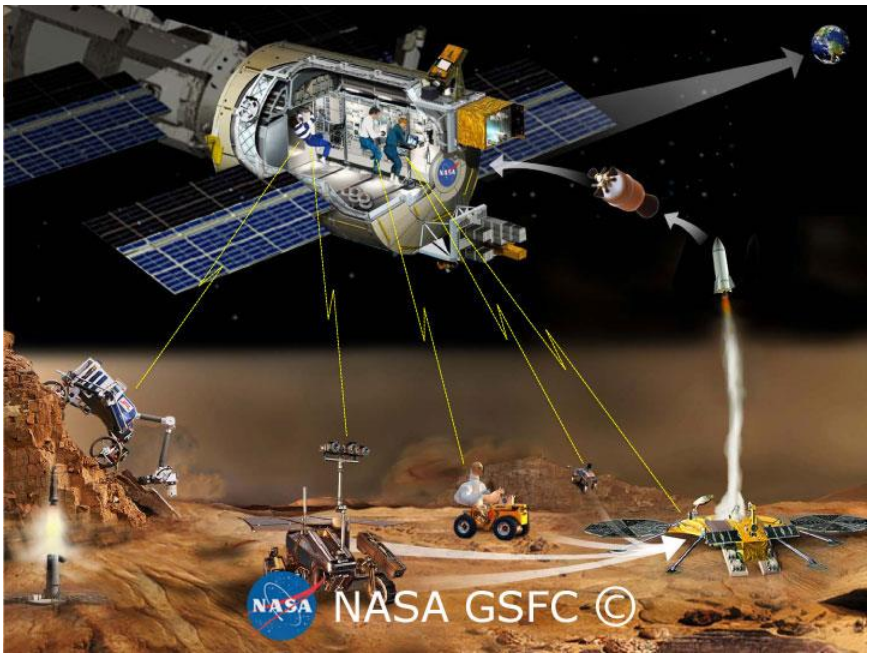

Figure 26. The telerobotic command and control of robotic agents is a rapidly advancing field. Recent demonstrations from ISS suggest that this technology could be useful for lunar /Mars CC/SIS machine operations, circumventing the signal time delay associated with extraterrestrial surface operations management from Earth mission control and ground station networks.[Credit NASA GSFC 2012]

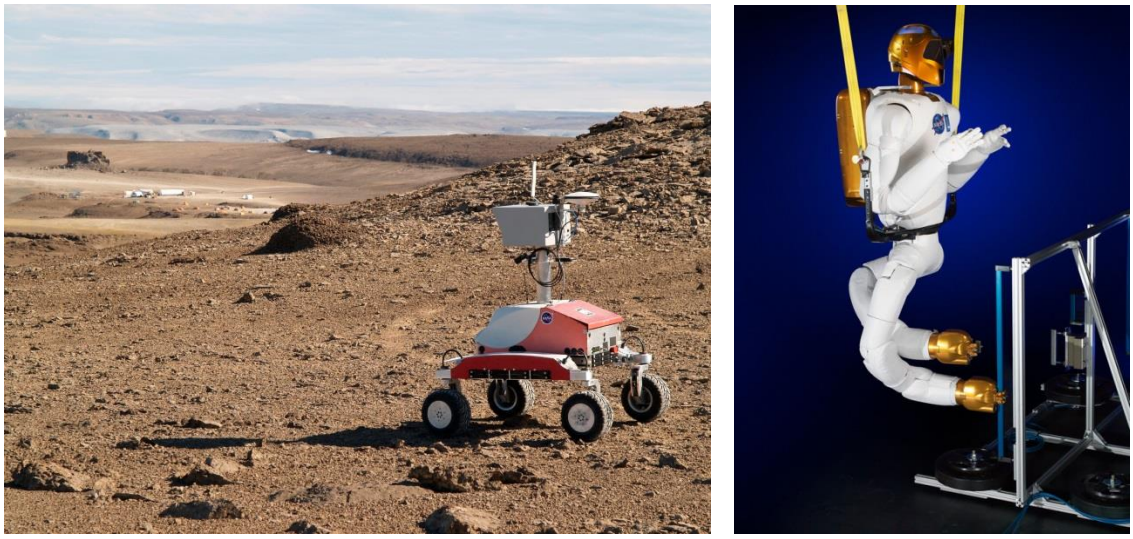

Figure 27. The telerobotic technologies employed in K10 rover and the Robonaut 2 robotic assistant could play an important role in lunar CC/SIS development and operations.[Image credit NASA Ames, NASA JSC]

Lunar CC Power System

Since the lunar CC is being proposed to operate in the polar regions of interest to investigators and settlement designers, this architecture hopes to use solar energy to generate the power necessary for CC operation. Hence the lunar south polar sites chosen (Malapert, Leibnitz) that have long periods of uninterrupted, continuous sunlight. Currently, electrical energy via PV arrays and direct solar heating are the two main methods being investigated. Solar energy concentrators and piped beams via fused silica core fiber optics and allied optical wave guides have shown promise and also being looked into (Figure 28). Transient shadowing of solar power arrays or concentrators due to low solar elevation at polar sites may be compensated using booms to elevate them as needed.

The lunar Mars CC machine is being designed to operate at a peak load of about 10kW. Multijunction and solar cells employed on spacecraft and those being made from lll-V group of materials (gallium arsenide and indium phosphide) efficiency exceed 40% presently, and they may provide the compact PV arrays that would power the lunar CC machine (Figure 29). Heat rejection systems will have to be sized accordingly.

Figure 28. Optical waveguide solar energy concentrators could be used to pipe energy directly to the end effector of the CC or SIS systems. Since the construction system is meant to operate in

the luanr polar region in areas with constant solar illumination, this may be one way to economically harness the energy that is needed to utilize ISRU feedstock with high melting points.[Credit T.Nakamura PSI]

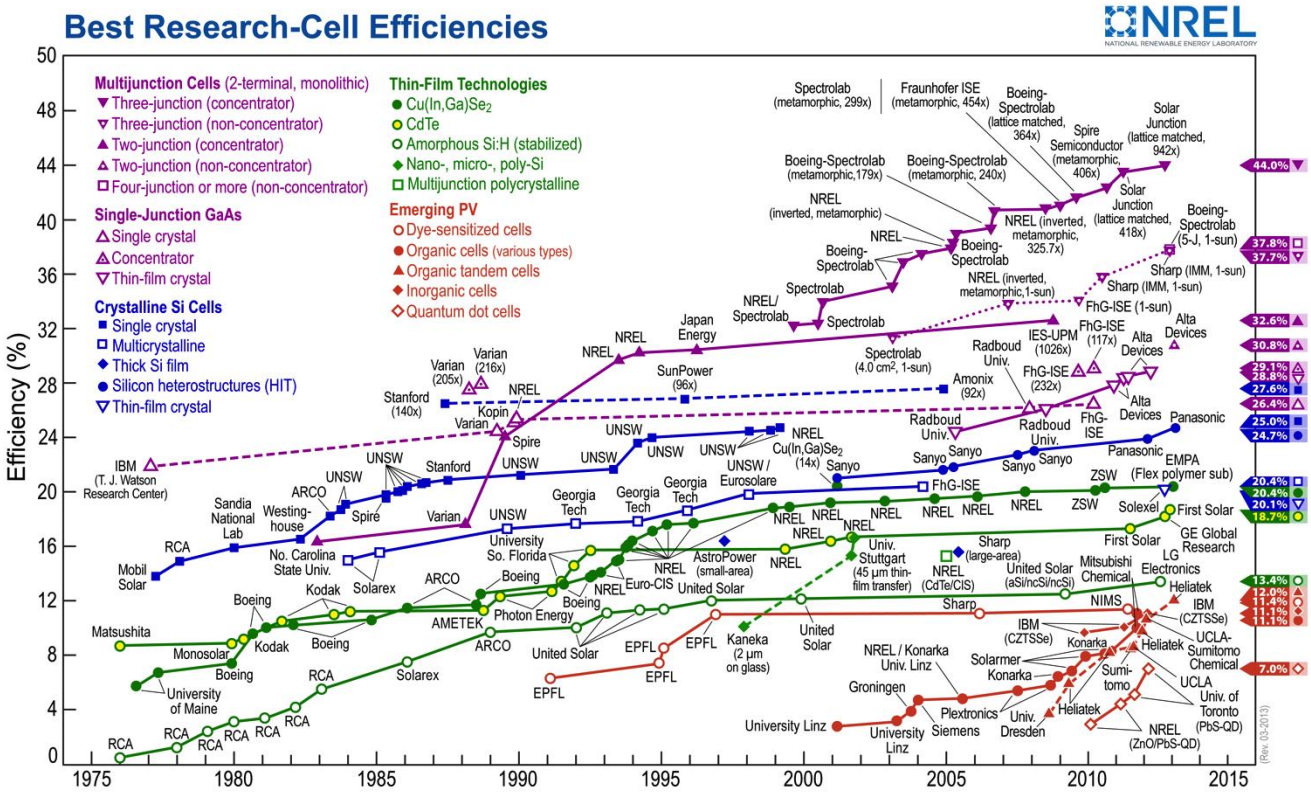

Figure 29. NREL table shows the increasing efficiency of photovoltaic cells. PV arrays for space applications continue to improve in energy conversion efficiency and a 10kW flexible array for a lunar CC/SIS machine operating at 40% efficiency would have a spread of just 3X5m and weigh less than 50kg including deployment and stowage system.

CC and SIS Operations in the Extraterrestrial Environment

Contour Crafting and SIS technologies are currently maturing in the Earth environment. The core systems and allied technologies will need rigorous testing and suitable modifications for sustained and reliable operations on extraterrestrial and planetary surfaces.

The Moon and Mars and its satellites Phobos and Deimos are considered prime candidates for early CC/SIS extraterrestrial deployment because these are the destination bodies of current interest to NASA and other space agencies.

Some of the salient features that differentiate the environments on these extraterrestrial surfaces that will require the construction system modifications suited for each destination include:

1. Gravity – Relative to Earth's gravity of 1G, our closest celestial neighbor, the Moon, poses just 1/6th G and Mars has 3/8th G (Figure 30, 31). Gravity fed systems like hoppers and conveyor belts that operate routinely on Earth will need to be designed to accommodate flow rates and friction effects among other parameters. Peristaltic and augur tube pumps, magnetic separation sieves and conveyor belts are among the feedstock feeder components that will need to be modified depending on the extraterrestrial destination.

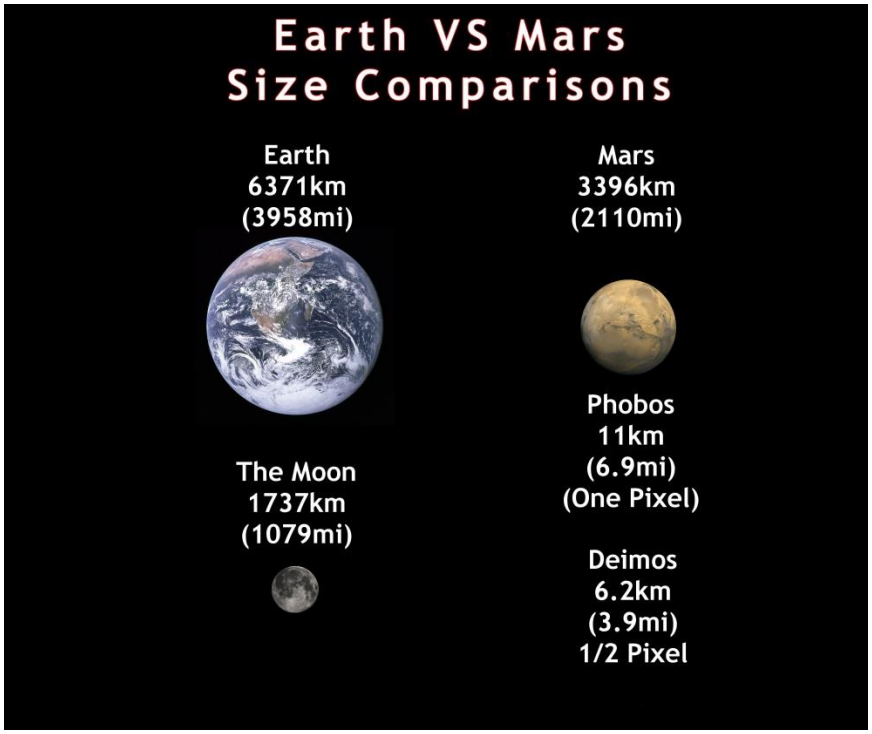

Figure 30. Mars poses 3/8th G and the Moon 1/6th G. Phobos and Deimos present microgravity conditions similar to those found on smaller asteroid fragments. Gravity, or the lack thereof, will affect all extraterrestrial activity, both human and robotic., and systems will have to be designed to operate reliably in low gravity conditions, an environment that is hard to simulate on Earth.

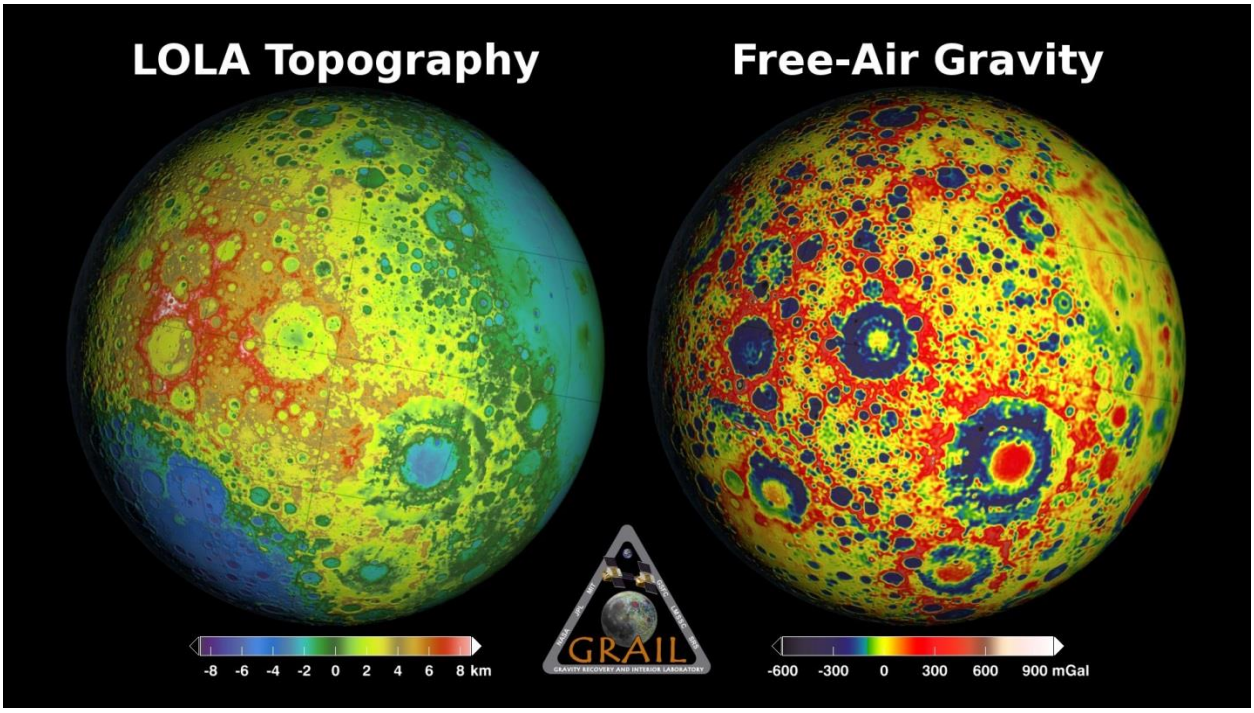

Figure 31. The most recent Lunar Reconnaissance Orbiter(LRO) Lunar Orbiter Laser Altimeter(LOLA) imagery(left) and The Gravity Recovery and Interior Laboratory (GRAIL) mission maps(right) made by spacecraft Ebb and Flow have provided the most detailed topography and lunar gravity maps to date. This data will help in mission planning, ranging from orbit selection to picking geological exploration sites and perhaps even a site for permanent settlement activities [Credit M.Zuber MIT, ASU, NASA 2012]

2. Orbital Parameters –Orbit, Diurnal Period, Thermal Cycling and Seasons– Since the Earth-Moon system is in heliocentric orbit, they share a similar solar constant of 1.36kW/m^2. The Earth's 24 hour cycle that we operate the CC/SIS systems in is somewhat comparable to Mars that has an approximately similar diurnal period of 24 hours and 40 minutes while the Moon, in a tidally locked orbit around Earth has a long synodic period of 29.53 Earth days. This is an important differentiator since surface conditions are dramatically affected by diurnal temperature variations and solar radiation, especially in lunar vacuum , where the unfiltered solar radiation arrives unhampered on the surface and stays in the lunar sky for approximately 14.5 Earth days in the lower latitudes. Since the Moon has very little axial tilt, there are no seasonal variations. However, the sun stays over the horizon at the poles for most of the year. Since the Polar Regions receive less insolation, the thermal cycling in those regions are much milder than in the lower latitudes and equatorial regions (see Figure 32).

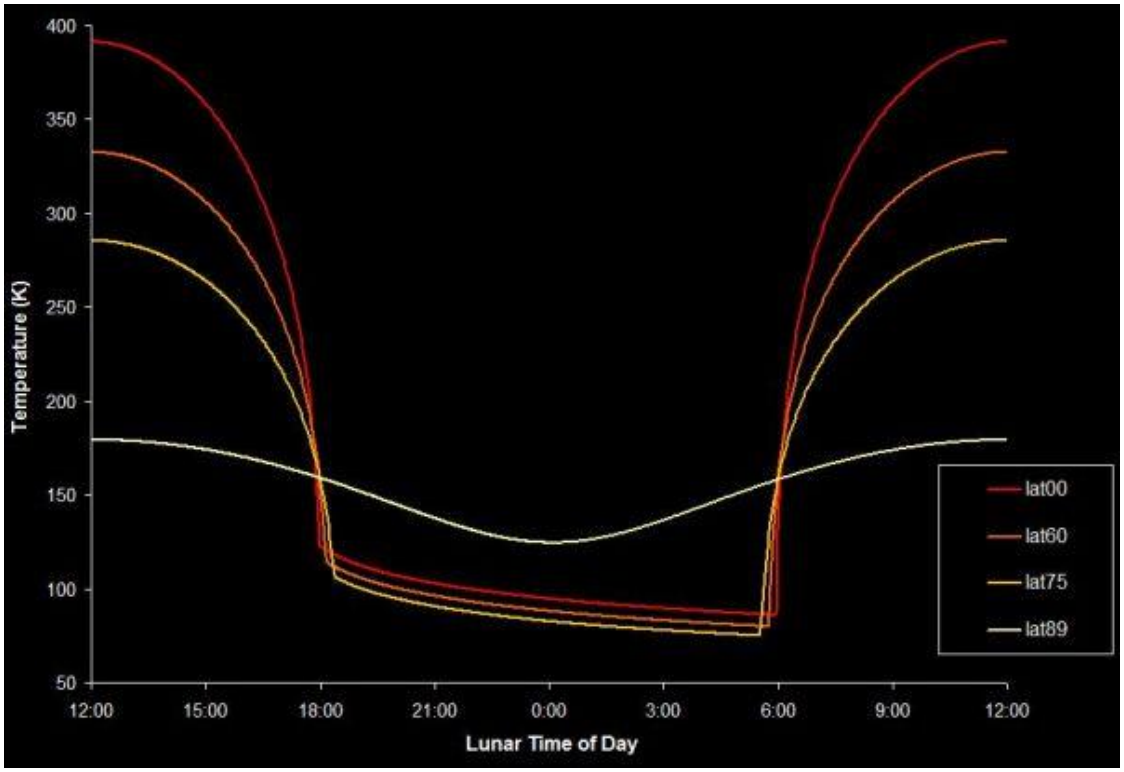

Figure 32. On the Moon, since the Polar Regions receive less insolation, the diurnal thermal cycling in those areas are much milder than in the lower latitudes and equatorial regions. Milder thermal cycling is another reason to establish settlements and infrastructure in those regions, as it will also help the CC machine to operate in a more steady thermal environment. [Image credit NASA LRO Diviner Expt. UCLA]

And in the very thin Martian atmosphere, compounded by twice the distance to the sun as the Earth and resulting solar constant of 0.589kW/m^2, the pronounced eccentricity of the planet's orbit (see Figure 33] and an axial tilt that is similar to Earth, the energy transport mechanisms create seasons as well as dramatic weather phenomena like dust devils and long duration dust storms that can block out the sun for most of the year. The construction machines will have to be resilient in order to weather these fluctuations over the commissioning period, allowing it to operate reliably from months to years of operation. The CC machine feedstock will also need to be tailored to resist deleterious effects by the low pressure CO_2 atmosphere.

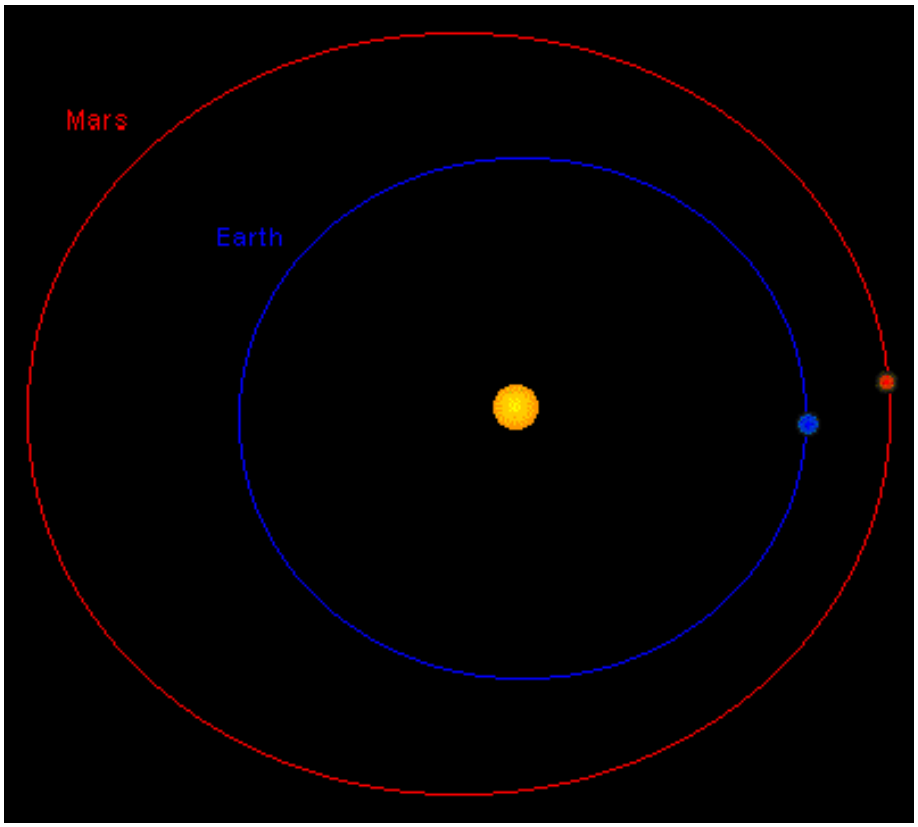

Figure 33. The pronounced eccentricity of Mars orbit causes extreme weather. Dust storms are known to block out the sun for months at a time. Such conditions will call for alternative power systems for reliable Martian CC operation.

3. Atmosphere - While the atmosphere of the Earth provides the thermal inertia to support life, our Moon, lacking such a blanket due to its inability to hold one because of weak gravity, sees sharp diurnal variations resulting from direct solar radiation. Micrometeoritic impacts constantly pummel the lunar surface, creating a fine top layer of lunar dust that is continually charged by the solar wind. This dust is highly abrasive and will affect the mechanical components of the construction machinery and must be dealt with. On Mars, the thin atmosphere is highly energetic, carrying fine dust at velocities that exceed hurricanes on Earth and creating long lasting dust storms that can blanket the entire hemisphere at times. Low visibility can impair some construction operations and so enhanced vision systems may be necessary on the construction machines destined for Mars settlement and infrastructure development (see Figure 34).

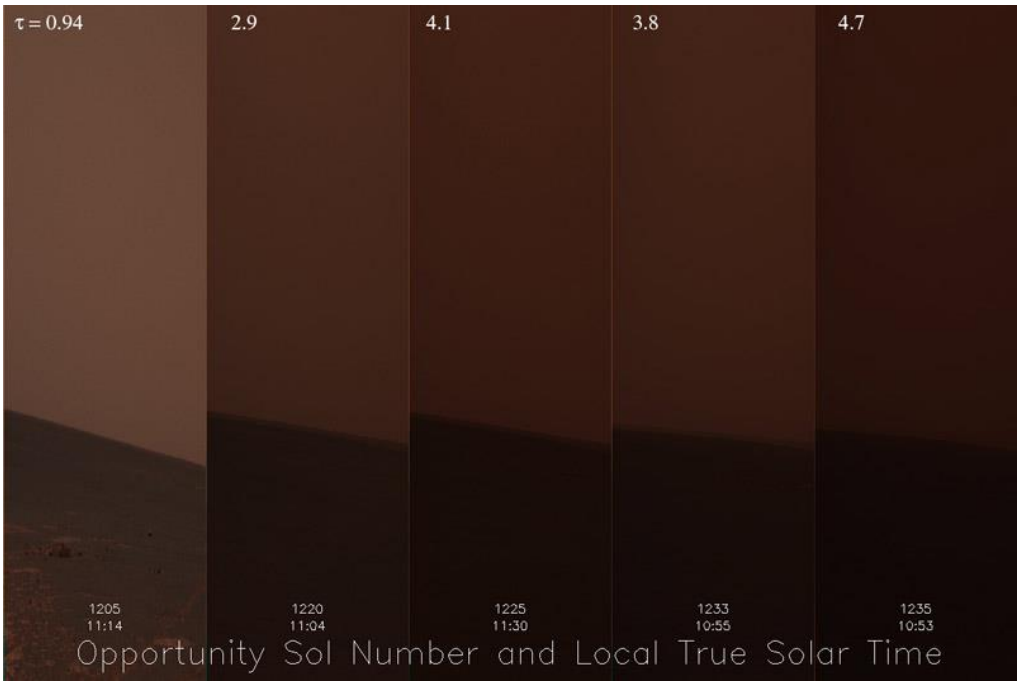

Figure 34. Dust storm recorded by Opportunity shows how visibility is impaired by long lasting event. Solar power generation declined by 80%, severely affecting nominal operations and communications. The Martian version of CC/SIS machine may have special auxiliary power systems to compensate for events such as these.[Image credit NASAJPL]

4. Radiation - The Earth's atmospheric blanket effectively filters both energetic solar electromagnetic and particulate radiation, allowing a much more benign radiation environment than found in space, or on the surface of the Moon or Mars. The Mars Science Laboratory Curiosity has been monitoring radiation levels, both during interplanetary transit and on the Martian surface (see figure 35). NASA continues to accumulate radiation dose data on space missions and a comparison chart shows the range of dosage received on Earth surface to interplanetary missions (see Figure 36). Radiation will affect electronics and other sensitive components of the construction system as well. So radiation hardening procedures will have to be implemented on the Lunar and Martian construction system as with any spacecraft or extraterrestrial surface vehicle.

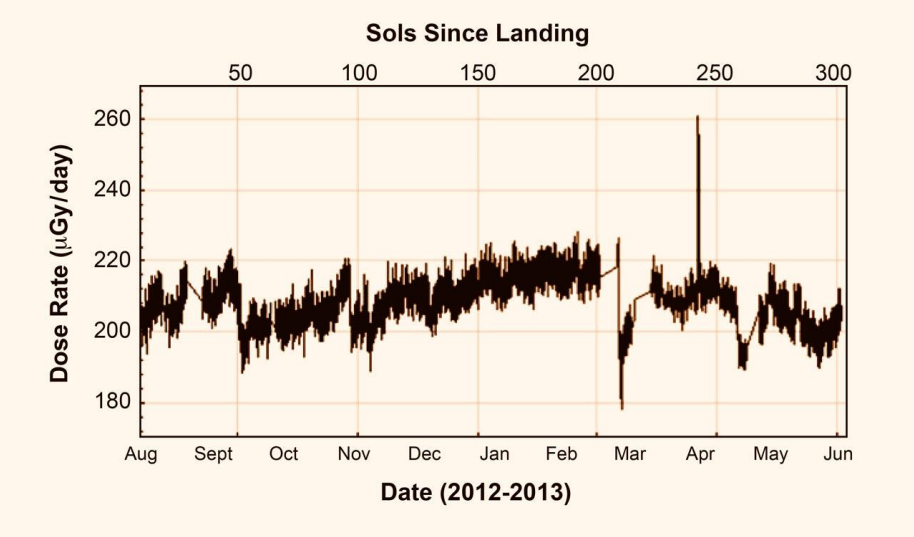

Figure 35. The Mars Science Laboratory(MSL) measured radiation on the martian surface. It registered the spike during an energetic solar particle event in April 2013.The CC/SIS machines will have to be radiation hardened to protect sensitive components. [Image credit NASA JPL-MSL]

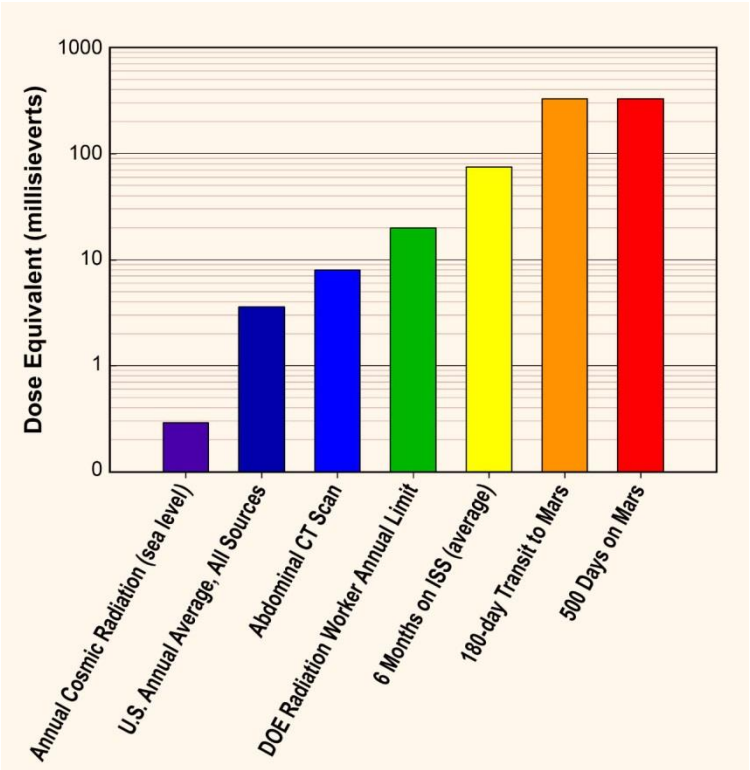

Figure 36. Comparison of radiation dosage in different space and terrestrial environments. Polymer additives have been suggested to moderate and absorb GCR and energetic particles. The CC machine feedstock could use additive powders like Boron Nitride or Boron Carbide to

absorb energetic neutrons, ameliorating radiation for crew and sensitive equipment in surface facilities. [Image credit NASA]

In order to circumvent the difficulties posed by the harsh conditions discussed above, recent literature favors building settlements inside extraterrestrial lava tubes. Such geologic structures may also exist on Mars as shown in recent images of the region surrounding the Pavonis Mons volcano (see Figure 37). Such a strategy circumvents the difficulties posed by many of the extraterrestrial surface environments discussed above, providing a more stable thermal and radiation regime for CC operations. However, critical physical infrastructure like the landing pad will have to be built, commissioned and serviced to reliably weather ambient conditions on the extraterrestrial surface.

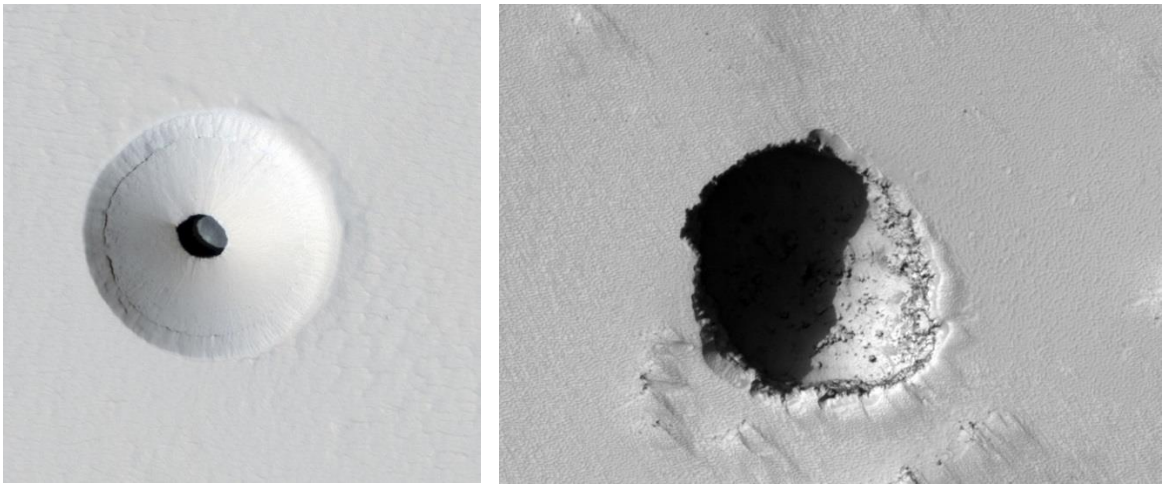

Figure 37. A pit crater on a Martian volcano at Mons Pavonis. Such features may also point to sulfur deposits that could be used for production of sulfur concrete(Credit: Mars Reconnaissance Orbiter, NASA, JPL, HiRISE-University of Arizona]

Lunar and Mars Terrain for Landing Pad

Several missions flown to the lunar and Mars surface to date provide evidence that these extraterrestrial surfaces possess the required stability and soil load bearing qualities to build a permanent landing pad. The following images shot on the surface over the last four decades (1969 – 2012) show that both the surface of the Moon and Mars are strewn with boulders, rocks and outcrops of bedrock. Apollo 11 images clearly show rocks of various sizes scattered over an otherwise smooth terrain.[See figure 38] Astronaut footprints indicate that the surface dust can be tamped down without need for excessive impact force.[See figure 39] The MSL Curiosity rover is continuing to provide detailed information about the geologic nature of the terrain and aqueous processes are evident. Mars landers show rocks of all sizes (Figure 40) and the flat sedimentary rock formations (see Figure 41), once cleared of dust and debris may be ideal foundations on which the SIS machine can process the in-situ material to create a landing pad.

When prestabilized using proven precursory methods like excavating, raking, tamping and leveling of the pristine terrain, followed by extrusion by a CC system to lay down the landing pad apron with sulfur concrete, it is possible to create a serviceable landing pad with a durable surface for repeated lunar or Martian landings. The CC machine, fitted with excavation scoops and rakes, may be able to do the entire job without the need for other dedicated tools and systems. This may be doable if the feed material which is a mix of regolith and sulfur is brought to the site and is in the reach of the CC machine.

If the site for a landing pad is carefully selected with attention paid to topography, not only for ease of lander navigation and service but also from the point of view of geology and ISRU, then it may be possible to build and commission a landing pad quickly.

Figure 38. This image shot of the lunar surface in the sea of tranquility region by Apollo 11 crew show the rocks and boulders strewn all over the area in the vicinity of the lunar lander.(Credit: Apollo 11 Lunar Surface Journals]

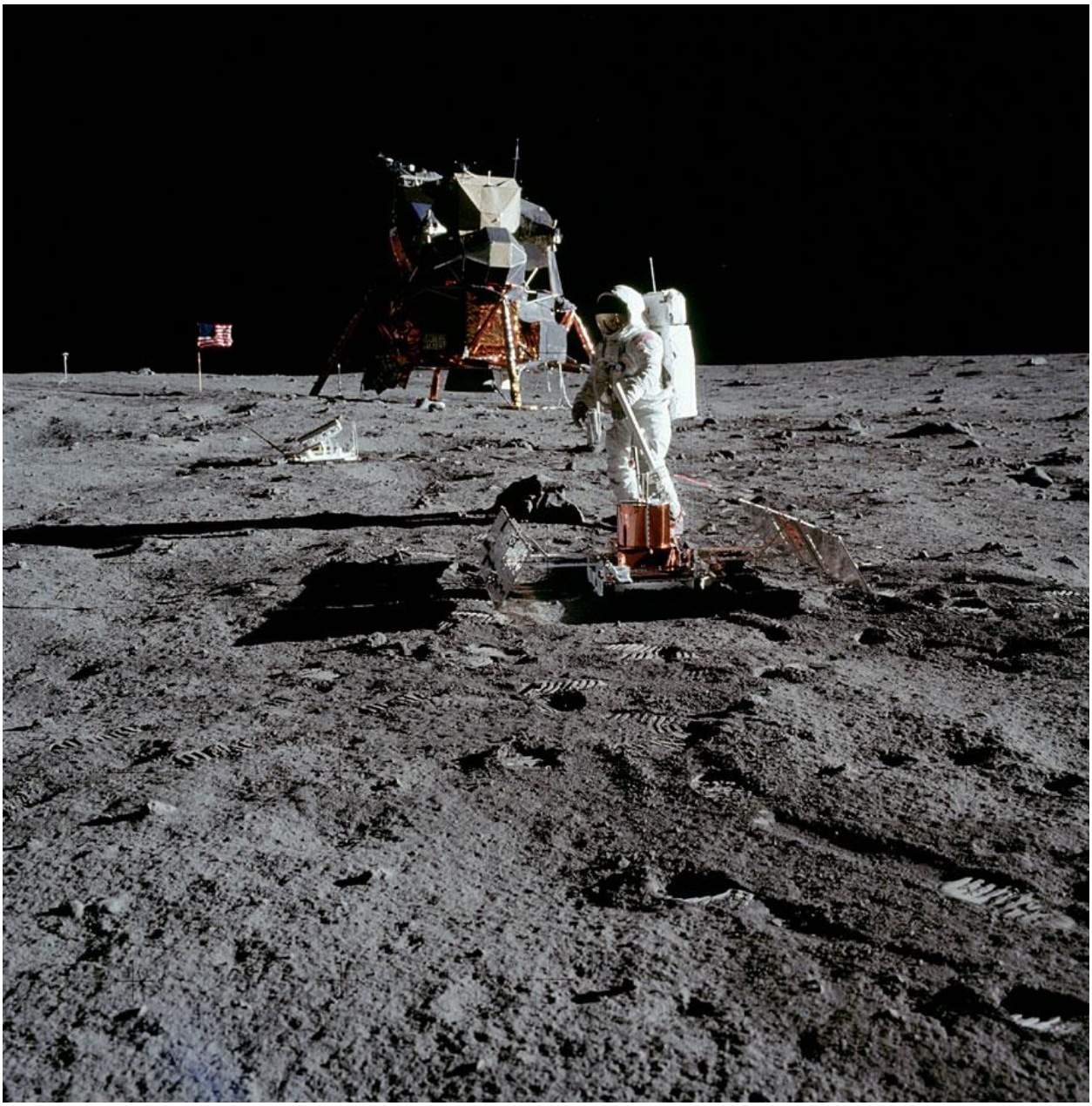

Figure39. This Apollo image shows the dust laden lunar surface. The footprints suggest that the surface could be prestabilized by raking to remove rocks and then by tamping it level before lunar CC machine starts to deposit a concrete surface, layer by layer to create a serviceable landing pad for repeated sorties by heavy landers.[Credit: Apollo Lunar Surface Journals]

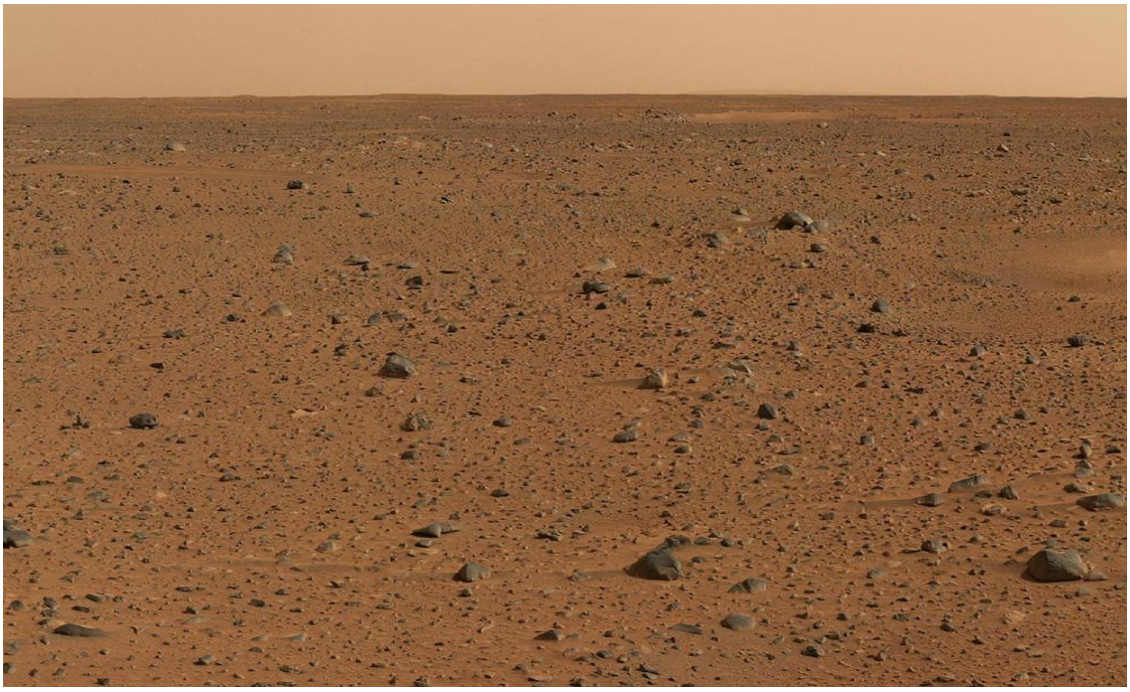

Figure 40. The surface of Mars is also strewn with rock and boulders of all shapes and sizes

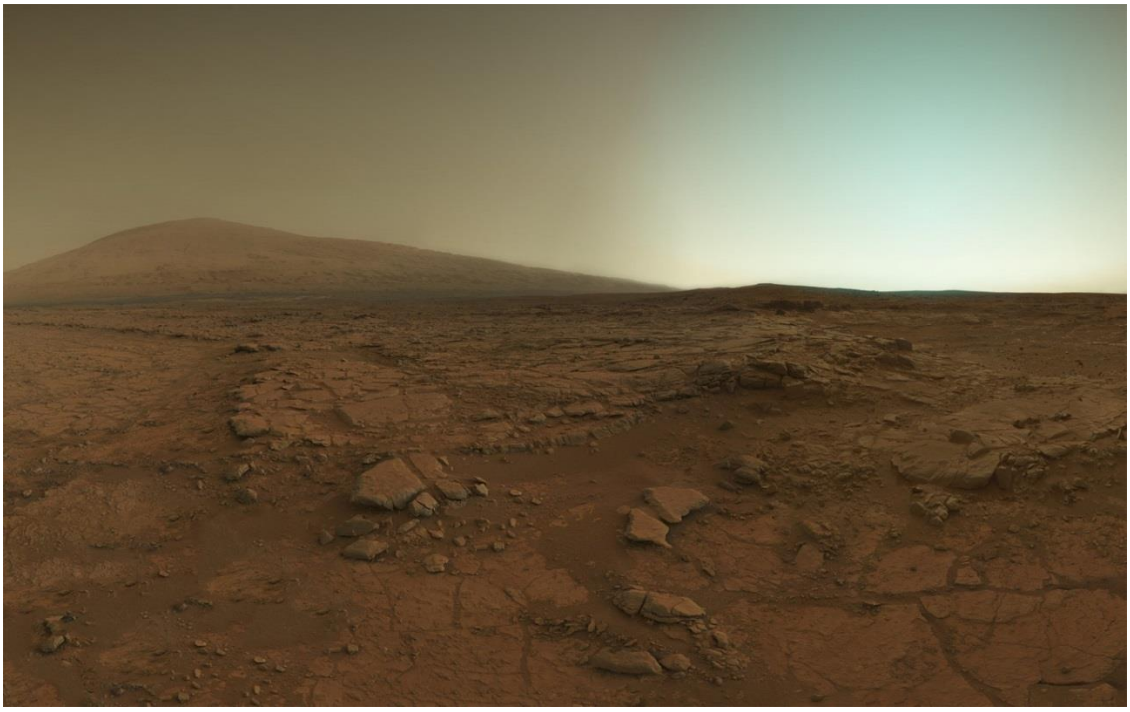

Figure 41. Large flat rock outcrops like these sedimentary formations on Mars are potential sites for landing pads because it offers a strong foundation on which the CC machine can begin extruding the concrete with minimal preparation.

Figure 42. A recent image of Mt. Sharp on Mars from the Mars Science Laboratory Curiosity shows a terrain with ample ISRU materials that could be used as CC feedstock using Martian sulfur as binder.

The Evolution of the Construction Technology

Employing current best practice in design and engineering, it is prudent to evolve the proposed construction system for extraterrestrial application in a step by step approach. Simulations are the way to test and evolve the system. Simulations on analogous terrain on Earth would be followed by the commissioning the system on the Moon. The first extraterrestrial CC and SIS machines might be tested on the Moon because it is much closer, requires less transport and logistics effort and energy, quick abort capability if crew need evacuation, and allows for better telerobotic command and control, if Earth based mission control is employed.(see Figure 43]. Once the machines are proven on the Moon, they can be adapted for Mars. This progressive sequence fits

well with NASA baseline plans and follows the recommendation of NRC and independent commissions that have studied the future of space activities, both human and robotic.

	Moon	Mars
Distance from Earth	384,000 km	58,000,000 – 400,000,000 km
Two-Way Communication Time	2.6 seconds	6 – 44 minutes
One-way Trip Time	4 days	180-210 days
Stay Time	7 days (sortie mission)	495 – 540 days
Total Mission Duration	18 days (sortie mission)	895 – 950 days
Aborts	Anytime return	Limited to early in the mission or multi-year
Logistics Delivery	Daily	Every 26 months
Total Mission Mass (Note: ISS ~ 400 t)	~200 t	~800 – 1,200 t
Total Delta-V (LEO to surface and back)	9.5 km/s	12 – 14 km/s

Figure 43. After CC and SIS machine development and high fidelity simulations on Earth, the first extraterrestrial construction machines might be tested on the Moon because it is much closer, requires less transport and logistics effort and energy, quick abort capability if crew need evacuation, and allows for better telerobotic command and control, if Earth based mission control is employed.[Table credit: B.Drake Journal of Cosmology 2010]